THE INVOLVEMENT OF RENAL TUBULE EPITHELIAL CELLS IN THE PATHOPHYSIOLOGY OF CALCIUM OXALATE NEPHROLITHIASIS

De betrokkenheid van epitheliale niertubuluscellen bij de pathofysiologie van calcium oxalaat niersteenziekte

PROEFSCHRIFT

ter verkrijging van de graad van doctor
aan de Erasmus Universiteit Rotterdam
op gezag van Rector Magnificus
Prof. dr P.W.C. Akkermans M.A.
en volgens het besluit van het College voor Promoties

De openbare verdediging zal plaatsvinden
op woensdag 25 november 1998 om 11.45 uur

door
Carl Friedrich Verkoelen
geboren te Rotterdam

PROMOTIE-COMMISSIE

Promotor:	Prof. dr F.H. Schröder
Overige Leden:	Prof. dr G. van Meer Prof. dr W. Weimar Dr. H.R. de Jonge
Co-Promotor:	Dr. J.C. Romijn

Onwetendheid is de heerlijkste eigenschap die er bestaat omdat men haar zonder enige moeite kan aanleren en omdat zij de geest voor zwaarmoedigheid behoedt.

Giordano Bruno

Ter nagedachtenis aan mijn vader

Voor Carlie en Sjors

Dit proefschrift werd bewerkt binnen de afdeling Urologie, Faculteit der Geneeskunde en Gezondheidswetenschappen, Erasmus Universiteit Rotterdam en Academisch Ziekenhuis Dijkzigt Rotterdam en werd ondersteund door de Nier Stichting Nederland (projekten C92.1235 en C95.1494).

Het verschijnen van dit proefschrift werd mede mogelijk gemaakt door een financiële bijdrage van de Nier Stichting Nederland, Bussum, de Stichting Urologisch Wetenschappelijk Onderzoek (SUWO), Rotterdam, Yamanouchi Pharma BV, Leiderdorp en Pfizer BV, Rotterdam.

ISBN 90 5166 663 2

Uitgeverij Eburon
Postbus 2867
2601 CW Delft
info@eburon.nl

Foto omslag: Pim Visser - Calcium oxalaat monohydraat kristallen (SEM opname)

ABBREVIATIONS

α-MG	α-methyl glucoside
AF	apical fluid
ALH	ascending limb of Henle
AP	alkaline phosphatase
A->B	apical to basal solute transport flux
BF	basal fluid
B->A	basal to apical solute transport flux
CaOx	calcium oxalate
CCD-A	apical fluid collecting duct buffer
CCD-B	basal fluid collecting duct buffer
CD	collecting duct
CM	culture medium
COM	calcium oxalate monohydrate
CS-A	chondroitin-4-sulfate
CS-B	dermatan sulfate
CS-C	chondroitin-6-sulfate
CSLM	confocal laser scanning microscopy
DLH	descending limb of Henle
DMSO	dimethylsulfoxide
dpm	desintegrations per minute
DT	distal tubule
FCS	fetal calf serum
γ-GT	γ-glutamyltranspeptidase
GAGs	glycosaminoglycans
H	heparin
HA	hyaluronic acid
HS	heparan sulfate
IMCD	inner medullary collecting duct
Jox	oxalate transport
Jv	water transport
KHB	Krebs Henseleit buffer
KS	keratan sulfate
LDH	lactate dehydrogenase
MOPS	na-morpholinopropane sulfonic acid
MTT	3-(4,5-dimethylthiazol-2-yl) -2,5-diphenyl tetrazolium bromide
Ox	oxalate
P	plasma

PAH	*para*-aminohippurate
PCA	perchloric acid
PCT	proximal convoluted tubule
PD	potential difference
P^{mann}	mannitol permeability
PT	proximal tubule
S1-segment	early proximal tubule
S2-segment	late proximal tubule
S3-segment	straight portion of the proximal tubule
SEM	scanning electron microscopy
SP54	pentosanpolysulfate
SSPs	semi-synthetic polysaccharides
TEM	transmission electron microscopy
TER	transepithelial electrical resistance
THP	Tamm Horsfall protein
TF	tubular fluid
UF	ultrafiltrate

CONTENTS

Chapter 1

GENERAL INTRODUCTION

Chapter 1

General introduction

1.1 Nephrolithiasis

Renal stone disease is a common disorder in industrialized countries where up to 10% of the population will develop kidney stones during lifetime [1-5]. Because of the rising incidence, it is often considered one of the "diseases of affluence". Indeed epidemiological studies made apparent that the prevalence of the disease fluctuates in parallel with economy, with peaks during time of abundance and troughs during war and recession [6,7,8]. Another depressing fact is the high stone recurrence rate, showing new stone formation in about 50% of cases over a 10-year period. Much improvement has been made in the management of renal calculi with the advent of extracorporeal stone destructive techniques and refinements in endoscopic surgery [1]. The removal of stones, however, does not alter the propensity for recurrent stone formation and it has been suggested that the enthousiasm surrounding such advances reduced the need to search for metabolic causes of stone formation [5,6]. This attitude may have fuelled the stone recurrence problem. Moreover, kidney stones cause considerable suffering and the clinical procedures to remove stones have a substantial economic impact [1-5]. Measures should therefore be taken to prevent stone recurrence. Calcium is the most common component of kidney stones, being present in approximately 70% of all stones found. It is generally accepted that increases in urinary supersaturation and the subsequent nucleation of crystalline material is the basis for the formation of a renal stone [9-12]. Excessive intakes of meat protein, oxalate and potentially sodium, as well as insufficient intakes of vegetable fibers, calcium and fluid, all can lead to increased urinary supersaturation [6-9]. This does not necessarily implicate however, that nephrolithiasis is primarily a nutritional disease. Rather, nutrition should be regarded as an additional factor that causes subjects with underlying disorders to become stone formers [6,7,8,13]. Many such underlying abnormalities have already been recognized, including subtle forms of primary hyperparathyroidism, incomplete forms of distal renal tubular acidosis, abnormal structure of macromolecular inhibitors, primary or enteric hyperoxaluria. Most disorders underlying stone disease are still unknown and no treatment can be designed against them. Among these there are patients with membrane transport protein abnormalities. For example, some stone forming individuals can be identified a faster anion-exchange (band 3) mediated oxalate flux across their red blood cell membranes [14-

16]. It is not clear though if this aberrant transport of oxalate in erythrocytes represents a more general cellular oxalate transport abnormality which also may affect oxalate transport across the membranes of epithelial cells in the intestine and/or kidney. Other inherited forms of kidney stone disease are those associated with mutations in the gene encoding a chloride channel (CLC-5), including Dent's disease and X-linked ressesive nephrolithiasis [4]. These disorders are characterized by excessive urinary excretion of calcium (hypercalciuria) and abnormally high urinary levels of low molecular weight proteins (low molecular weight proteinuria). At the present time, there are many uncertainties about the mechanism responsible for hypercalciuria in these syndromes, but the presence of low molecular weight proteinuria in Dent's disease subjects has prompted consideration of a defect in absorptive endocytosis in the proximal tubule. CLC-5 could be essential for proximal tubular endocytosis by providing an electrical shunt necessary for the efficient acidification of vesicles in the endocytotic pathway [17]. For decades all stone formers have rightly been advised to increase their fluid intake, but the inadequacy of this as the sole approach to therapy is reflected by the high recurrence rates. Our understanding of the stone-forming process is still incomplete and therefore future research is required in the field of prevention of recurrent calcium stone disease.

1.2 Saturation, supersaturation, crystal nucleation and stone formation

Important functions of the kidney are to conserve essential nutrients, to eliminate potentially toxic substances and to reduce the quantity of salt and water excreted in the final urine, usually to less than 1 percent of the volume filtered at the glomerulus. A number of interdependent functions of nephron segments are responsible for the production of concentrated urine [18]. One of the side-effects of this process is that the tubular fluid in segments beyond the thin limbs of Henle frequently becomes oversaturated with stone salts. Because of its unique composition, being a combination of anions, cations, and small and macromolecular organic components, the tubular fluid is capable of holding ions in solution at levels above saturation conditions by the formation of numerous stable soluble complexes [9-12]. When the concentration of the salt components increases beyond saturation levels, a state of thermodynamically unstable supersaturation exists in the tubular fluid. Under certain conditions, this oversaturated state induces crystal nucleation, which is accompanied by a reduction of excess free energy and a thermodynamically more stable environment. The free energy of the solution continues to decrease as new crystal components are

withdrawn from the solution and incorporated into the crystal structure (crystal growth). Once formed, the crystal particles can bind to each other to form larger particles (agglomeration) [9-12]. Crystal formation or growth does not require continuous supersaturation of the tubular fluid, since intermittent supersaturation during periods of dehydration or after meals is sufficient. The formation of urinary stones can not be explained by urinary supersaturation alone. Urine is frequently supersaturated with calcium oxalate in all individuals and crystals are seen in most urine specimens. In healthy individuals, crystals are washed out in the urine, whereas in stone formers crystalline material is retained in the kidney [1,12,19].

1.3 Calcium or oxalate?

In the past, calcium intake was regarded to play the main role in stone formation for the very reason that most renal stones contain this element. For a long time, the restriction of calcium from the diet has been a mainstay of dietary advice for the prevention of recurrent nephrolithiasis. Later it became clear that this advice was inappropriate and even potentially dangerous given the potential impact of low calcium levels on total body calcium content (i.e. bone density). In addition, it was demonstrated that individuals with a high calcium intake may actually form fewer stones presumably because calcium forms complexes with oxalate in the gastro-intestinal tract, leading to reduced oxalate absorption and decreased urinary oxalate excretion. A restriction in dietary calcium is now only advised to hypercalciuric patients with excessive calcium intake or to those who remain hypercalciuric despite pharmacologic therapy [6,11,20,21,22]. One of the key advances in our understanding of calcium stone disease has been the appreciation of the importance of oxalate. Urine oxalate excretions correlate strongly with both frequency of stone episodes and with crystalluria while these correlations are much weaker with urinary concentrations of calcium. Oxalate therefore appeared to be a much more important determinant of calcium oxalate supersaturation than calcium [23,24]. The incidence of mild hyperoxaluria in patients with idiopathic calcium stone disease has been reported to range from 15-50% [25]. The amount of oxalate that is excreted in the urine depends on dietary intake, intestinal absorption, endogeneous production and renal handling [26-30]. Although the largest amount of urinary oxalate (90%) derives from the production of oxalate in the liver (from ascorbate, glycolate, glycin, hydroxyproline, and α-hydroxy-ß-ketoadipate), a primary disorder in the metabolism of oxalate has not (yet) been demonstrated in most calcium stone formers [26-31]. After ingestion

of oxalate containing food, normally only a small amount of oxalate (~ 10%) is absorbed from the gastrointestinal tract. In addition, most foods have a relatively low oxalate content and dietary intake of excessive oxalate is relatively uncommon, even in stone formers. Nevertheless, as small increments in oxalate can substantially contribute to the degree of urinary supersaturation and since there is no effective pharmacologic therapy available to reduce the excretion of oxalate in urine, calcium stone formers are generally adviced to reduce the consumption of oxalate-rich foodstuffs such as rhubarb, spinach, nuts, chocolate and tea [1,2,3,11,13,20,24].
Despite the important role of oxalate in calcium stone disease, relatively little is known about the maintanance of the mass body balance of oxalate. For a long time there was a lack of reliable methods to measure oxalate in urine and plasma. In addition, oxalate did not receive much interest in renal physiology since it did not seem to have a biological function. The recent development of improvements in the precision of oxalate assays [32-39], as well as the recent finding that low concentrations of oxalate (1 μM) can play an important role in certain physiological processes [40-44], may lead to better understanding of oxalate homeostasis in the future.

1.4 Renal handling of oxalate

Oxalate is a small dicarboxylate anion ($C_2O_4^{2-}$) that is freely filtered into Bowman's space. Urinary oxalate levels are then adjusted by tubular secretion and/or reabsorption. Higher urinary levels of oxalate could be explained by an enhanced secretory pathway for oxalate in the kidney [14-16,26-28]. In the erythrocytes of idiopathic calcium stone formers an abnormal oxalate transmembrane flux was found. It was speculated that the red blood cell abnormality may represent a more generalized cellular oxalate transport abnormality, which could affect gastrointestinal absorption as well as renal secretion which in turn could lead to hyperoxaluria [14-16]. In fact these reports prompted us to study oxalate transport mechanisms in cell culture, as described in this thesis. Much of the available information about the mechanisms involved in cellular oxalate transport has been derived from studies with isolated membrane vesicles [45-53]. However, transport processes in vesicles do not imperatively reflect transport in intact and functional epithelia [53]. Microperfused renal tubules have been used as a model for such an intact epithelium but this approach is technically demanding and is limited by the small volume of the luminal compartment. Alternatively, transport studies can be performed under electro-physiologically controlled conditions across sheets of polarized and

functional epithelia mounted in a two compartment system. A model to study oxalate transport across stripped intestinal tissue has already been presented [54-57]. Unfortunately, this approach is not feasible with renal tissue. Cultured epithelial cells could serve as an alternative *in vitro* model to study renal oxalate transport.

1.5 Crystal retention

The presence of crystals can be detected in the urine of all individuals and does, therefore, not necessarily reflect a pathological situation. Development of a renal stone requires the retention of crystals inside the kidney [1,9,12]. It is not clear, however, how crystals become trapped. Growth and agglomeration could result in the formation of particles that are too large to freely pass the renal tubules. It is also possible that crystals even when they are much smaller than the diameter of the lumen attach to the renal epithelial cell surface [9,12,19]. Morphological evidence for the latter possibility was obtained from observations in patients with disorders in intestinal oxalate absorption and oxalate metabolism [58-62] and in hyperoxaluric rats [63,64]. It remains to be established why crystal retention apparently does not take place in the kidneys of healthy persons. Possibly, still unidentified cell surface characteristics or substances in the urine are able to prevent crystal adherence. Alterations in the amount or structure of such components at the cell surface or in the tubular fluid could create conditions that are favorable for crystal retention [9,65-67].

1.6 Inhibitors of stone formation

A compound may be referred to as an inhibitor of stone formation if it interferes with the nucleation, growth, agglomeration or retention of crystals and thereby diminishes the process of stone formation. Many investigators have searched for naturally occurring urinary inhibitors of crystallization. The inhibitors revealed sofar can be divided roughly into two major catagories (a) macromolecular organic molecules, such as Tamm-Horsfall protein, nephrocalcin, osteopontin, crystal matrix protein, uronic acid-rich protein, GAGs, and (b) small organic and inorganic compounds such as citrate, pyrophosphate, magnesium, and trace metals. Although much has been done to understand the mode of action of these inhibitors, their exact role in the pathogenesis of renal stones is still largely unclear [68-73].

1.7 Renal tubular cells and nephrolithiasis

Renal tubular cells could be involved in calcium oxalate stone formation in several ways. They actively transport most inorganic stone components, such as calcium, phosphate and perhaps oxalate, and are also actively involved in the reabsorption of water. These processes directly influence the concentration of stone salts in the tubular fluid. Furthermore, the cells produce urinary glycoproteins that serve as inhibitors of crystallization and the terminal residues of cell surface glycoconjugates may act as binding site for crystals. It is therefore conceivable that abnormalities in the biosynthesis of glycoproteins and their carbohydrate side-chains not only influence the inhibitory capacity of the tubular fluid but also could predispose the tissue for crystal retention.

1.8 Renal cell culture

Renal epithelial cells in tissue culture have been widely used as a model in renal physiology and cell biology research. Tissue cultures of renal tubular cells form monolayers of highly differentiated and polarized cells with apical microvilli and junctional complexes [74-78]. The advantage of cell lines above primary cultures is that they are convenient to culture and form monolayers more reproducibly. Cells can be stored frozen and returned to culture at a later date, which allows additional experiments to be performed with the same material. The disadvantage of cell lines is that they do not necessarily correspond exactly to a distinct segment of the nephron but rather retained some of the characteristics. Although there are no cell lines available isolated from stone forming individuals, more knowledge of normal renal cell function could provide information on processes that are possibly abnormal or altered in renal stone disease. Several permanently growing cell lines with characteristics of distinct nephronal segments are presently available. The choice of a specific cell model system depends on which mechanisms are to be studied. The cell lines used in the experiments described in this thesis are LLC-PK_1 cells that have retained many characteristics of the proximal tubule [79], and MDCK cells that have widely been used as a model system for the distal/collecting duct [80,81]. Whatever model system is used, it is a general requirement for performing physiologically relevant studies that the cultures morphologically and functionally mimic as much as possible the cell phenotype found *in vivo*.

1.9 Oxalate transport and crystal-cell interaction studies in cell culture

In order to move transcellularly from the peritubular capillaries to the tubular fluid, solutes have to cross two barriers: the basolateral plasma membrane, which is in contact with the internal milieu facing the mesenchymal space and blood supply, and the apical plasma membrane, which is in contact with the external milieu and faces the tubular fluid. To study oxalate transport in cell culture, cells are grown as monolayers in a two compartment culture system in which the apical compartment is separated from the basal compartment by the epithelial layer. Culture medium is added to both compartments of which the apical compartment is representative for the tubular fluid and the basal compartment for the peritubular plasma. In such a model system, radiolabeled oxalate is applied either to the apical or basal compartment and the appearance of tracer in the opposite compartment is measured in time. Net transport is defined as the difference between the two unidirectional fluxes.

Crystal-cell interactions are studied with calcium oxalate monohydrate (COM) crystals and MDCK cells, also these cells are generally cultured on permeable supports in a two-compartment culture system. A suspension of radiolabeled COM crystals is prepared by mixing [^{14}C]oxalate with calcium. Crystal adherence is quantitated by measuring cell-associated radioactivity and morphologically inspected using various techniques, including light microscopy (LM), scanning electron microscopy (SEM), transmission electron microscopy (TEM) and confocal laser scanning microscopy (CLSM).

1.10 Scope of this thesis

The aim of the present investigations was to obtain more basic information about cellular processes that are possibly involved in the pathophysiology of calcium stone disease. The major questions were (1) is oxalate actively transported by renal tubular cells? and (2) can calcium oxalate crystals adhere to the renal cell surface? Oxalate transport experiments are described in *Chapters 2 and 3*. In *Chapter 4,* a model system is presented to study crystal-cell interaction. With this model the effect of naturally occuring and semi-synthetic polysaccharides on crystal-cell interaction was studied as described in *Chapter 5*, the effect of epithelial injury on crystal binding in *Chapter 6,* and nephron site-specific protection from crystal binding in *Chapter 7.* Finally, in *Chapter 8* our results are discussed in relation to the latest understanding on the possible role of renal tubular cells in calcium oxalate nephrolithiasis.

References

[1] Menon M, Koul H (1992) Calcium oxalate nephrolithiasis. J Clin Endocrin Metab 74:703

[2] Levy FL, B Adams-Huet, CYC Pak (1995) Ambulatory evaluation of nephrolithiasis. An update of a 1980 protocol. Am J Med 98:50

[3] Monk RD. Clinical approach to adults (1996) Seminars Nephrology, 16:375

[4] Lloyd SE, Pearce SHS, Fisher SE, Steinmeyer KS, Schwappach B, Scheinman SJ, Harding B, Bollino A, Devoto M, Goodyer P, Rigde SPA, Wrong O, Jentch TJ, Craig IW, Thakker RV (1996) A common molecular basis for three inherited kidney stone diseases. Nature 379:445

[5] Curhan GC, WC Willett, EB Rimm, D Spiegelman, MJ Stampfer (1996) Prospective study of beverage use and the risk of kidney stones. Am J Epidemiol 143:240

[6] Jaeger Ph (1994) Prevention of recurrent calcium stones: diet versus drugs. Miner Electrolyte Metab 20:410

[7] Robertson WG (1987) Diet and calcium stones. Mineral Electrolyte Metab 13:228

[8] Goldfarb S (1994) Diet and nephrolithiasis. Annu Rev Med 45:235

[9] Mandel N (1996) Mechanisms of stone formation. Sem Nephrol 16:364

[10] Smith LH (1987) Pathogenesis of renal stones. Min Electr Metab 13:214

[11] Parks JH, Coe FL (1996) Pathogenesis and treatment of calcium stones. Sem Nephrol 16:398

[12] Kok DJ, Khan SR (1994) Calcium oxalate nephrolithiasis, a free or fixed particle disease. Kidney Int 46:847

[13] Coe FL, Favus MJ (1991) Nephrolithiasis. In the Kidney, Brenner BM and Rector FC (eds) pg 1728

[14] Baggio B, Gambaro G, Marchini F, Cicerello E, Borsatti A (1984) Raised transmembrane oxalate flux in red blood cells in idiopathic calcium oxalate nephrolithiasis. The Lancet 2:12

[15] Gambaro G, Baggio B (1992) Idiopathic calcium oxalate nephrolithiasis: a cellular disease. Scanning Microscopy 6:247

[16] Borsatti A (1991) Calcium Oxalate nephrolithiasis: defective oxalate transport. Kidney Int 39:1283

[17] Günther W, Lüchow A, Cluzeaud F, Vandewalle A, Jentsch TJ (1998) CLC-5, the chloride channel mutated in Dent's disease, colocalizes with the proton pump in endocytotically active kidney cells. Proc Natl Acad Sci USA 95:8075

[18] Knepper MA, Rector FC (1991) Urinary concentration and dilution. In The Kidney, Brenner BM and Rector FC (eds) pg 445

[19] Finlayson B, Reid F (1978) The expectation of free and fixed particles in urinary stone disease. Invest Urol 15:442

[20] Coe FL, Parks JH, Murray JF (1997) Diet and calcium:The end of an era? Ann Int Med 126:553

[21] Robertson WG (1990) Epidemiology of urinary stone disease. Urol Res 18:S3

[22] Parivar F, Low RK and Stoller ML (1996) The influence of diet on urinary stone disease. J Urol 155:432-440.

[23] Robertson WG, Peacock M (1980) The cause of idiopathic calcium stone disease: Hypercalciuria or hyperoxaluria? Nephron 26:105

[24] Robertson WG, Peacock M, Heyburn PJ, Marshal DH, Clark PB (1978) Risk factors in calcium stone disease of the urinary tract. Brit J Urol 50:449

[25] Sutton RAL, Walker VR (1994) Enteric and mild hyperoxaluria. Miner electrol Metab 20:352

[26] Williams AW, Wilson DM (1990) Dietary intake, absorption, metabolism and excretion of oxalate. Sem Nephrol 10:2

[27] Wandzilak TR, Williams HE (1990) The hyperoxaluric syndromes. Endocr Metab Clin N Am 19:851

[28] Williams HE, Wandzilak TR (1989) Oxalate synthesis, transport and the hyperoxaluric syndromes. J Urol 141:742

[29] Larsson L, Tiselius HG (1987) Hyperoxaluria. Min Electr Metab 13:242

[30] Menon M, Mahle CJ (1982) Oxalate metabolism and renal calculi. J Urol 127:148

[31] Poore RE, Hurst CH, Assimos DG, Holmes RP (1997) Pathways of hepatic oxalate synthesis and their regulation. Am J Physiol 272:C289

[32] Samuell CT, Kasidas GP (1995) Biochemical investigations in renal stone formers. Ann Clin Biochem 32:112

[33] Wilson DM, Liedtke RR (1991) Modified enzyme-based colorimetric assay of urinary and plasma oxalate with improved sensitivity and no ascorbate interference: Reference values and sample handling procedures. Clin Chem 37:1229

[34] Boer P, Beutler JJ, van Rijn HJM, Berckmans RJ, Koomans HA, Dorhout Mees EJ. Urinary oxalate excretion during intravenous infusion of diuretics in man. Nephron 54:187

[35] Schwille PO, Manoharan M, Rumenapf G, Wölfel G, Berens H (1989) Oxalate measurements in the picomol range by ion chromatography: Values in fasting plasma and urine of controls and patients with idiopathic calcium urolithiasis. J Clin Chem Clin Biochem 27:87

[36] Kasidas GP, Nemat S, Rose GA (1990) Plasma oxalate and creatinine and oxalate/creatinine clearance ratios in normal subjects and in primary hyperoxaluria. Evidence for renal hyperoxaluria. Clin Chim Acta 191:67

[37] Barratt TM, Kasidas GP, Murdoch I, Rose GA (1991) Urinary oxalate and glycolate excretion and plasma oxalate concentrations. Arch Dis Childhood 66:501

[38] Hagen L, Walker VR, Sutton RAL (1993) Plasma and urinary oxalate and glycolate in healthy subjects. Clin Chem 39:134

[39] Hatch M (1993) Oxalate status in stone-formers. Two distinct hyperoxaluric entities. Urol Res 21:55

[40] Wang T, Giebisch G, Aronson PS (1992) Effects of formate and oxalate on volume absorption in rat proximal tubule. Am J Physiol 263:F37

[41] Wang T, Agulian SK, Giebisch G, Aronson P (1993) Effects of formate and oxalate on chloride absorption in rat distal tubule. Am J Physiol 264:F730

[42] Wang T, Egbert AL, Abbiati T, Aronson PS, Giebisch G (1996) Mechanisms of stimulation of proximal tubule chloride transport by formate and oxalate. Am J Physiol 271:F446

[43] Wareing M, Green R (1994) Effects of formate and oxalate on fluid reabsorption from the proximal convoluted tubule of the anaesthesized rat. J Physiol 447:347

[44] Aronson PS (1996) Role of ion exchangers in mediating NaCl transport in the proximal tubule. Kidney Int 49:1665

[45] Aronson PS (1989) The renal proximal tubule: A model for diversity of anion exchangers and stilbene-sensitive anion transporters. Annu Rev Physiol 51:419

[46] Karniski LP, Aronson PS (1985) Chloride/formate exchange with formic acid recycling: A mechanism of active chloride transport across epithelial membranes. Proc Natl Acad Sci USA 82:6362

[47] Karniski LP, Aronson PS (1987) Anion exchange pathways for Cl^- transport in rabbit renal microvillus membranes. Am J Physiol 253:F513

[48] Knickelbein RG, Aronson P, Dobbins JW (1986) Oxalate transport by anion exchange across rabbit ileal brushborder. J Clin Invest 77:170

[49] Knickelbein RG, Dobbins JW (1990) Sulfate and oxalate exchange for bicarbonate across the basolateral membrane of rabbit ileum. Am J Physiol 259:G807

[50] Kuo SM, Aronson PS (1988) Oxalate transport via the sulfate/HCO_3 exchanger in rabbit renal basolateral membrane vesicles. J Biol Chem 263:9710

[51] Löw I, Friedrich T, Burckhardt G (1984) Properties of an anion exchanger in rat renal basolateral membrane vesicles. Am J Physiol 246:F334

[52] Yamakawa K, Kawamura J (1990) Oxalate:OH exchange across rat renal cortical brush border membrane. Kidney Int 37:1105

[53] Murer H, Kinne R. (1980) The use of isolated membrane vesicles to study epithelial transport processes. J Membrane Biol 55:81

[54] Hatch M, Vaziri ND (1991) Segmental differences in intestinal oxalate transport. FASEB J 5:A1138

[55] Hatch M, Freel RW, Vaziri ND (1993) Characteristics of the transport of oxalate and other ions across rabbit proximal colon. Pflügers Arch 423:206

[56] Hatch M, Freel RW, Vaziri ND (1994) Intestinal excretion of oxalate in chronic renal failure. J Am Soc Nephrol 5:1339

[57] Hatch M, Freel RW, Vaziri ND (1994) Mechanisms of oxalate absorption and secretion across the rabbit distal colon. Pflügers Arch 426:101

[58] Lieske CL, Spargo BH, Toback FG (1992) Endocytosis of calcium oxalate crystals and proliferation of renal tubular epithelial cells in a patient with type 1 primary hyperoxaluria. J Urol 148:1517

[59] Mandell I, Krauss E, Millan JC (1980) Oxalate-induced acute renal failure in Crohn's disease. Am J Med 69:628

[60] Morgenroth K, Backmann R, Blaschke R (1968) On the formation of deposits of calcium oxalate in the human kidney in oxalosis. Beitr Path Anat 136:454

[61] Saxon A, Busch GJ, Merrill JP, Franco V, Wilson RE (1974) Renal transplantation in primary hyperoxaluria. Arch Intern Med 133:464

[62] Wharton R, D'agati V, magun AM, Whitlock R, Kunis CL, Appel GB (1990) Acute detoriation of renal function associated with enteric hyperoxaluria. Clin Nephrol 34:116

[63] Kahn SR, Hackett RL (1991) Retention of calcium oxalate crystals in renal tubules. Scann Microsc 5:707

[64] Bruijn WC de, Boevé ER, van Run PRWA, van Miert PPMC, Romijn JC, Verkoelen CF, Cao LC, Schröder FH (1994) Etiology of experimental calcium oxalate monohydrate nephrolithiasis in rats. Scanning Micr 3:541-550

[65] Lieske JC, R Leonard, H Swift, G Toback (1996) Adhesion of calcium oxalate monohydrate crystals to anionic sites on the surface of epithelial cells. Am J Physiol 270:F192

[66] Lieske JC, Leonard R, Toback FG (1995) Adhesion of calcium oxalate monohydrate crystals to renal epithelial cells is inhibited by specific anions. Am J Physiol 268:F604

[67] Lieske JC, Toback FG (1996) Interaction of urinary crystals with renal epithelial cells in the pathogenesis of nephrolithiasis. Sem Nephrol 16:458

[68] Nakagawa Y, Abram V, Parks JH, Lau S-H Kawooya JK, Coe FL (1985) Urine glycoprotein crystal growth inhibitors. Evidence for a molecular abnormality in calcium oxalate nephrolithiasis. J Clin Invest 76:1455

[69] Lieske JC, Coe FL (1996) Urinary inhibitors and renal stone formation. In Kidney stones medical and surgical management. Coe FL, Favus MJ, Pak CYC, Parks JH and Premminger GM (eds), Chapter 3:65

[70] Worcester E (1996) Inhibitors of stone formation. Sem Nephrol 16:474

[71] Kok DJ (1997) Intratubular crystallization events. World J Urol 15:219
[72] Coe FL, Nakagawa Y, Parks JH (1991) Inhibitors within the nephron. Am J Kidney Dis 17:407
[73] Bek-Jensen H, Tiselius H-G (1990) Inhibition of calcium oxalate crystallization by urinary macromolecules. Urol Res 19:165
[74] Handler JS, Perkins FM, Johnson JP (1980) Studies of renal cell function using cell culture techniques. Am J Physiol 238:F1
[75] Kreisberg JI, Wilson PD (1988) Renal cell culture. J Electron Microsc Techn 9:235
[76] Gstraunthaler GJA (1988) Epithelial cells in tissue culture. Renal Physiol Biochem 11:1
[77] Simons K, Fuller SD (1985) Cell surface polarity in epithelia. Ann Rev Cell Biol 1:243
[78] Handler JS (1989) Overview of epithelial polarity. Annu Rev Physiol 51: 729
[79] Hull RN, Cherry WR, Weaver GW (1976) The origin and characteristics of a pig kidney cell strain, LLC-PK_1. In Vitro 10:670
[80] Gausch CR, Hard WL, Smith TF (1966) Characterization of an established line of canine kidney cells (MDCK). Proc Soc Exp Biol Med 122:931
[81] Valentich JD (1981) Morphological similarities between the dog kidney cell line MDCK and the mammalian cortical collecting tubule. Ann NY Ac Sci 372:384

Chapter 2

ABSENCE OF A TRANSCELLULAR OXALATE TRANSPORT MECHANISM IN LLC-PK$_1$ AND MDCK CELLS CULTURED ON POROUS SUPPORTS

CF Verkoelen, JC Romijn, WC de Bruijn[1], ER Boevé, LC Cao, FH Schröder

Department of Urology and [1]AEM-Unit, Clinical Pathological Institute. Erasmus University Rotterdam, The Netherlands

Scanning Microscopy (1993) 7:1031-1040

Abstract

Transepithelial oxalate transport across polarized monolayers of LLC-PK_1 cells, grown on collagen-coated microporous membranes in Transwell culture chambers, was studied in double-label experiments using [^{14}C]-oxalate together with [^{3}H]-D-mannitol as an extracellular marker. The [^{14}C]-labeled glucose analog α-methyl-glucoside (α-MG) was used as functional marker for active proximal tubular sugar transport. Cellular uptake of oxalate and α-MG at both the apical and basolateral plasma membrane was determined. When added to the upper compartment, α-MG was actively taken up at the apical membrane, directed through the cells to the basolateral membrane and transported to the lower compartment, indicating functional epithelial sugar transport by LLC-PK_1 cells. In LLC-PK_1 cells the uptake of α-MG at the apical membrane was approximately 50 times higher than that at the basolateral membrane. In contrast to this active transport of sugar, LLC-PK_1 cells did not demonstrate oxalate uptake either at the apical or basolateral plasma membrane. The apical-to-basolateral (A->B) flux of oxalate in LLC-PK_1 cells was identical to the basolateral-to-apical (B->A) oxalate flux in these cells. Moreover these flux characteristics were similar to those found for D-mannitol, indicating paracellular movement for both compounds. From these data, it is concluded that, under the experimental conditions used, LLC-PK_1 cells do not exhibit a specific transcellular transport system for oxalate.

Introduction

Hyperoxaluria is considered a major risk factor in calcium oxalate (CaOx) urolithiasis [1,2,11,20,21,30]. Amongst idiopathic CaOx stone formers, mild hyperoxaluria is frequently found. It has been postulated that cellular transport defects, located in the epithelium of the gastrointestinal tract and/or in the epithelium of the renal proximal tubule, could lead to increased urinary oxalate concentrations as a result of hyperabsorption from the normal diet and/or enhanced tubular secretion [1,2,10,11,30]. Oxalate is an apparently useless end-product of metabolism. Excretion in the urine seems to be the sole route for its elimination [10,30]. In man [16] as well as in several animal species [23,30], it was demonstrated that tubular secretion is an important

pathway in oxalate excretion. Clearance studies in rats [28] and rabbits [24] indicated that tubular secretion of oxalate takes place in the proximal convoluted tubule but not further down the nephron.

The objective of this paper is to present a tissue culture model system for studying renal tubular oxalate transport and its possible regulation. The system employs a two-compartment culture chamber in which established renal tubular cell lines are grown on polycarbonate collagen-coated permeable supports. Under such conditions, the cells form differentiated polarized monolayers with apical microvilli, apical tight junctions, desmosomes and basolateral infoldings and retain the morphological and functional features of transporting renal epithelia [6,8,9]. Although the same renal epithelial cell lines have been widely used during the last decade to study epithelial transport systems [5], oxalate transport across monolayers cultured on porous supports, has not been published before. The functional integrity of LLC-PK_1 monolayers was assessed in parallel by studying vectorial transport of α-MG, a non-metabolizable probe for the proximal tubular apical sodium-glucose co-transport carrier [12,14,15].

Materials and Methods

Cell lines

Two established renal tubular cell lines, LLC-PK_1 (CRL 1392) and MDCK (strain II), obtained from the American Type Culture Collection (Rockville, MD, USA), were used in this study, at passage numbers 201-230 and 20-30, respectively. The porcine kidney cell line LLC-PK_1 [7], was used as a model for renal proximal tubular epithelium [5,8,9], whereas the Madin-Darby Canine Kidney cell line MDCK [4] is assumed to originate from the cortical collecting duct of the nephron [5,9]. Both cell lines were cultured in Dulbecco's Modified Eagle's Medium (DMEM) supplemented with 10 % fetal calf serum (SANBIO, Uden, The Netherlands), 20 mM Hepes buffer (GIBCO-BRL, UK), 100 IU/ml penicillin and 100 μg/ml streptomycin. Cells were grown in plastic tissue culture flasks at 37^0 C in a humidified atmosphere of 5 % CO_2 in air. Subculturing was performed weekly by use of 0.05% trypsin/0.02% EDTA (GIBCO-BRL, UK).

Transmission Electron Microscopy

For morphological inspection at the ultrastructural level, cells were fixed in 1.5% (v/v) glutaraldehyde in 0.1 M cacodylate/HCL buffer for 1h at 37^0C. After aldehyde fixation, cells were postfixed in 1% (w/v) OsO_4 in the same buffer

system, to which $K_4Fe(CN_6).3H_2O$ was added to a final concentration of 0.05 M, for 1 h at room temperature. Subsequently the cells were routinely dehydrated and embedded in Epon. Ultrathin sections (30-50 nm) were sectioned with diamond knives collected on unfilmed 400 mesh copper grids and inspected in a Zeiss EM 902, transmission electron microscope (Zeiss, Oberkochen, FRG) operating at 80 kV.

Growth on porous filter supports

Transwell cell culture chambers (Costar Transwell-COL, Badhoevedorp, The Netherlands, diameter 24.5 mm, 0.45 μm pore size), containing a collagen-coated transparent microporous membrane were used to obtain monolayers of polarized cells. When placed in a six-well cluster plate, such monolayers separate the culture chamber into two individually accessible compartments, which makes it possible to study directed transcellular solute fluxes and uptake via the apical or basolateral plasma membrane. Cells were seeded at subconfluent density (1-2 x 10^6 cells per insert of 4.71 cm^2), rinsed with phosphate-buffered saline (PBS) the following day and re-fed with fresh culture medium twice a week. Transport and uptake studies were usually performed 9 days after cell seeding.

Transport and uptake studies

Transepithelial fluxes and cellular uptake of [^{14}C]-oxalate or α-[^{14}C]-methyl-glucoside were measured using Transwell cell culture chambers. Such measurements were carried out as dual-label experiments in combination with D-[^{3}H]-mannitol. As this compound is not transported transcellularly, it is generally used as a marker of paracellular leakage in transport flux studies, and a marker for extracellular trapping of radioactive tracers in uptake studies. Prior to use, monolayers were rinsed three times and preincubated for 15 minutes with MOPS-buffer (pH 7.3), containing 119 mM NaCl, 5.3 mM KCl, 6.6 mM Na acetate.$3H_2O$, 0.25 mM $CaCl_2.2H_2O$, 1.3 mM $MgSO_4.7H_2O$, 2.0 mM KH_2PO_4, 6.6 mM $NaHCO_3$ and 9.2 mM sodium morpholinopropane sulfonic acid (MOPS). Incubation buffer volumes were 2600 μl in the lower compartment (facing the basolateral cell membrane) and 1500 μl in the upper compartment (facing the apical cell membrane), as recommended by the supplier in order to avoid differences in hydrostatic pressure. To study transepithelial transport, the following combinations of radiolabelled compounds (final concentration: 50μM in MOPS-buffer each) were added to either the upper or the lower compartment of Transwell culture chambers: [^{14}C]-oxalate (3.7KBq/ml) plus D-[^{3}H]-mannitol (14.8KBq/ml), or α-[^{14}C]-methyl-glucoside (3.7KBq/ml) plus D-[^{3}H]-mannitol (14.8KBq/ml). Tracer-free MOPS-buffer was supplemented to the opposite compartment. Appearance and disappearance of radioactive tracers in both compartments was determined by counting radioactivity in 50μl aliquots from

both compartments in a ß-scintillation counter (Packard) 0, 1, 2, 3 and 4 hours after the start of incubation. Fifty µl aliquots of tracer-free MOPS-buffer were added to keep the hydrostatic pressure unaffected. Prior to performing cellular uptake studies, monolayers were rinsed three times and preincubated for 15 minutes with MOPS-buffer at 37°C. To start the uptake, the buffer was aspirated from either the lower or the upper compartment and replaced by MOPS-buffer containing radioactive tracers. To discontinue uptake at 0, 15, 30 and 60 minutes, the filter insert with monolayer was rapidly (a few seconds) dipped in three successive ice-cold PBS baths. The porous support was cut out from the inserts by a scalpel and transferred to an Eppendorf tube containing 500 µl 1 M perchloric acid (PCA) to extract the radioactive compounds. After two cycles of freezing and thawing, the tubes were centrifuged for 2 minutes at maximum speed in an Eppendorf centrifuge. In this way, > 99% of the radioactivity was extracted from the pellet. From the supernatant 400 µl was used to determine ^{3}H- and ^{14}C-dpms by scintillation counting. The pellet was washed twice with 1 ml 1 M PCA and the dry pellet dissolved in 100 µl 1N NaOH to determine the amount of protein per filter. Protein concentrations were measured using the Bio-Rad protein assay reagent (Bio-Rad Laboratories, Richmond, CA, USA).

Calculation of transepithelial fluxes and cellular uptake

Clearance of solutes from the apical (upper) to the basolateral (lower) compartment (A->B) was calculated by:

$$C_{A\to B}\ (\mu l) = V_L \cdot \frac{L}{U} \qquad (1)$$

where V_L is the volume of the lower compartment (2600 µl). L and U are amounts of radioactivity (dpm/µl) detected after 0, 1, 2, 3 and 4 hours in the lower and upper compartment respectively.

Similarly the B->A clearance was calculated by:

$$C_{B\to A}\ (\mu l) = V_U \cdot \frac{U}{L} \qquad (2)$$

where V_U is the volume in upper compartment (1500 µl).

Assuming that the area of the monolayer is equal to the area of the filter, solute transport fluxes (in pmol/cm^2.min.) could be calculated from equation (1) and (2), using 4.71 cm^2 filter inserts and solute concentrations of 50 μM, according to the formula:

$$Flux = \frac{C\ (\mu l)\ .\ 50\ (pmol/\mu l)}{t\ (minute)\ .\ 4.71\ (cm^2)} \qquad (3)$$

Solute uptake (in fmol/μg protein.min.) by the monolayers after 0, 15, 30 and 60 min. incubation, was calculated from the measured radioactivity (dpm per filter), the specific activity (dpm/fmol) and the amount of protein (μg) per filter, using the formula:

$$Uptake = \frac{dpm}{dpm/fmol\ .\ \mu g\ protein\ .\ t\ (minute)} \qquad (4)$$

Results

Cell morphological studies

In some experiments, filter membranes were selected for cellular ultrastructural inspection. In Fig.1A, a cross-section is shown of MDCK cells, eight days after confluency, as a neat row of unicellular columnar epithelial cells. At the apex, short villi were present. In between the cells, prominent tight junctions and rather small intercellular clefts and some wider clefts at the basal portion of the cells towards the membrane material were visible. Inside the cell cytoplasm was well preserved with numerous lysosomal structures. In Fig.1B, a similar cross-section is shown from the LLC-PK$_I$ cells eight days after confluency. The cells lost their strict unicellular aspect and formed a pseudo-stratified epithelial layer, with apical microvilli which are much longer than those present at the MDCK cell apex. Also in this case, patent tight junctions were observed, though the intercellular clefts were much wider. The cytoplasm was well preserved. Basement membrane material was seen outside the basal cell membrane.

Effect of culture time on transport characteristics of LLC-PK$_I$ monolayers

Mannitol fluxes, measured daily in four hour flux experiments, reached a stable level within two days after seeding the cells at subconfluent density

(1-2 x 10^6 cells/filter). In contrast, the A->B transport of α-MG increased with days in culture, attaining a maximal value after 9-11 days (Fig.2). Apparantly this time in culture is needed by these monolayers to fully develop their transport capacity. Based on this observation, all further transport and uptake studies were performed 9-11 days after seeding the cells at subconfluent density. The integrity of the monolayer was monitored morphologically by phase-contrast light microscopy and functionally by determining the D-[^{3}H]-mannitol flux.

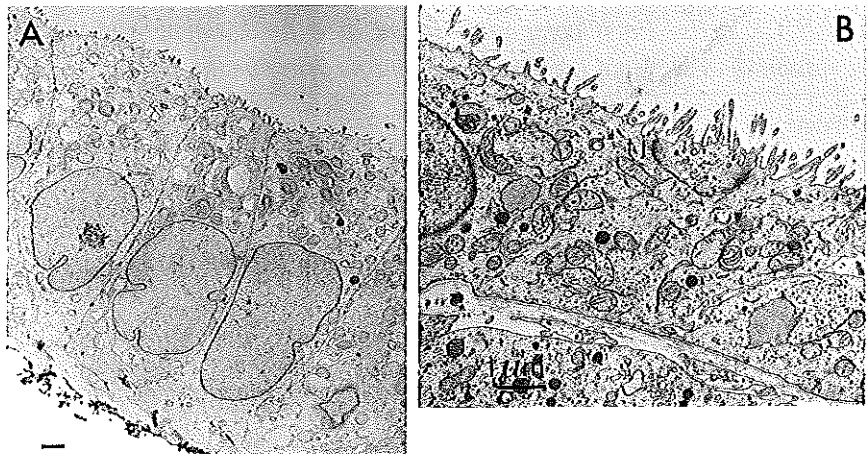

Fig.1 Transmission electron microscopic (TEM) image of MDCK (A) and LLC-PK$_1$ (B) cells cultured on porous supports.

Transport and uptake of α-methyl-glucoside

Monolayers of LLC-PK$_1$ cells exhibited vectorial transport for α-MG: the mean A->B α-MG flux (38.6 pmol/cm^2.min), as measured in the four-hour flux experiments, was 7 times higher (Table 1) than the mean B->A flux (5.5 pmol/cm^2.min.). In contrast, MDCK cells did not demonstrate vectorial α-MG transport in either direction (Table 1). Similar results were obtained with respect to intracellular uptake of α-MG. The uptake of α-MG at the apical membrane proceeded linearly with time for at least 60 min (Fig.3). Although the uptake at the basolateral membrane also increased with time, the level of uptake (9.3 fmol/μg protein.min.) was approximately 50 times lower than the uptake at the apical membrane (452 fmol/μg protein.min.) and may represent B->A leakage followed by apical uptake (Table 3). Fluxes of mannitol across LLC-PK$_1$ monolayers, presumed to be paracellular, were low and similar in both directions (Table 1). The apparent uptake of mannitol was

very low, non-directional (Tables 3 and 4) and independent of time (Fig.3) reflecting non-specific trapping of tracer. These results show that LLC-PK_1 cells, under the experimental conditions used, retained the capacity for directed α-MG transport. In contrast, experiments performed with MDCK cells demonstrated that this cell line did not possess a transport system for α-MG (Tables 1 and 3).

Table 1. *Transport fluxes of α-methyl-glucoside and mannitol in pmol/cm^2.min across 9 days cultured polarized monolayers of LLC-PK_1 and MDCK cells. Each compound added at a final concentration of 50 μM. Mean $\pm$ S.D. from three independent measurements.*

Transport Flux (pmol/cm^2.min)	LLC-PK_1		MDCK	
	α-MG	mannitol	α-MG	mannitol
apical-to-basolateral	38.6 $\pm$ 5.1	9.6 $\pm$ 3.4	1.2 $\pm$ 0.1	1.6 $\pm$ 0.1
basolateral-to-apical	5.5 $\pm$ 1.0	9.4 $\pm$ 2.5	1.5 $\pm$ 0.1	1.7 $\pm$ 0.2

Table 2. *Transport fluxes of oxalate and mannitol in pmol/cm^2.min across 9 days cultured polarized monolayers of LLC-PK_1 and MDCK cells. Each compound added at a final concentration of 50 μM. Mean $\pm$ S.D. from three independent measurements.*

Transport Flux (pmol/cm^2.min)	LLC-PK_1		MDCK	
	oxalate	mannitol	oxalate	mannitol
apical-to-basolateral	8.3 $\pm$ 2.3	8.0 $\pm$ 2.2	2.1 $\pm$ 0.5	1.7 $\pm$ 0.5
basolateral-to-apical	12.1 $\pm$ 2.8	10.2 $\pm$ 2.3	1.9 $\pm$ 0.2	1.2 $\pm$ 0.1

Transport and uptake of oxalate

Particle size measurements in a Coulter Multisizer II (Coulter Electronic Ltd, Luton, UK) demonstrated that using 50 μM oxalate, which was the final oxalate concentration during the transport experiments, the solubility product of calcium oxalate was not exceeded in the presence of 0.25 mM $CaCl_2$, a constituent of the incubation buffer. This implies that ionized oxalate was present under such conditions. Transport fluxes of oxalate across monolayers of LLC-PK_1 cells in either direction (A->B: 8.3 and B->A: 12.1 pmol/cm^2.min), were not significantly different from transport fluxes of mannitol (A->B: 8.0 and B->A: 10.2 pmol/cm^2.min) within the same experiment (Table 2).

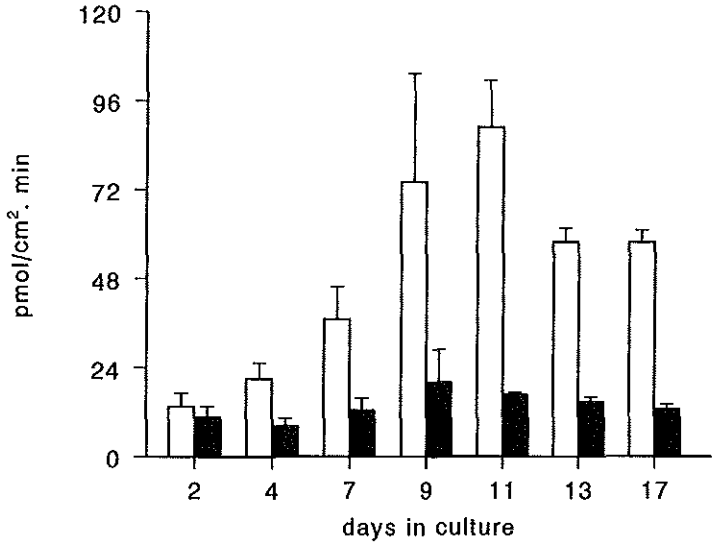

Fig.2 A->B transcellular α-methyl-glucoside transport capacity across LLC-PK_1 monolayers in time. The cells were plated on microporous membranes at subconfluent densities on day "0". Solute flux experiments were performed using α-[^{14}C]-methyl-glucoside (open bars) and D-[^{3}H]-mannitol (closed bars), added to the apical compartment. After each transport experiment the monolayers were rinsed extensively with PBS to remove radiolabeled tracers, re-fed with fresh DMEM and the experiments were repeated with the same monolayers every two or three days during a time period of 17 days. Bars represent means ± S.D. from three individual cell culture chambers.

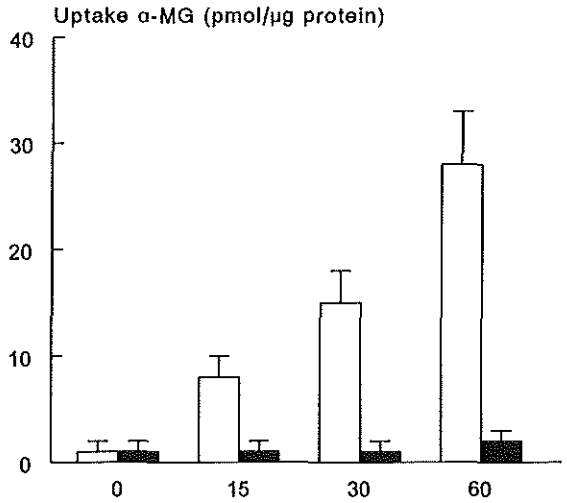

Fig.3. Apical uptake of α-[^{14}C]-methyl-glucoside (open bars) and D-[^{3}H]-mannitol (closed bars) in LLC-PK$_1$ cells grown as monolayers on microporous membranes, after 9 days in culture. Each time point represents the mean ± S.D. of three independent determinations in pmol/μg protein.

Flux measurements using filters without cells showed that radioactively labelled compounds were evenly distributed over both compartments after about four hours following addition to one of the compartments. When filters were covered with LLC-PK$_1$ monolayers, equal distribution of oxalate and mannitol was achieved after approximately 20 hours. No accumulation of oxalate in any of the compartments was observed upon longer incubation, in contrast to α-MG that was transported against its concentration gradient. Hence, the equilibration of oxalate over the two compartments was retarded by the cellular barrier compared to the equilibration rate observed through filters without cells, but reflected passive diffusion. Moreover, the uptake of oxalate by LLC-PK$_1$ cells from either compartment (apical = 1.01 and basolateral = 1.31 fmol/μg protein.min.), was in the same low range as values found for the extracellular marker D-mannitol (apical = 0.87 and basolateral = 1.75 fmol/μg protein.min., Table 4).

Table 3. Uptake of α-methyl-glucoside compared to the extracellular trapping of mannitol in fmol/μg protein.min in 9 days cultured polarized monolayers of LLC-PK$_1$ and MDCK cells. Each compound added at a final concentration of 50 μM. Mean ± S.D. of three independent measurements.

Uptake fmol/ μg protein.min	LLC-PK$_1$		MDCK	
	α-MG	mannitol	α-MG	mannitol
apical	452 ± 80	2.1 ± 0.50	0.93 ± 0.03	0.63 ± 0.12
basolateral	9.3 ± 0.90	1.3 ± 0.10	0.48 ± 0.05	1.15 ± 0.10

Table 4. Uptake of oxalate compared to the extracellular trapping of mannitol in fmol/μg protein.min in 9 days cultured polarized monolayers of LLC-PK$_1$ and MDCK cells. Each compound added at a final concentration of 50 μM. Mean ± S.D. of three independent measurements.

Uptake fmol/ μg protein.min	LLC-PK$_1$		MDCK	
	oxalate	mannitol	oxalate	mannitol
apical	1.01 ± 0.07	0.87 ± 0.12	1.21 ± 0.18	0.69 ± 0.13
basolateral	1.31 ± 0.30	1.75 ± 0.13	1.18 ± 0.12	1.57 ± 0.41

Experiments performed with higher concentrations of oxalate (up to 500 μM) together with lower concentrations of calcium (down to 100 μM) in order not to exceed the solubility product, did not result in significant oxalate uptake by these cells either. Uptake experiments performed with MDCK cells resulted in uptake patterns for oxalate and mannitol that were similar to those found for LLC-PK$_1$ cells (Table 3 and 4). Although the level of paracellular leakage among both cell lines differed, the extracellular trapping of mannitol, as determined in the uptake experiments, was of the same order of magnitude in both cell lines.

Discussion

The present data demonstrate that LLC-PK_1 monolayers were unable to take up oxalate from either the apical or the basolateral membrane and, as a consequence, to mediate active transcellular oxalate transport. In contrast, similar monolayers developed active sugar uptake at the apical plasma membrane within the same time period. Since A->B directed sugar transport (reabsorption) is a well documented characteristic of renal proximal tubular cells [12,15], this result indicates the functional integrity of LLC-PK_1 monolayers under the conditions used. In accordance with their renal cortical collecting duct origin, monolayers of MDCK cells did not show to possess transcellular α-MG or oxalate transport capacity in either direction.

The absence of oxalate transport in the LLC-PK_1 cell line is in contrast to the findings of Wandzilak et al. [27], who recently reported uptake of oxalate by this cell line. The authors claim that oxalate uptake was dependent on the buffers used. Uptake of oxalate was found to occur in Na-gluconate or mannitol buffers to a much greater extent than in PBS or Earl's Salt Solution. We repeated some uptake experiments with Na-gluconate buffer and found that the presence of this buffer resulted in disruption of tight junctions and subsequent loss of epithelial polarity. The amount of radioactive tracers in the monolayer was slightly increased in time not only for oxalate but also for mannitol, indicating non-specific uptake in this buffer. Na-gluconate buffer is often used to study isolated cell membranes, which in contrast to viable cells [3,9,12-15,17-19] or tissues [22,24,28], do not require physiological conditions. In addition, Sigmon et al. [25] demonstrated uptake of oxalate in suspensions of rat renal cortical and papillary cells, using a buffer (Krebs-Ringer Bicarbonate) very similar to our buffer, indicating that cellular oxalate uptake is not necessarily prevented in the presence of this buffer.

According to our experiments, the absence of a transcellular oxalate transport system at the basolateral plasma membrane of LLC-PK_1 cells can be explained in several ways. Firstly, dedifferentiation processes as a result of genetic drift during culture of immortal cell lines may have led to loss of certain cellular properties [9], including the ability to transport specific compounds. Despite the fact that the LLC-PK_1 cell line exhibits various transport systems, it appears to lack others [12,19]. Another possibility is that oxalic acid is transported by the paracellular shunt pathway. This permeation pathway, controlled by a number of

determinants such as pH, the passage of current, osmotic loads, calcium concentration, cytoskeletal function [23] and surface charge [29], selectively regulates the passive diffusion of ions and small water-soluble solutes. In so-called "leaky" epithelia, like the epithelium of the renal proximal tubule, passive movement of ions is predominantly via the paracellular route [23]. It is conceivable that alterations in determinants that control the paracellular flux could result in a renal leak for oxalate and consequently lead to hyperoxaluria. Interestingly, LLC-PK_1 monolayers showed a six times higher mannitol flux than MDCK monolayers (Table 1 and 2). This observation is in agreement with the more leaky, low-resistance paracellular pathway in proximal tubular epithelium (LLC-PK_1) compared to tighter epithelium of distal parts of the nephron (MDCK).

Finally, the possibility exists that the cell lines used in this investigation are the descendants of tubular cells devoid of any specific oxalate transport system. Oxalate secretion is most probably restricted to a specific portion of the renal proximal tubule. It is difficult to pinpoint the exact original location of established renal cell lines and assignment of their origin is principally based on the observed properties. LLC-PK_1 cells exhibit apical sodium-dependent transport systems for sugars, amino acids and phosphate, and basolateral sodium-dependent neutral amino acid and inorganic phosphate transport systems [5] as well as a sodium-independent 3-O-methylglucose transport mechanism [13]. Such transport systems are indicative of renal proximal tubular epithelium. More specifically LLC-PK_1 cells demonstrate properties, like anion-selective occluding junctions [3,17,18] and the bioenergetics of Na^+-coupled glucose transport [5], that correspond to those observed in the pars recta (S3-segment) of the proximal tubule [26]. Using intratubular microinjection, free-flow micropuncture, and droplet precession techniques, Weinman et al. [28] demonstrated that oxalate secretion is located predominantly in the early portions (S1, S2-segments) of the proximal convoluted tubule of the rat. This location of oxalate secretion was confirmed by clearance and microperfusion studies in isolated segments of renal proximal tubule of the rabbit [24]. No significant oxalate transport seemed to occur in segments of the nephron beyond the proximal convoluted tubule in these species. Micropuncture studies of tubular transport in the pig kidney demonstrated that para-amino hippurate (PAH), the more traditional marker for renal proximal tubular organic acid transport, is secreted in the S2-segment of the proximal

convoluted tubule and not in the pars recta [22]. Pig kidney derived LLC-PK_1 cells lack the probenecid sensitive Na^+-dependent PAH transport system, suggesting that LLC-PK_1 originates from the pars recta, a segment that is possibly not involved in oxalate secretion.
In conclusion, the results of this study demonstrate that a specific oxalate transport system is missing in LLC-PK_1 cells. Unless it appears that oxalate transport is predominantly regulated by the paracellular shunt pathway, the characterization of renal oxalate handling will require other sources of renal proximal tubular cells, capable of transcellular oxalate transport. Irrespective of species (rats, rabbits and possibly pigs), the early proximal convoluted tubular part of the nephron (S1, S2-segments) seems to be the most promising region to find epithelial cells that are involved in the secretion of oxalate. Therefore we will continue our efforts to determine and characterize renal oxalate secretory transport mechanisms by focusing our attention on the development of techniques to isolate and establish renal cell types, originating from specific segments of the nephron [9].

This study was supported by the Dutch Kidney Foundation through grant C 92.1235. The authors wish to thank Dr. W.G. Robertson from the King Faisal Specialist Hospital and Research Centre in Riyadh, Saudi Arabia, for helpful discussions.

References

[1] Baggio B, Gambaro G, Marchini F, Cicerello E (1984) Raised transmembrane oxalate flux in red blood cells in idiopathic calcium oxalate nephrolithiasis. The Lancet 7:12

[2] Borsatti A (1991). Calcium Oxalate nephrolithiasis: defective oxalate transport. Kidney Int 39:1283

[3] Bosch L Van Den, De Smedt H, Borghgraef R (1991) Influence of PMA and a low extracellular $Ca2^+$ concentration on the development of the Na^+-dependent hexose carrier in LLC-PK_1 cells. Biochim Biophys Acta. 1092:244

[4] Gausch CR, Hard WL, Smith TF (1966) Characterization of an established line of canine kidney cells (MDCK). Proc Soc Exp Biol Med. 122:931

[5] Gstraunthaler GJA (1988) Epithelial cells in tissue culture. Renal Physiol Biochem 11:1

[6] Handler JS (1989) Overview of epithelial polarity. Annu Rev Physiol 51:729

[7] Hull RN, Cherry WR, Weaver GW (1976) The origin and characteristics of a pig kidney cell strain, LLC-PK_1. In Vitro 10:670

[8] Ip TK, Aebischer P, Galletti PM (1988) Cellular control of membrane permeability. Implications for a bioartificial renal tubule. Trans Am Soc Artif Intern Organs 34:351

[9] Kreisberg JI, Wilson PD (1988) Renal cell culture. J Electron Microsc Techn 9:235

[10] Menon M, Mahle CJ (1982) Oxalate metabolism and renal calculi. J Urol 127:148

[11] Menon M, Koul H (1992) Calcium oxalate nephrolithiasis. J Clin Endocrin Metab 74:703

[12] Miller JH (1992) Sodium-sensitive, probenecid-insensitive p-aminohippuric acid uptake in cultured renal proximal tubule cells of the rabbit. Soc Exp Biol Med 199:298

[13] Mullin JM, Kofeldt LM, Russo LM, Hagee MM, Dantzig AH (1992) Basolateral 3-O-methylglucose transport by cultured kidney (LLC-PK_1) epithelial cells. Am J Physiol 262:F480

[14] Mullin JM, Fluk L, Kleinzeller A (1986) Basal-lateral transport and transcellular flux of methyl α-D-glucoside across LLC-PK_1 renal epithelial cells. Biochim Biophys Acta 885:233

[15] Mullin JM, McGinn MT, Snock KV, Kofeldt LM (1989) Na^+-independent sugar transport by cultured renal (LLC-PK_1) epithelial cells. Am J Physiol 257:F11

[16] Oswald H, Hautman R (1979) Renal elimination kinetics and plasma half-life of oxalate in man. Urol Int 34:440

[17] Rabito CA (1986) Occluding junctions in a renal cell line (LLC-PK_1) with characteristics of proximal tubular cells. Am J Physiol 250:F734

[18] Rabito CA (1986) Reassembly of the occluding junctions in a renal cell line with characteristics of proximal tubular cells. Am J Physiol. 251:F978

[19] Rabito CA, Karish MV (1982) Polarized amino acid transport by an epithelial cell line of renal origin (LLC-PK_1). J Biol Chem 257:6802

[20] Robertson WG, Peacock M, Heyburn PJ, Marshal DH, Clark PB (1978) Risk factors in calcium stone disease of the urinary tract. British J Urol 50:449

[21] Robertson WG, Peacock M (1980) The cause of idiopathic calcium stone disease: hypercalciuria or hyperoxaluria? Nephron 26:105

[22] Roch-Ramel F, White F, Vowles L, Simmonds HA, Cameron JS (1980) Micropuncture study of tubular transport of urate and PAH in the pig kidney. Am J Physiol 239:F107

[23] Schneeberger EE, Lynch RD (1992) Structure, function, and regulation of cellular tight junctions. Am J Physiol 262:L647

[24] Senekjian HO, Weinman EJ (1982) Oxalate transport by proximal tubule of the rabbit kidney. Am J Physiol 243:F271

[25] Sigmon D, Kumar S, Carpenter B, Miller T, Menon M, Scheid C (1991) Oxalate transport in renal tubular cells from normal and stone-forming animals. Am J Kidney Dis 17:376

[26] Tisher CC, Madsen KM (1991) Anatomy of the kidney. In: The Kidney. Brenner BM, Rector FC (eds), WB Saunders Company, Philadelphia, Chapter I, pp 3

[27] Wandzilak TR, Calo L, Andre SD, Williams HE (1992) Oxalate transport in cultured porcine renal epithelial cells. Urol Res 20:341

[28] Weinman EJ, Frankfurt SJ, Ince A, Sansom S (1978) Renal tubular transport of organic acids. Studies with oxalate and para-aminohippurate in the rat. J Clin Invest 61:801

[29] Weinstein SW, Jones SM, Weinstein RJ (1989) Evidence that alteration of charge modifies proximal tubular shunt pathway permselectivity. Am J Physiol 257:F1079

[30] Williams HE, Wandzilak TR (1989) Oxalate synthesis, transport and the hyperoxaluric syndromes. J Urol 141:742

Discussion with Reviewers

A.P. Soler: The clinical importance of the paper requires some comments on the doses of oxalate used in the assays. Also, it will be necessary to add data and references in relation to normal and pathological plasma and urinary values of oxalate. Furthermore, I would like to know if it is possible that some oxalate transport might occur in the presence of very high urinary levels of the molecule? Could it exist a very low affinity cellular transport system?

Authors: The average serum oxalate concentration is 1-2 μM [30,32]. Mean values of 24-h excretion of oxalate are 350 $\pm$ 10 μmol (n = 60) in normal subjects and 430 $\pm$ 20 μmol (n = 65) in recurrent stone-formers [21]. The concentration profile of oxalate along the nephron as determined by Hautman and Oswald showed a gradual increase from 1 μM in Bowman space up to 300 μM in the final urine [32]. Routinely, our transport studies were performed with 50 μM oxalate. Experiments

performed with much higher oxalate concentrations up to 500 μM, or much lower oxalate concentrations down to 1 μM, never resulted in cellular uptake of radioactive labeled oxalate, which makes the existence of any oxalate transport system in these cells unlikely.

R.L. Hackett: Oxalate, 500 μM, when incubated with DMEM with or without 10% fetal calf serum in the presence or absence of cells will form calcium oxalate crystals. Did you check your medium for presence of crystals when using oxalate at that concentration? Alternatively, what is the effect on cell function when cells are incubated with the reduced levels of calcium you utilized to avoid crystal formation?
Authors: The transport studies were performed in MOPS-buffer and not in DMEM. To study possible oxalate uptake under extreme conditions, we performed a small number of experiments using varying amounts of oxalate and calcium. In these experiments, care was taken that the solubility product for CaOx was not exceeded. Short-term incubations in the presence of the lowest calcium concentration used in this study (100μM) did not lead to morphological or functional changes of the monolayers.

Reviewer V: This paper presents evidence that LLC-PK1 cells in culture do not transport oxalate, which appears to be in opposition to a 1992 study from Dr. Williams' research group. Explanation is offered as to why the current data is different, but the arguments are not compelling. The primary concern about the manuscript is the observation that these cells do not transport oxalate. Although many negative observations form the basis for significant publications, the current data should be part of a larger investigation defining exactly why oxalate transport was not observed and in what cells in this segment of the nephron oxalate transport is observed, i.e. a comparitive study with some positive as well as negative observations.
Authors: To our opinion this manuscript provides a constructive contribution to study oxalate transport in functional renal tubule epithelia in culture. As indicated in the discussion, this study will be part of a larger investigation and hopefully we will be able to present more positive observations in the near future.

J. Kavanagh: Even if the structural integrity of the monolayer is not well preserved in gluconate buffer, Wandzilak et al. seem to have demonstrated active uptake of oxalate by LLC-PK_1 (and MDCK) cells. Could the differences in the buffers used explain the absence of transport in your system and was the pH controlled by MOPS or MES/Tris when you tested the gluconate buffer?
Authors: The use of (MES/Tris buffered) Na-gluconate buffer not only resulted in the loss of epithelial polarity but also led to the apparent intracellular uptake of the extracellular marker mannitol. This indicates gluconate-buffer induced cell damage, which was confirmed by microscopical studies.

J. Kavanagh: Were other salts present which could affect the ionized oxalate concentration or inhibit active transport?
Authors: The transport experiments in this study were performed in MOPS-buffer containing physiological salt concentrations. It is known that anion exchange mechanisms exist in the proximal tubule [31]. Recently it has been suggested that the presence of chloride ions may negatively influence oxalate transport in proximal tubular cells (H Koul, personal communication). However, the biological significance of oxalate transport inhibited by physiological concentrations of other anions remains to be determined. When we succeed to establish primary cultures of renal tubular cells exhibiting oxalate transport, we will study stimulating and inhibiting effects of anion gradients (Cl^-, HCO_3^-).

R.L. Hackett: Your evidence that oxalate flux did not involve a transcellular pathway was based only on a comparison with mannitol flux. Did you poison anion transport systems, as did Sigmon et al, in order to demonstrate the absence of an active transporter?
Authors: Since the values measured for oxalate "transport flux" and "uptake" did not significantly exceed background levels (assessed with radiolabelled mannitol) in any of our experiments, it was not considered relevant to apply anion-exchange inhibitors such as disulfonic stilbenes (SITS, DIDS).

R.L. Hackett: MDCK cells at 9-10 days post-seeding begin to demonstrate morphological evidence of regressive changes. Would you comment on that in relation to your transport studies?
Authors: Compared to monolayers cultured on tissue culture plastics, monolayers cultured on microporous membranes can be maintained much longer without loss of morphological or functional integrity. LLC-PK_1 cells cultured on microporous membranes have been maintained in culture for up to 28 days without loss of glucose transport capacity [8].

A.P. Soler: The data in Table 3 showing the apical and basolateral uptake of αMG in LLC-PK1 cells, contradict the results of previous works, demonstrating the absence of basolateral αMG uptake in this cell line. One possible explanation for this could be that the relatively high values observed don't represent the basolateral uptake of αMG by LLC-PK_1 cells, but rather a "re-uptake" of αMG from the apical surface of the cells after a paracellular diffusion of the molecule.
Authors: We also assumed that the basolateral uptake of αMG in LLC-PK_1 cells was the result of initial apical-to-basolateral diffusion and referred to this possibility in the Results section when describing Table 3.

C.A. Rabito: I think there is a conceptual error in the role of the paracellular pathway in the transepithelial transport of oxalate as presented in the discussion. In the absence of active secretion, there should be a net reabsorption and no secretion of oxalate along the proximal tubule. The isotonic fluid reabsorption that occurs along the proximal tubule (and that amount to 85% of the total glomerular filtrate) will increase the concentration of oxalate in the tubular fluid and allow its diffusion (reabsorption) to the blood side of the epithelium. It is only a large reduction and not increase in the permeability of the occluding junctions to oxalate that may explain the presence of hyperoxaluria in absence of active oxalate secretion.
Authors: The expression "renal leak" as depicted in the discussion, emphasizes increased urinary excretion of oxalate. We subscribe the postulation that only a decrease in the permeability of the occluding junctions of proximal tubular epithelium could result in enhanced amounts of oxalate excreted into the urine.

C.A. Rabito: The absence of transepithelial oxalate transport in LLC-PK_1 cells comes not as a suprise since most if not all the characteristics of this cell line correspond to the S3 segment of the renal proximal tubule and this nephron segments lack of an specific oxalate secretion system. The significance of this meticulous paper, however, resides in the fact that it contradicts the results obtained by Wandzilak et al. in the same cell line with a less rigorous technique. Whereas the difference may merely represent technical differences (as discussed in this paper) other possibilities such as difference in cell lineage, difference in passage number, etc. should also be considered. For instance, we have isolated from the original LLC-PK_1 cell provided by ATCC at least two different clones designated LLC-PK_{1A} and LLC-PK_{1B4}. These two clones show totally different properties with reference to their Na^+-dependent sugar transport system and Na^+-H^+ exchange system. Also it is well known that the transport characteristics of different renal epithelial cell lines change with the number of passages in culture.

Authors: We cannot exclude the possibility that some of the characteristics of the LLC-PK_1 cells used in our studies are not identical to those used by Wandzilak et al. However, as discussed, we consider it more likely that the segmental origin of the LLC-PK_1 cells accounts for the observed lack of oxalate transport. The recognition that these cells probably descend from the S3 segment of the renal proximal tubule encouraged us to develop techniques to establish in vitro primary cultures of defined proximal cells. As a matter of fact attempts to isolate and culture S1,S2 cells of rat renal proximal tubuli were recently initiated in collaboration with Prof MF Horster from the Physiological Institute of the University of Munich [33].

Additional References

[31] Aronson PS (1989) The renal proximal tubule: A model for diversity of anion exchangers and stilbene-sensitive anion transporters. Annu Rev Physiol 51:419

[32] Hautman R, Osswald H (1983) Concentration profiles of calcium and oxalate in urine, tubular fluid and renal tissue: Some theoretical considerations. J Urol 129:433

[33] Horster MF, Sone M (1990) Primary culture of isolated tubule cells of defined segmental origin. Methods-Enzymol 191:409

Chapter 3

LLC-PK$_1$ CELLS AS MODEL SYSTEM TO STUDY PROXIMAL TUBULE TRANSPORT OF WATER AND OTHER COMPOUNDS RELEVANT FOR RENAL STONE DISEASE

CF Verkoelen, DJ Kok, BG van der Boom,
[1]HR de Jonge, FH Schröder and JC Romijn.

Departments of Urology and [1]Biochemistry.
Erasmus University Rotterdam, The Netherlands

Accepted for publication in Urological Research

Abstract

$LLC\text{-}PK_1$ cells were cultured on a permeable support in a two compartment culture system. Confluent monolayers received an ultrafiltrate-like solution at the apical side and a plasma-like solution at the basolateral side. The distribution of various solutes, including phosphate, calcium, and oxalate over both compartments was measured in time. The transport of water was monitored by alterations in fluid concentrations of radiolabeled inulin. Bicarbonate, glucose, and phosphate were transported rapidly from the apical to basolateral side of the monolayer. Sodium and chloride were reabsorbed without major consequences for the osmolality in the apical and basal fluid. Calcium and potassium were also reabsorbed, but to a smaller extent than sodium. The luminal concentration of oxalate gradually increased to values that were at least three times higher (12.0 ± 0.4 μmoles/l) than those in the contraluminal fluid (3.8 ± 0.1 μmoles/l. However, since the luminal rise of oxalate completely matched the rise of inulin in the apical fluid this appeared to be the passive consequence of active water reabsorption rather than of net directed oxalate transport. The $LLC\text{-}PK_1$ model could prove useful to study the regulation of proximal tubule water transport and its effect on luminal stone salt concentrations under different physiological conditions.

Introduction

Calcium oxalate and phosphate salts are extremely poorly soluble in biological fluids. In renal tubular fluid their concentration products easily exceed the value needed for spontaneous crystal formation. Although these crystals by themselves are not necessarily harmful, because they normally are eliminated with the urine, their possible retention could ultimately lead to the formation of a renal stone [11,12,13,17,29,30,31]. Causes for retention may be formation of crystals inside the nephron at an abnormal site, in abnormal numbers or with abnormal sizes and aberrant interactions between crystals and the epithelial cells lining the renal tubules [11-14,29]. The first event in stone development probably is the precipitation of calcium phosphate crystals in the Limb of Henle. This is followed by calcium oxalate crystallization in the distal tubule and collecting ducts, whereby previously formed calcium phosphate crystals may act as a heterogenous nucleator [11,12,16]. The first crystallization step is sensitive to variations

in the concentration of calcium and phosphate at the end of the proximal tubule, the latter is sensitive to calcium and oxalate concentrations and pH in the distal tubule and collecting ducts [12,13,16,27,28]. Most filtered phosphate is actively reabsorbed in the proximal tubule. Factors that influence phosphate reabsorption include the amount of filtered phosphate, dietary intake, the level of ionized calcium and acid-base status [25]. Also the bulk of filtered calcium is reabsorbed in the proximal tubule. Calcium transport is primarily passive in this segment of the nephron and is influenced by the amount of filtered calcium, dietary calcium and phosphate intake, calcium complexation in the tubular fluid, defects in sodium and water reabsorption, and acid-base status [25]. No recent data are available for site specific oxalate handling in the kidney. This information is important given the impact that, due to the high calcium to oxalate ratio in the tubular fluid, relatively small changes in oxalate concentrations have on the level of urinary calcium oxalate supersaturation [20]. Taken together, proximal tubular handling of water, calcium, phosphate and oxalate is an important variable determining the risk of crystal formation in the nephron. The question is whether abnormalities in this handling can explain the formation of too many and too large particles as witnessed in recurrent stone former urines [17]. Such abnormal proximal tubule functions may not be apparent in the final collected urine, since processes occuring in late nephron parts will counteract them to guard overall homeostasis [25]. On a 24-h basis, the values for calcium, phosphate and oxalate excretion in idiopathic stone formers do not differ much from those in non-stone formers. Mean urinary oxalate values, for example, may be slightly increased but the ranges largely overlap [10,20,22,26]. However, the combination of high normal excretions of these stone salts do give significantly increased levels of tubule fluid supersaturation [4,27]. In addition, transient differences in solute concentrations which may result from proximal tubule dysfunction have been reported. After an oxalate load, oxalate is excreted rapidly in the urine and with high peaks [18], but the peaks are higher in stone formers [8] and also urinary phosphate levels are higher in postprandial urine of stone forming individuals [23,24]. In view of these data, transport functions of the proximal tubule are of interest for idiopathic calcium stone formation. In the present study, we have investigated proximal tubule transport in LLC-PK_1 cells, a cell line that has retained in culture many of the characteristics of the mammalian proximal tubule [9,19] Although this cell line has extensively been used to study transport, as far as we know, our approach to study the reabsorption of

water was not reported earlier, especially not in relation to its effect on luminal stone salt concentrations. The alterations in the composition of the luminal fluid are interpreted in the light of crystallization risks in the nephron.

Materials and methods

LLC-PK_1 cells were seeded at a high density ($1x10^6$ cells/4.52 cm^2) on permeable supports in a two compartment culture system (Transwell-clear polyester membrane, Costar Badhoevedorp, The Netherlands). Transport experiments were performed 8-9 days post-seeding. Earlier we demonstrated that this time is needed for the development of functional LLC-PK_1 monolayers [32]. Fresh culture medium, Dulbecco's modified MEM (DMEM, Gibco BRL, Paisley, UK) supplemented with 10% fetal calf serum (FCS) was added to the cells every other day. To study solute transport, DMEM supplemented with 10 mM HEPES, pH 7.4, but without serum, representative for ultrafiltrate, was applied to the apical compartment, whereas DMEM, 10 mM HEPES, pH 7.4, supplemented with 10% FCS, resembling the peritubular fluid, was applied to the basal compartment. The osmolality of both solutions was approximately 335 mosmol/kg. The initial volumes in the apical and basal compartment were 1500 and 2600 μl, respectively. These volumes were chosen such that artificial fluid movement, caused by hydraulic pressure differences and unrelated to cellular processes, was prevented as much as possible. Fluid from both compartments was collected after 24 and 48 h for the determination of the various solutes. In another series of experiments 0.1 μCi/ml [^{14}C]oxalate (final concentration 5 μM) or 0.1 μCi/ml [^{14}C]-labeled α-methylglucoside (αMG, a non-metabolizable glucose-analog) in a final concentration of 1 mM were applied to both compartments and their distribution measured in time (radioactively labeled compounds obtained from Amersham Int., Buckinghamshire, UK). In addition, the transepithelial transport of water (J_v) was monitored using radiolabeled inulin ([^{3}H]inulin). Since the monolayers are practically impermeable for relatively large molecules such as inulin, alterations in [^{3}H]inulin concentrations are indicative for the transepithelial movement of water. The apical and basal compartment both received 5 μCi/ml [^{3}H]inulin. To determine fluid transport (J_v), a 100 μl aliquot was taken from the apical and basal fluid at different time points and counted in a ß-scintillation counter. The volume (V_t) in μl is calculated as follows: $V_t = dpm_0 . V_0/dpm_t$, in which dpm_t = dpm/100μl at t, V_0 is the initial volume in μl, and dpm_0 is the amount of radioactivity per 100μl at the start of the experiment. Fluid transport (J_v) in μl/h.cm^2 is than calculated by: $J_v = (V_0 - V_t).(t.A)^{-1}$, in which t= time (h) and A = the area of the filter inserts (4.52 cm^2). It should be noticed that the relatively long incubation times (24 and 48 h) in this study were required to

measure water transport-induced alterations in fluid [^{3}H]inulin concentrations. To avoid fluid evaporation as much as possible during this period, the studies were performed in a humidified atmosphere and care was taken that the incubator was opened only for sampling. The various solute concentrations and osmolality were measured by standard clinical chemical methods. The measured solute concentrations can be interpreted in several ways. The change in apical concentration will bear relevance to the risk for crystal formation and retention. Alterations in absolute amounts in a compartment, obtained by multiplying the concentration of a solute with the volume at a given time, are indicative for net reabsorption or secretion. Changes in the absolute amounts of the apical plus basal compartment indicate net production or metabolism. To compare our findings with *in vivo* data, the apical fluid concentration at a certain time point (AF_t) to initial apical fluid (AF_0) concentration ratio is calculated (AF_t:AF_0) in analogy to tubular fluid to ultrafiltrate concentration ratio (TF:UF) [25].

Results

Solute concentrations

The concentrations of sodium and chloride in both compartments did not change much during the complete course of the experiment (Table 1). The AF_t:AF_0 concentration ratio's for sodium and chloride are slightly increased from 1.0 at t=0 to 1.05 and 1.11, respectively after 48h, which most likely is explained by some fluid evaporation (Fig.1). The luminal concentrations of bicarbonate, glucose and phosphate are dramatically reduced already in 24 h and further decline thereafter (Table 1). The basal fluid concentrations of bicarbonate and glucose also decrease in time, whereas that of phosphate rises (Table 1). The AF_t:AF_0 ratio's of bicarbonate, glucose and phosphate in 48 h decrease to respectively, 0.07, 0.003 and 0.13 (Fig.1). Luminal fluid potassium and calcium are elevated in time, whereas they remain practically unaltered in the basolateral fluid (Table 1). The AF_t:AF_0 concentration ratio's for potassium and calcium in 48 h increase to respectively, 1.41 and 1.99 (Fig.1). The osmolality in both compartments remains practically unaltered during the course of the experiment (Table 1). The pH remained unaltered in both compartments during the first 24h, whereas after 48h the fluid slightly acidified (Table 1).

Table 1. Time-dependent solute transport by LLC-PK$_1$ cells. The apical compartment received DMEM without serum, representative for ultrafiltrate and the basal compartment received DMEM containing 10% serum to resemble the renal peritubular space (n=6).

t	sodium (mM)		chloride (mM)		bicarbonate (mM)	
	apical	basal	apical	basal	apical	basal
0 h	153.8 ±1.3	156.6 ±1.0	119.7 ±0.7	119.4 ±0.8	18.1 ±0.3	17.7 ±0.3
24 h	155.6 ±0.8	163.8 ±1.6	129.4 ±1.1	125.6 ±0.7	4.8 ±0.5	12.0 ±0.8
48 h	161.4 ±3.4	170.9 ±.4	132.6 ±2.61	132.8 ±1.7	1.3 ±0.4	8.1 ±0.5

t	glucose (mM)		phosphate (mM)		potassium (mM)	
	apical	basal	apical	basal	apical	basal
0 h	24.1 ±0.2	23.1 ±0.1	0.80 ±0.06	0.83 ±0.06	5.10 ±0.04	5.13 ±0.03
24 h	7.1 ±2.0	21.0 ±0.1	0.23 ±0.06	0.83 ±0.06	7.29 ±0.03	4.77 ±0.1
48 h	0.07 ±0.06	17.1 ±0.4	0.10 ±0.0	1.13 ±0.06	7.19 ±0.6	5.28 ±0.1

t	calcium (mM)		osmolality (mosmol/l)		pH	
	apical	basal	apical	basal	apical	basal
0 h	1.66 ±0.01	1.65 ±0.03	334 ±3	336 ±3	7.4 ±0.1	7.4 ±0.1
24 h	2.66 ±0.1	1.46 ±0.01	334 ±4	336 ±3	7.4 ±0.1	7.3 ±0.1
48 h	3.31 ±0.03	1.57 ±0.05	351 ±1	349 ±1	7.2 ±0.1	7.2 ±0.1

The total amount of apically applied [^{14}C]α-MG is almost quantitatively transported to the basolateral fluid in time (Table 2), reflected by a $AF_t:AF_0$ of 0.07 after 48h (Fig.1). Luminal oxalate, on the other hand, shows a time-dependent increase which is accompanied by decreased values at the basolateral side of the monolayers (Table 2), resulting in $AF_t:AF_0$ concentration ratio's of 1.7 and 2.4, after respectively 24 and 48 h (Fig.1).

Fluid transport (J_v)

As calculated from changes in [^{3}H]inulin concentrations (Table 2 and Fig.2), the volume in the basal compartment steadily increased in time from 2600 μl at t=0, to 2920±120 μl at 8 h (not included), 3399±130 μl at 24 h and 3726±163 μl at 48 h (Table 2), 24 and 48 h, whereas in the apical compartment the fluid concomittantly decreased from 1500 μl at t=0, to 1201±60, 939±56 and 658±19 μl at respectively t=8 (not included in Table 2), 24 and 48 h. The apparent rise in total volume (apical plus basal compartment), which after 48 h approximates 109% of the initial total volume (=4100 μl), most likely is to be ascribed to some fluid evaporation that slightly increased the concentration of radiolabeled inulin, which is also reflected in a slight overall rise in osmolality (Table 1). When the reabsorption of water was monitored continuously it appeared that J_v was linear up to 8 hours at a rate of 8.1±1.0 $\mu l.cm^{-2}.h^{-1}$ (not shown), to decrease to 5.2±0.3 and 3.0±0.1 $\mu l.cm^{-2}.h^{-1}$, after 24 and 48 h, respectively.

Net solute transport

When these time-dependent volume changes are used to calculate absolute solute amounts in the compartments, it becomes evident that in spite of unaltered sodium and chloride concentrations, net NaCl transport occured from the apical to basal compartment. Such calculations also show that, for example, after 48h, only 3% of the bicarbonate, 0.1% of the glucose and 5.5% of the phosphate are still present in the apical fluid. In contrast to phosphate and α-MG, reabsorbed bicarbonate and glucose are not quantitatively recovered in the basal fluid. It also becomes clear that in spite of the rise in their luminal concentration, the absolute amount of potassium and calcium is reduced in the apical fluid. Although the concentration of oxalate in the apical compartment reached values more than 3-fold higher compared to those in the contraluminal compartment (Table 2), calculation of the absolute amounts at the different time points showed that this is not caused by net oxalate transport (7.5±0.15, 7.72±0.18 and 7.48±0.25 nmoles luminal oxalate, respectively at t=0, 24 and 48 h).

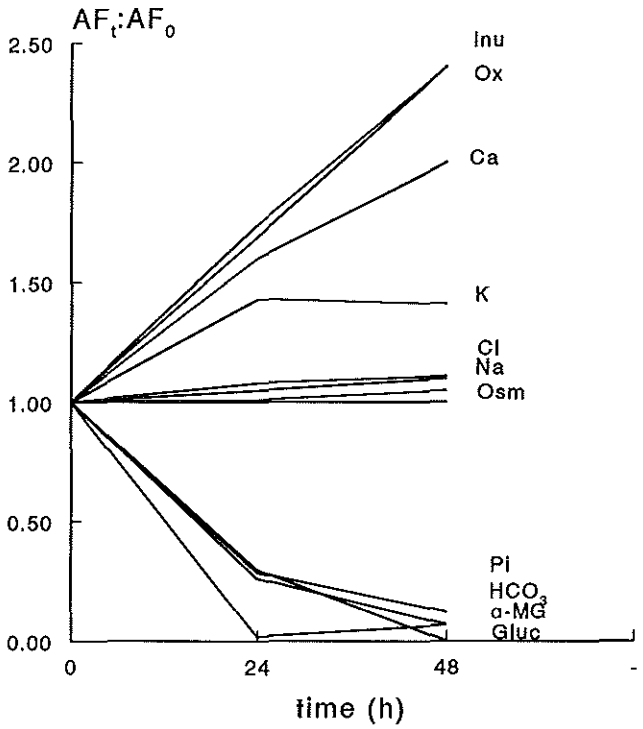

Fig.1 Alterations in the composition of the apical fluid can be expressed as concentration ratio between the apical fluid at the start (AF_0) and end (AF_t) of an incubation period (AF_0:AF_t). When these data are compared with the ultrafiltrate (UF) to tubular fluid (TF) concentration ratio's (TF:UF) in the mammalian proximal tubule [25], there is a striking similarity between these in vivo data and the data obtained from our cell culture model. The reabsorption of essential nutrients is indicated by decreased AF_0:AF_t of glucose, bicarbonate and phosphate. In spite of the relatively large amount of fluid that is transported from the apical to basal compartment, little change is observed in AF_0:AF_t of sodium and chloride, indicating isosmotic reabsorption of NaCl. The AF_0:AF_t for oxalate is almost similar to that for inulin, indicating that the concentration of oxalate increases in the apical compartment due to water reabsorption.

Table 2. Handling of α-MG, oxalate and inulin by LLC-PK$_1$ cells. Both compartments received [^{14}C]oxalate or [^{14}C]α-MG and the distribution of tracers was measured in time. In double label experiments the distribution of [^{3}H]inulin (dpm/100 μl) was monitored to measure the transepithelial movement of water (J_v) (n=6).

t	α-MG (mM)		oxalate (μM)		inulin (dpm/100μl)	
	apical	basal	apical	basal	apical	basal
0 h	1.0 ±0.05	0.9 ±0.03	5.0 ±0.1	5.0 ±0.1	965 ±55	950 ±40
24 h	0.02 ±0.008	1.2 ±0.04	8.7 ±0.2	4.0 ±0.2	1631 ±96	741 ±28
48 h	0.07 ±0.03	1.2 ±0.06	12.0 ±0.4	3.8 ±0.07	2325 ±69	676 ±30

Discussion

Proximal tubular functions may play a crucial role in calcium oxalate nephrolithiasis. The handling of phosphate, calcium, and water by the proximal tubule influences the risk that calcium phosphate crystallizes in the loop of Henle [12,13]. The presence of calcium phosphate particles and the composition of the fluid emerging from the loop of Henle in turn influence the risk of calcium oxalate crystallization in the distal tubule and collecting ducts [12,28]. It is therefore of interest in urolithiasis research to study the composition of the fluid leaving the proximal tubules and how it is regulated. Here, we assessed whether some of these transport functions can be studied in LLC-PK$_1$ cells. Although this cell line has widely been used during the last decade to study many transport mechanisms, these studies did not specifically adress the possible relationship between processes involved in renal stone disease. LLC-PK$_1$ cells were allowed to process an ultrafiltrate-like solution in time, during which we examined fluid transport (J_v), alterations in osmolality and pH, and the vectorial movement of solutes, including compounds that play an important role in stone formation such as calcium, phosphate, and oxalate.

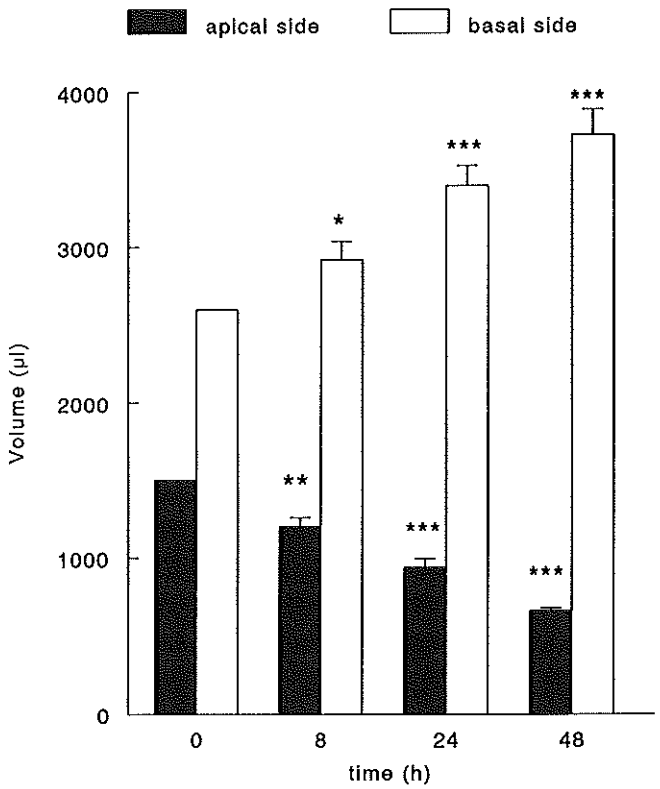

*Fig.2 Volume in the apical (closed bars) and basal (open bars) compartment after 0, 8, 24 and 48 hours, as calculated from changes in the [^{3}H]inulin concentrations. During this time period in which the cells received an ultrafiltrate-like solution at the apical side and the same solution including serum at the basolateral side of the monolayers, a decrease in the apical volume is observed that is accompanied by a volume increase in the opposite compartment, indicating that water is transported from the apical to the basal compartment. Results from a representative experiment, values are means $\pm$ SD of three independent measurements. *,**,*** Compared to the amount of fluid at t=0, significantly decreased or increased in respectively, the apical and basolateral compartment, analyzed with Student's t-test. *0.025>P>0.01, **P<0.01, ***P<0.001.*

The various solutes were processed in a specific manner by the cells. Luminal fluid bicarbonate, glucose and phosphate rapidly decreased, whereas sodium and chloride practically remained unaltered and potassium and calcium increased. During the same time period, however, the luminal concentration of [^{3}H]inulin, an extracellular marker that diffuses hardly or

not through the paracellular shunt pathway, increased more than 2-fold, whereas in the basal fluid it decreased, indicating that fluid was transported from the apical to basolateral side of the monolayers. Experiments, in which BSA (6%) was added to either the apical or basal compartment, to both sites of the monolayer or omitted from both compartments (data not shown), indicated that J_v was not influenced in this study by the presence or absence of serum proteins. The transport of water was recognized earlier in LLC-PK_1 cells by the formation of "domes" which are fluid filled blisters caused by the transepithelial apical to basal directed transport of water that becomes trapped between the cultured cell layer and the solid culture dish [7]. In agreement with our data, analysis of the basolateral fluid collected from such domes by micropuncture showed that the concentrations of sodium and chloride were nearly the same in the dome fluid and the apical medium, while bicarbonate, glucose and phosphate were actively reabsorbed. Our results indicate that NaCl and water are transported isosmotically from the apical to basal compartment, which is supported by the observation that the osmolality in both compartments remained practically unchanged during the complete course of the experiment (Table 1). Calcium and potassium are also reabsorbed but to a lesser extent than NaCl (Table 1), suggesting that their transport is passive and lags behind that of NaCl and water. At the end of the proximal tubule, the TF:UF concentration ratio's for calcium and potassium indeed are higher than that for sodium [25]. It should be emphasized, however, that under the experimental conditions used the various transport processes most likely are influenced by the alterations that take place in time. After 48 hours, for example, glucose, bicarbonate and phosphate are almost completely depleted from the apical compartment and, in addition, the fluid in both compartments was slightly acidified at this time-point. Since metabolic acidosis partitions potassium out of cells, this may have contributed to the lower reabsorption of potassium as compared to sodium. Whereas most reabsorbed solutes are transported almost quantitatively from the apical to basal compartment, glucose and bicarbonate are not completely recovered at the basolateral side of the monolayers. Since apically applied α-MG, which is a non metabolizable analog of glucose, is almost quantitatively transported to the basal compartment, this indicates that an amount of glucose is lost by cellular metabolism. The reduction in bicarbonate most likely is explained by CO_2 release after H_2CO_3 formation and its subsequent dissociation in CO_2 and H_2O. It should be noticed that when we performed these experiments with MDCK cells, the luminal concentrations of bicarbonate, glucose and phosphate were largely

unaffected and also inulin was not significantly changed (data not shown), indicating that the above described results are specific for cells with proximal tubule characteristics.

Next, we studied the handling of oxalate by LLC-PK_1 cells. In previous studies, we demonstrated with more convential methods that oxalate is not preferentially transported to either side of LLC-PK_1 monolayers [32,33]. Nevertheless, others found that LLC-PK_1 cells express oxalate transport proteins, including an apical membrane oxalate/chloride exchanger and basolateral membrane oxalate/sulphate and oxalate/bicarbonate exchangers [15]. In the present study, it was observed that the luminal concentration of radiolabeled oxalate gradually increased to values that after 48 hours were at least three-fold higher than those in the basal compartment (Table 2). Although this increase in apical oxalate suggested that oxalate was secreted, the rise in oxalate appeared to match that of inulin (Table 2), indicating that the luminal increase of oxalate is the passive consequence of water reabsorption. Thus, again we found that is no net directed transport of oxalate across LLC-PK_1 monolayers.

What is the significance of these findings to stone formation? Since the phosphate concentration is a main determinant of the first nucleation of calcium phosphate in the loop of Henle, the regulation of phosphate reabsorption in the proximal tubule is of importance. It was recently shown that stone formers frequently have an inappropriately high postprandial, PTH-independent phosphaturia [23,24]. The risk for calcium phosphate formation will be increased by diminished proximal tubule phosphate reabsorption. Indirectly, this will also speed-up the formation of calcium oxalate crystals further on in the nephron [12,13]. Small increases of the time a crystal spends inside a tubule can have magnifying effect on its size and subsequent risk for retention [12]. The site where crystals initially are formed may also be of importance. Several data point out that the epithelium in late nephron parts is protected against particle adhesion [6,29]. So, perhaps a shift in crystal formation to earlier parts of the nephron, that might not be protected from crystal binding, increases the risk for crystal retention.

Variations in oxalate concentration are especially important as they have a disproportional effect on the calcium oxalate formation product [20]. After filtration, oxalate might undergo bidirectional transport along the renal tubules [34]. For a long time, calculation of the renal clearance of oxalate was hampered by the lack of reliable methods to measure the relatively low concentrations of oxalate in plasma. Only recently this vital information in

the understanding of the renal handling of oxalate is becomming available. Two studies, in which the clearance of oxalate was examined in relatively large populations of calcium stone formers and healthy individuals, showed that the mean oxalate/creatinine clearance ratio in both groups was close to unity [10,26]. From these studies it was concluded that the mild hyperoxaluria observed in many patients may result from enhanced intestinal absorption or increased endogeneous production, but not from an abnormal renal handling of oxalate. Two other studies, however, in which smaller but more homogeneous groups of hyperoxaluric stone formers were investigated, found an oxalate/creatinine ratio above unity, suggesting net renal oxalate secretion [8,22]. Taken together, it is still not clear whether or not there exists a transcellular renal transport pathway that contributes to the urinary excretion of oxalate. Perhaps net oxalate secretion only occurs in patients with a specific cellular transport defect [8] or under specific physiological conditions. For example, large increases in net acid production during metabolic acidosis or after a diet high in animal protein, causes compensatory mechanisms that contribute significantly to the risk of stone formation [1,2]. A mild metabolic acidosis leads to decreased urinary citrate and increased urinary phosphate, calcium and, according to some reports, also oxalate [2]. The model system presented in this paper seems especially suitable to study the cellular handling of citrate and stone salts during acid-base disturbances. Sofar, our results demonstrate that under normal conditions there exists an equilibrium in the bidirectional transepithelial movement of oxalate across functional LLC-PK_1 monolayers. These results are in agreement with an oxalate/inulin (creatinine) ratio that is equal to unity (Fig.1). Although the monolayers are relatively leaky, an apical to basal directed oxalate concentration-gradient is generated, which is induced by water reabsorption. This observation indicates that oxalate becomes trapped at the luminal side of the monolayers.

The transport of water in the kidney has an important effect on filtered waste products. Intratubular concentrations of xenobiotics that are to be eliminated by the kidney gradually increase as a result of renal water reabsorption [5]. Although this common physiological process also has a large impact on the concentration of oxalate and thus on the formation product of its calcium salt, it has received little attention as possible factor in the pathophysiology of renal stone disease. Approximately 99% of the water filtered at the glomerulus is reabsorbed by the kidney [25]. Even in the absence of active secretion, this process will lead to approximately a 100-fold increase in the tubule fluid oxalate concentration up to the

collecting ducts. Assuming that the concentration of oxalate in ultrafiltrate is comparable to that in plasma (2-5 μM), this implies that along the length of the nephron the concentration of oxalate will rise passively to about 200-500 μM in the collecting duct [12]. The question is whether an essential physiological process such as renal water transport could be altered in stone forming individuals. Evidence has emerged that apical membrane anion exchange mechanisms play an important role in the reabsorption of salt and water in the kidney [3]. The transport of NaCl in proximal and distal tubules of rodents is effected by a process that couples apical Na^+/H^+ exchange to chloride/oxalate (formate) exchange. Oxalate was found to stimulate NaCl and water reabsorption by recycling across the luminal membrane whereby anions required for chloride exchange are continually replenished intracellularly. Although speculative, increased ion-exchance activity in the nephron could lead to enhanced water reabsorption resulting in higher luminal oxalate concentrations and the subsequent precipitation of stone salts in earlier segments of the nephron. Since the urine volume is fine-regulated in the collecting duct, higher levels of water reabsorption in early segments may be without consequences for urine volume and go unnoticed. In other words, it is possible that in stone forming individuals the tubular fluid reaches the collecting duct more concentrated than in healthy subjects. In summary, the results from this study demonstrate that functional monolayers of LLC-PK_1 cells process an ultrafiltrate-like solution, with stone salt concentration within the normal range, in a strikingly similar way as that described in the mammalian renal proximal tubule. Although there is no net directed transport of oxalate, its concentration in the luminal fluid increases as a passive consequence of isosmotic water reabsorption. This model may prove useful to study the regulation of NaCl and water transport in the proximal tubule, the effect of different calcium concentrations on the transport of phosphate, as well as the effect of metabolic acidosis on the cellular handling of compounds that are involved in renal stone disease. This information may provide new insights in processes that occur in the renal proximal tubule which may influence the risk for crystallization and stone formation in later segments of the nephron.

Supported by the Dutch Kidney Foundation through grant C95.1494.

References

[1] Alpern RL (1997) Trade-offs in the adaptation to acidosis. Kidney Int 47:1205

[2] Alpern RJ (1997) The clinical spectrum of chronic metabolic acidosis: Homeostatic mechanisms produce significant morbidity. Am J Kidney Dis 29:291

[3] Aronson PS (1996) Role of ion exchangers in mediating NaCl transport in the proximal tubule. Kidney Int 49:1665

[4] Bek Jensen H, Tiselius HG (1997) Evaluation of urine composition and calcium salt crystallization properties in standardized volume-adjusted 12-h night urine from normal subjects and calcium oxalate stone formers. Urol Res 25:365

[5] Besseghir K, Roch-Ramel F (1987) Renal excretion of drugs and other xenobiotics. Renal Physiol 10:221

[6] Bigelow MW, Wiessner JH, Kleinman JG, Mandel NS (1997) The dependence on membrane fluidity of calcium oxalate crystal attachment to IMCD membranes. Calcif Tissue Int 60:375

[7] Corman B, Roy C, Roinel N, de Rouffignac C (1984) Fluid composition of basolateral space of kidney cells in culture and its modification by intracellular cAMP. Am J Physiol 246:C546

[8] Gambaro G, Petrarulo M, Nardelotto A, Marangella M, Baggio B (1995) Erythrocyte transmembrane flux and renal clearance of oxalate in idiopathic calcium nephrolithiasis. Kidney Int 48:1549

[9] Gstraunthaler GJA (1989) Epithelial cells in tissue culture. Renal Physiol Biochem 11:1

[10] Hatch M (1993) Oxalate status in stone-formers. Two distinct hyperoxaluric entities. Urol Res 21:55

[11] Kok DJ, Khan SR (994) Calcium oxalate nephrolithiasis, a free or fixed particle disease. Kidney Int 46:847

[12] Kok DJ (1997) Intratubular crystallization events. World J Urol 15:219

[13] Kok DJ (1996) Crystallization and stone formation inside the nephron. Scann Microsc 10:471

[14] Kok DJ, Papapoulos SE, Bijvoet OLM (1990) Crystal agglomeration is a major element in calcium oxalate urinary stone formation. Kidney Int 37:51

[15] Koul H, Ebisuno S, Renzulli, Yanagawa M, Menon M, Scheid C (1994) Polarized distribution of oxalate transport systems in LLC-PK_1 cells a line of renal epithelial cells. Am J Physiol 266:F266

[16] Lupták J, Bek-Jensen H, Fornander AM, Höjgaard I, Nilsson MA, Tiselius HG (1994) Crystallization of calcium oxalate and calcium phosphate at supersaturation levels corresponding to those in different parts of the nephron. Scanning Microsc 8:47

[17] Menon M, Koul H (992) Calcium oxalate nephrolithiasis. J Clin Endocrin Metab 74:703

[18] Nguyen NU, Henriet MT, Dumoulin G, Widmer A, Regnard J (1994) Increase in calciuria and oxaluria after a single chocolate bar load. Horm Metab Res 26:383

[19] Rabito CA (1986) Sodium cotransport processes in renal epithelial cell lines. Min Electrol Metab 12:32

[20] Robertson WG, Peacock M (1980) The cause of idiopathic calcium stone disease: hypercalciuria or hyperoxaluria? Nephron 26:105

[21] Robertson WG, Heyburn PJ, Peacock M, Hanes FA, Swaminathan R (1979) The effect of high animal protein intake on the risk of calcium stone-formation in the urinary tract. Clin Sci 57:285

[22] Schwille PO, Manoharan M, Rümenapf G, Berens H (1989) Oxalate measurements in the picomol range by ion chromatography: values in fasting plasma and urine of controls and patients with idiopathic calcium urolithiasis. J Clin Chem Clin Biochem. 27:87

[23] Schwille PO, Herrmann U, Schmiedl A, Kissler H, Wipplinger J, Manoharan M (1997) Urinary phosphate excretion in the pathophysiology of idiopathic recurrent calcium urolithiasis: hormonal interactions and lipid metabolism. Urol Res 25:417

[24] Schwille PO, Schmiedl A, Herrmann U, Wipplinger J (1997) Postprandial hyperinsulinaemia, insulin resistance and inappropriately high phosphaturia are features of younger males with idiopathic calcium urolithiasis: attenuation by ascorbic acid supplementation of a test meal. Urol Res 25:49

[25] Seldin DW and Giebisch G (eds), *The kidney, Physiology and Pathophysiology,* Second Edition, Raven Press, New York, 1992

[26] Sutton RAL, Walker VR (1994) Enteric and mild hyperoxaluria. Min Electrol Metab. 20:362

[27] Tiselius HG (1997) Estimated levels of supersaturation with calcium phosphate and calcium oxalate in the distal tubule. Urol Res 25:153

[28] Tiselius HG, Fornander AM, Nilsson MA (1997) Studies on the crystallization process following addition of calcium phosphate crystals to solutions with a composition corresponding to that in the collecting duct. Scanning Microsc, in press

[29] Verkoelen CF, van der Boom BG, Houtsmuller AB, Schröder FH, Romijn JC (1998) Increased calcium oxalate monohydrate crystal binding to injured renal tubular epithelial cells in culture. Am J Physiol, 274:F958

[30] Verkoelen CF, Romijn JC, de Bruijn WC, Boevé ER, Cao LC, Schröder FH (1995) Association of calcium oxalate monohydrate crystals with MDCK cells. Kidney Int 48:129

[31] Verkoelen CF, van der Boom BG, Schröder FH, Romijn JC (1997) Cell cultures and nephrolithiasis. World J Urol 12:229

[32] Verkoelen CF, Romijn JC, de Bruijn WC, Boevé ER, Cao LC, Schröder FH (1993) Absence of a transcellular oxalate transport mechanism in LLC-PK_1 and MDCK cells cultured on porous supports. Scann Microsc 3:1031

[33] Verkoelen CF, Romijn JC (1995) Oxalate transport and calcium oxalate renal stone disease. Urol Res 24:183

[34] Williams HE, Wandzilak TR (1989) Oxalate synthesis, transport and the hyperoxaluric syndromes. J Urol 141:742

Chapter 4

ASSOCIATION OF CALCIUM OXALATE MONOHYDRATE CRYSTALS WITH MDCK CELLS

CF Verkoelen, JC Romijn, WC de Bruijn[1], ER Boevé, LC Cao, FH Schröder.

Department of Urology and [1]AEM-Unit, Clinical Pathological Institute. Erasmus University Rotterdam, The Netherlands

Kidney International 48:129-138, 1995

Abstract

Association of calcium oxalate monohydrate crystals with MDCK cells. Many factors are presently known that determine the risk of calcium oxalate (CaOx) stone formation in the kidney, although the early events in the pathogenesis of this disease are still to be elucidated. One of these early events is the interaction of intraluminal crystals with the epithelial cells lining the renal tubules. In this study we determined the interaction of approximately 2 μm calcium oxalate monohydrate (COM) crystals with monolayers of Madin-Darby Canine Kidney (MDCK) cells grown on porous supports in a two compartment culture system. Crystal-cell interaction studies were performed after the monolayers reached their highest level of γ-glutamyltranspeptidase (γ-GT) enzyme activity, a marker for brush border development. A number of technical aspects was evaluated, such as the size and morphology of the crystals and the influence of incubation time, temperature and pH on crystal-cell interaction. Kinetic data demonstrate that an equilibrium between free and associated particles is reached within 30 minutes. Crystal-cell interaction is often associated with cell damage. However, evidence is provided that in an environment that is saturated with calcium oxalate, MDCK cells are capable to interact with a certain amount of COM crystals without sustaining measurable injury. After initial attachment to the cell surface, crystals are taken up and subsequently eliminated again from the monolayers. The model system described in this paper provides a tool for detailed studies of processes that are involved in renal cellular handling of luminal COM crystals.

Introduction

The association of crystals with renal tubular cells is considered a potential factor in the process of renal stone formation [1,2,3]. The mechanisms of crystal-cell interaction, however, are not yet well understood. The most common crystalline material in kidney stones is CaOx [1,3,4,5]. In a number of experimental systems exposure to CaOx crystals induced various types of cellular responses. It has been shown that CaOx crystals induced lysis of red blood cells [4,6], secretion of PGE_2 and collagenase by synovial fibroblasts [7] and enzyme release from rabbit polymorphonuclear leukocytes [8.9]. The damaging effect of

CaOx crystals to the membranes of human erythrocytes was concentration dependent [6]. Granulocyte-mediated damage of endothelial cells, caused by urate and CaOx crystals, has been used as a model for vascular disease in gout and oxalosis [10]. Phagocytosis of hydroxyapatite and CaOx crystals resulted in the generation of superoxide anions in cultured endothelial cells [11].

A number of techniques has been described to study the interaction between crystals and cultured renal cells. Emmerson et al. used scanning and transmission electron microscopy to characterize the morphological aspects of urate crystal interaction with MDCK cells [12,13]. A more quantitative approach has been described by Lieske et al. who demonstrated CaOx crystal endocytosis and subsequent induction of proliferation in BSC-1 and MDCK cells [5]. The interaction between CaOx crystals and primary cultures of rat inner medullary collecting duct (IMCD) cells has been investigated by phase-contrast microscopy [14], light microscopy [15] and by the use of radioactively labeled calcium oxalate crystals [16,17]. A mathematical model to describe the complex process of crystal-cell interaction, has been developed by Mandel and Riese et al. [16,18,19].

The present study describes the association of CaOx crystals with MDCK cells. These cells are selected because they exhibit many of the characteristics of collecting duct epithelium [20], a segment in the nephron that could be one of the primary sites for crystal fixation [16]. The size and morphology of preformed crystals and assay conditions are described in detail. Saturation kinetics of crystal-cell interaction are studied and evaluated. Furthermore, it is demonstrated that a calcium oxalate saturated environment with or without COM crystals is not necessarily damaging to renal tubular cells.

Materials and Methods

Cell culture

MDCK cells, strain II, [21] were obtained from the American Type Culture Collection (ATCC, Rockville, MD, USA) and used between passage numbers 30 and 50. The cells were cultured in Dulbecco's modified MEM supplemented with 10 % fetal calf serum, 20 mM HEPES, 2 mM L-glutamine, 100 IU/ml penicillin and 100 μg/ml streptomycin. The medium was refreshed every two days. The cells were routinely grown in plastic tissue culture flasks (Costar, Badhoevedorp, The Netherlands) at 37°C in a humidified atmosphere of 5% CO_2

in air. Subculturing was performed weekly with 0.05% trypsin/0.02% EDTA (GIBCO-BRL,UK). To obtain monolayers that express a high level of differentiation, crystal-cell interaction studies were performed with monolayers cultured on a porous surface [22] in a two compartment culture system (24 mm Transwells, 0.4 μm pore size, Costar, Badhoevedorp, The Netherlands). The medium volumes were 2600 μl in the basal and 1500 μl in the apical compartment. Cells were seeded at a density of 1 x 10^5 cells/Transwell and the monolayers were allowed to maturate for 8 days prior to performance of crystal-cell interaction studies. To determine the total number of cells, the monolayers were treated with 0.05% trypsin/0.02% EDTA and the cells were counted in a hemocytometer.

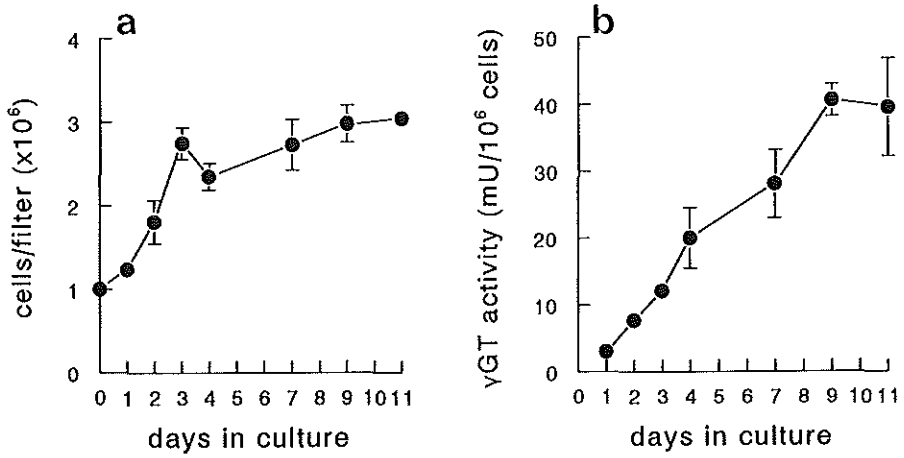

Fig.1. Growth curve of MDCK cells cultured on 24 mm Transwells (A) and the development of γ-GT enzyme activity in time (B).

Preparation of CaOx crystal suspensions

A solution of radioactive sodium oxalate was prepared by adding 1 ml 0.01 mCi/ml (0.37 MBq/ml) [^{14}C]oxalic acid (4.03 GBq/mmol, Amersham International plc., Buckinghamshire, UK) to 0.5 ml 200 mM sodium oxalate. A calcium chloride solution was prepared by adding 0.5 ml 200 mM calcium chloride to 8 ml aquadest. After mixing the two solutions at room temperature, resulting in a final concentration of 10 mM for both calcium and oxalate, [^{14}C]-labeled CaOx crystals were formed immediately. The crystal suspension was

allowed to equilibrate for three days. The crystals were then washed three times with (sodium and chloride-free) CaOx saturated water, resuspended and stored in 5 ml of this solution. The radioactive crystal suspension contained 2.92 mg CaOx crystals/ml.

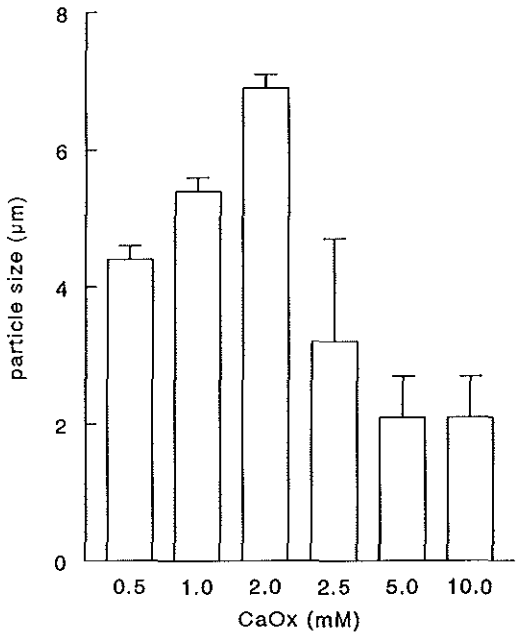

Fig.2. Coulter Multisizer measurements of COM crystals obtained from varying calcium oxalate concentrations (means ± SD; N=4).

X-ray diffraction

Crystal composition identification was performed by X-ray diffraction, using an X-ray generator PW 1729/00 connected to an Integrator/Interface PW 1842 (Philips).

Crystal size and number distribution

Size and number of the crystals were measured at various times after their preparation in a Coulter Multisizer (Coulter Electronic Ltd, Luton, UK). For each measurement a volume of 100 µl crystal suspension was added to 100 ml, 0.22 µm Millipore filtered CaOx saturated 0.9 % sodium chloride. Crystal size and number distribution were determined in 500 µl sample volumes using a 70 µm orifice tube.

Scanning electron microscopy (SEM)

To perform scanning electron microscopy, the crystals or cells cultured on porous supports were fixed in 2.5 % glutaraldehyde in 0.15 M cacodylate buffer for 4 hours. After washing in 0.1 M cacodylate buffer for 3 hours, the samples were postfixed in OsO_4 in 0.1 M cacodylate buffer for 4 hours, washed again in cacodylate buffer for 3 hours, dehydrated in graded series of ethanol and finally critical point dried. After mounting on stubs a conductive layer was sputtercoated on the samples and examined in a Philips SEM 525.

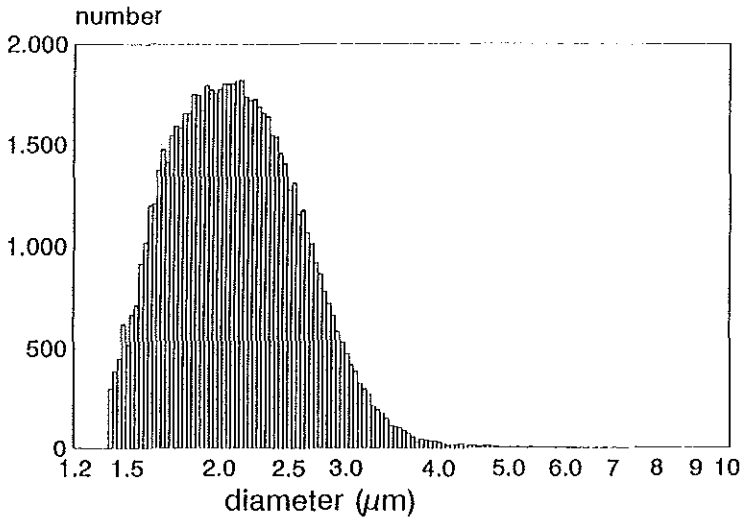

Fig.3. Particle number and size distribution of preformed COM crystals generated from 10 mM calcium oxalate.

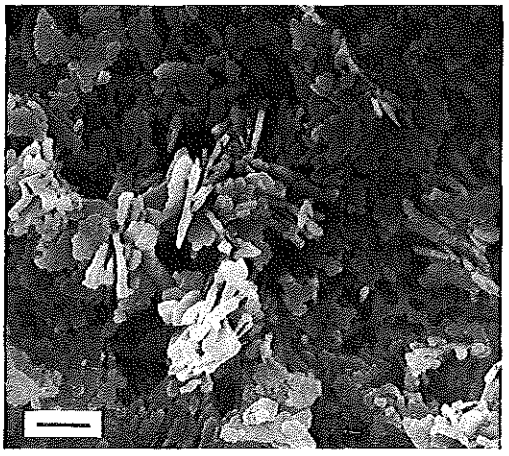

Fig.4. SEM-image of COM crystals.

Transmission electron microscopy (TEM)

Cells were fixed with 1.5 wt% glutaraldehyde in a 0.1 M cacodylate/HCl buffer pH 7.4 for 30 min. at 4°C, and postfixed with 1 wt% OsO_4 in cacodylate/HCl buffer to which $K_4Fe(CN)_6.3H_2O$ was added to a final concentration of 0.05 M, for 30 min. at room temperature. After several washing steps, the cells were dehydrated in ethanol series and embedded in Epon. Unstained ultrathin sections were obtained. These sections were observed in a Zeiss EM 902 transmission electron microscope (Zeiss, Oberkochen, Germany), operating at 80 kV. Analogue micrographs were obtained on Gevaert Scientia sheet film (Gevaert, Antwerpen, Belgium), developed in D19b (1:2 diluted) for 4 min. at room temperature.

Crystal-cell interaction studies

Crystal adherence was studied in a CaOx saturated buffer (buffer B) that was prepared by the addition an excess COM crystals (3 mg/ml), to a buffer (pH 6.7) containing (in mM): 118 NaCl, 5.3 KCl, 1.8 $CaCl_2$, 6.6 $NaHCO_3$, 1.3 $MgSO_4$, 2.0 NaH_2PO_4, and 20 HEPES. The cells were washed and preincubated with serum-free DMEM, 20 mM HEPES, 2 mM L-glutamine, 100 IU/ml penicillin and 100 μg/ml streptomycin added to both compartments. After one hour, filtered buffer B (0.45 μm) was added to the apical compartment and fresh serum-free DMEM to the basal compartment. Subsequently, 50 μl of the crystal suspension (146 μg), prepared as described above, was distributed homogeneously on top of the cells. After an incubation period of 60 minutes, the monolayers were rinsed in three successive buffer B baths, to remove non-associated crystals. The filter inserts were cut out with a scalpel and transferred to a scintillation vial. To extract radioactivity, 1 ml 1M perchloric acid was added and the amount of radioactivity was counted in a liquid scintillation counter (Packard, UK). Results were routinely expressed as dpm/filter. In some experiments the amount of associated crystals was calculated in μg and the results expressed in $\mu g/cm^2$.

Determination of cell damage

To study the possible damaging effect of the assay conditions, three experimental groups were formed; (I): untreated control cells; (II): cells incubated with buffer B alone; and (III): cells incubated with COM crystals in buffer B. The apical compartments received (I), (II) or (III), and fresh serum-free DMEM was added to the basal compartment in all three groups. After a one hour incubation period, the medium from the apical compartment was collected and centrifuged. The release of the brush border enzyme γ-glutamyl transpeptidase (γ-GT), and the cytosolic enzyme lactate dehydrogenase (LDH) were measured to reveal a possible direct damaging effect. The permeability of the tight junctions was measured using ^{3}H]mannitol and cell viability was assessed by Trypan Blue dye

exclusion and the MTT assay. To reveal a postponed effect of the various treatments, determination of the same markers was also carried out after an additional period of 24 hours during which the cells were maintained in DMEM supplemented with 10 % FCS.

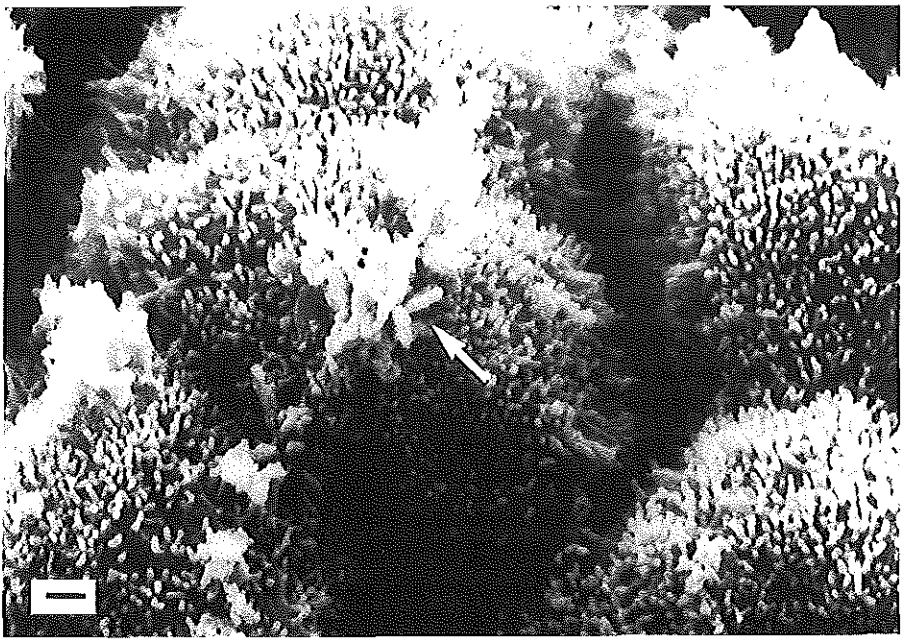

Fig.5. SEM-image of COM crystals attached to the surface of MDCK cells.

Enzyme determinations

γ-GT (EC 2.3.2.2) activity was determined spectrophotometrically, using L-γ-glutamyl-3-carboxy-4-nitroanilide as substrate and LDH (EC 1.1.1.27) was assayed with pyruvate as substrate. Cell monolayers were washed with PBS, scraped in 1 ml 50 mM Tris-HCl (pH 7.4) and sonicated for 30 s. on ice. After centrifugation for 10 min. at 2000 g the supernatant was used to measure γ-GT activity.

MTT assay

This assay reflects the amount of living metabolically active cells and is based on the reduction of a tetrazolium salt 3-(4,5-dimethylthiazol-2-yl)-2,5-diphenyl tetrazolum bromide (MTT obtained from Sigma, St Louis, MO) to a colored formazan product by mitochondrial enzymes and is a modification of the assay described previously [23]. MTT was added to both compartments (0.5 mg/ml) and the monolayers were incubated for 2 hour at 37°C. The medium was

carefully sucked of, and 5.0 ml buffered dimethylsulfoxide (DMSO) was added to both compartments. The plates were placed in a plate shaker to dissolve the purple-colored formazan after which the contents from both compartments were combined. From each group eight duplicate samples (0.2 ml) were transferred to a 96-well microtiter plate and the absorbance was read at 570 nm using a Biorad microplate reader, model 450.

Measurement of epithelial barrier integrity

Monolayers were rinsed and preincubated for 15 min. with MOPS-buffer (pH 7.3), containing (in mM): 119 NaCl, 5.3 KCl, 6.6 Na acetate, 0.25 $CaCl_2$, 1.3 $MgSO_4$, 2.0 KH_2PO_4, 6.6 $NaHCO_3$ and 9.2 Na-morpholinopropane sulfonic acid (MOPS). To study the permeability of mannitol (P^{Mann}), D-[^{3}H]mannitol (0.6 μCi per Transwell) in a final concentration of 50 μM was added to the apical compartment. Tracer-free MOPS-buffer was added to the basal compartment. The appearance of D-[^{3}H]mannitol in the basal compartment and the disappearance from the apical compartment was determined by counting radioactivity in 50 μl aliquots from both compartments in a liquid-scintillation counter 0, 15, 30 and 60 minutes after the start of incubation. P^{Mann} is expressed in pmol/cm^2.minute [24].

Mathematical model

To analyse crystal-cell interaction further, we have adapted the mathematical approach previously presented by Mandel and Riese et al.[18,19]. According to these authors, interaction can be described by the equation:

$Bd = ß/\alpha \times (1-e^{-(\alpha \times C)})$ (1), in which Bd represents crystal mass bound per total cell area and C represents the total crystal mass delivered per total cell area. The parameters $1/\alpha$ and ß can be calculated from the equation and are suggested to represent the maximum μg crystals/binding area ($1/\alpha$) and the cell area that can bind crystals/total area (ß), respectively.

Statistics

All experiments are performed at least two times. The results are presented as means $\pm$ S.D. of three independent filters. Statistical analysis was performed with ANOVA or Student's t-test. Differences were considered significant if $P < 0.05$.

Results

Cell culture

After seeding $1x10^6$ cells per 4.52 cm^2 Transwells, cultures reached confluency within three days as observed by phase-contrast light microscopy. The total cell number, however, continued to increase to obtain a maximal density of approximately $3x10^6$ cells/filter after 8-9 days (Fig.1A). The increase in cell density was accompanied by an increase of γ-GT. One day after seeding γ-GT activity was 3.0 $\pm$ 0.4 mU/10^6 cells and increased the following days to reach a maximal level of 40.6 mU/10^6 cells after 8-9 days in culture (Fig.1B).

Effects of different CaOx concentrations on crystal size

CaOx crystals were prepared as described under Methods with different concentrations of calcium oxalate and the size of the formed crystals was measured in a Coulter Counter Multisizer. At lower concentrations (0.5 - 2 mM) the average crystal size increased with the concentrations, reaching a maximum average diameter of 6.9 μm. However, at higher concentrations crystal size steeply declined reaching a constant level of about 2 μm at concentrations $\geq$ 5 mM calcium oxalate (Fig.2). For the crystal-cell interaction studies in this paper, final concentrations of 10 mM were used to prepare CaOx crystals. Crystal suspensions prepared as described in Methods contained approximately 140 x 10^6 particles/ml, with an average size of 2.03 $\pm$ 0.40 μm (Fig.3) Crystal size and number did not measurably change upon storage for several months at room temperature.

Crystal identification

X-ray diffraction analysis demonstrated that the suspension exclusively consisted of calcium oxalate monohydrate (COM) crystals. SEM images of these crystals demonstrated the typical plate-like shape (Fig.4).

SEM studies

Scanning electron microscopy (SEM) images showed that after an incubation period of one hour and subsequent removal of non-associated crystals, COM crystals were attached to the surface of MDCK cells. The crystals were not uniformly distributed over the monolayer, but seemed to cluster at certain locations at the cell surface (Fig.5).

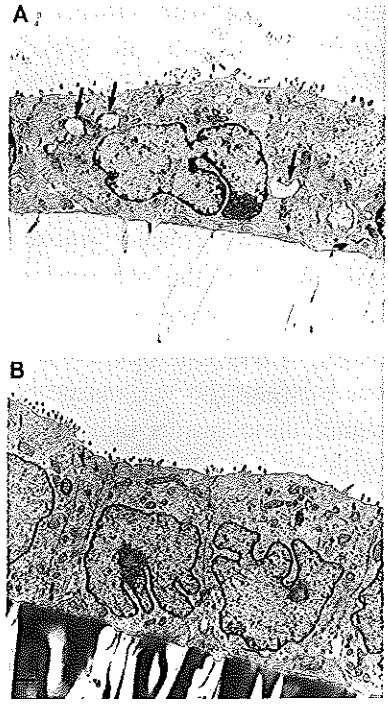

Fig.6. (A) TEM-image of an MDCK monolayer after incubation with COM crystals for two hours, demonstrating intracellular (arrows), and (B) these monolayers after an additional culture period of 72 hours, illustrating the elimination of crystals form the monolayer. Bar=1 μm.

TEM studies

The presence of intracellular crystal ghosts were studied with TEM images 2 and 72 hours after incubating MDCK cells with COM crystals. Two hours after incubation crystals were located inside the cells (Fig.6A). In monolayers cultured for an additional 72 hours following crystal exposure, most of the intracellular crystals had disappeared (Fig.6B).

Cellular damage and monolayer integrity after interaction with crystals

Enzyme release (γ-GT,LDH), MTT-conversion and epithelial barrier integrity of the monolayers were measured to assess possible damaging effects of the assay conditions to MDCK cells. After a one hour incubation period, γ-GT and LDH activities in the medium from all groups were equally low (Fig.7) and not dufferent from enzyme activities

in medium from cells cultured with DMEM + 10 % FCS in both compartments. After the removal of non-associated crystals, the monolayers in all three groups now received DMEM 10 % FCS and were cultured for an additional period of time. When measured again 24 hours later, the activities of both enzymes in the medium of the three groups were considerably increased. However, no significant differences were observed between the two treated groups and untreated controls (Fig.7A and 7B), indicating that the observed enzyme release reflected normal 24 hour turn-over. Likewise, with respect to MTT conversion (Fig.8A), P^{Mann} (Fig.8B), or Trypan Blue exclusion (Fig.8C), there were no obvious differences between the various groups measured after 1 and 24 hours. Taken together these results indicate that an incubation period of 1 hour with the CaOx saturated buffer with or without crystals, did not affect the viability of the cells, the total amount of cells nor the integrity of the monolayers to a measurable extent within 24 hours.

Effect of pH and temperature on crystal-cell interaction

The effect of pH on crystal-cell interaction was studied using buffer B, adjusted to pH 5.1, 6.3, 7.2 and 8.1, respectively. It was demonstrated that the highest amount of crystals became associated with the cells during incubations performed at pH 5.1. At higher pH values crystal association gradually decreased (Fig.9). this pH-dependent decrease was statistically significant ($P < 0.0003$; ANOVA). Incubations performed at 4°C resulted in a 5-fold lower amount of crystals associated with the monolayers than incubations performed at 37°C (Fig.10).

Crystal-cell interaction and saturation kinetics

Under all circumstances tested, only a fraction of applied crystals associated with the cells. When non-associated crystals were removed and added to another monolayer, the relative proportion of crystals that associated during this second round of incubation was nearly identical to the proportion of the original crystal suspension that was retained during the first round of incubation. This indicates that selective association based on crystal properties (e.g. size) did not occur. In addition, we looked whether stirring of the crystal suspension during the incubation would increase crystal retention. However, when crystals were frequently redistributed over the cell surface during a one hour incubation period, only a minor (5%) increase was observed.

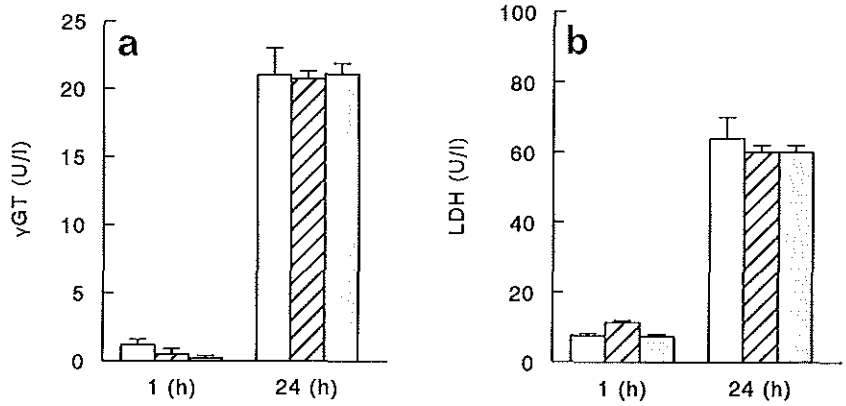

Fig.7.Release of γ-GT (A) and LDH (B) enzyme activity into the culture medium after a one hour treatment with buffer B (hatched bars) and buffer B including COM crystals (dotted bars) compared to untreated controls (open bars) measured after 1 and 24 hours.

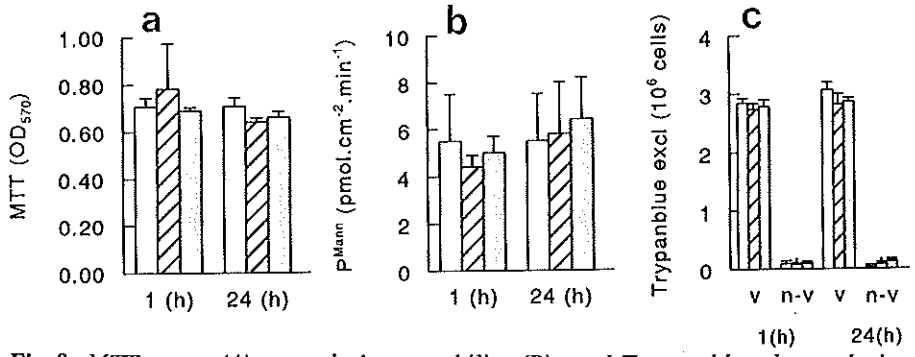

Fig.8. MTT-assay (A), mannitol permeability (B), and Trypan blue dye exclusion test (C) in MDCK monolayers treated with buffer B (hatched bars) and buffer B including COM crystals (dotted bars) compared to untreated controls (open bars) measured after 1 and 24 hours.

The kinetics of crystal-cell interaction were studied also by varying the amount of applied crystals (25-500 μl crystal suspension, corresponding to 73-1460 μg crystals) and incubation times (0-120 min.) Fig.11 shows that at all crystal dosages tested, saturation was achieved within 30 min. The maximum level of associated crystals never exceeded about 30-40% of applied crystals, which suggests that neither the amount of crystals added, nor the number of potential "binding sites" appeared to be limiting factors. Further analysis of crystal-cell interaction kinetics was performed

by application of the mathematical model developed by Mandel and Riese et al. A best fit curve was made by plotting the amount of associated crystals after a one hour incubation period against the amount of applied crystals ($\mu g/cm^2$). Using equation (1), the parameters $1/\alpha$ and ß, for MDCK cells and COM-crystals, were calculated to be 90 μg/cm2 and 0.29, respectively (Fig.12).

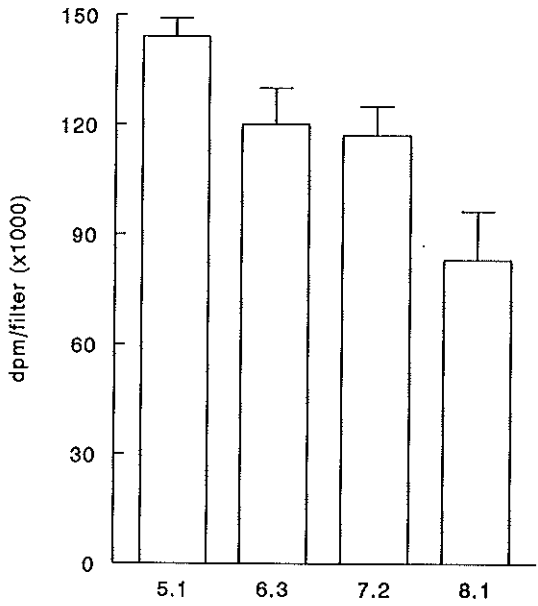

Fig.9. Crystal-cell interaction in buffer B with varying pH-values (means±SD). Statistical significant increase of dpm/monolayer with decreasing pH (ANOVA,N=3,P<0.0003).

Discussion

The presence of crystals in urine is one of the prerequisites for the formation of urinary stones [1,25,26]. The reaction of crystals with tubular epithelial cells could be an initiating mechanism in renal stone formation [1,2,4,26,27]. This paper describes the interaction between CaOx crystals and monolayers of MDCK cells cultured on permeable supports. After seeding $1x10^6$ cells/filter the monolayers are visually confluent in 3 days. However, the amount of cells per filter increased to reach the highest cell density after a culture period of 8-9 days (Fig.1A). In parallel the brush border enzyme γ-GT developed in time and reached

a maximal specific activity after 8-9 days of culture (Fig.1B). Similarly, it was reported that in LLC-PK_1 cells γ-GT activity and Na^+-dependent hexose transport, a characteristic of terminally differentiated epithelia, developed in parallel with cell density increase [28]. As the renal tubule brush border is the initial site of crystal-cell contact and γ-GT activity reflects development of the brush border in MDCK cells, an 8-days culture period was considered to create optimal conditions for crystal-cell interaction studies.

Crystals were generated by mixing equal concentrations of calcium and oxalate and consisted purely of calcium oxalate monohydrate (COM). The conditions used to prepare the crystals clearly influenced crystal characteristics, in particular crystal size. At relatively low concentrations the size of the formed crystals increased with the concentration possibly due to heterogeneous nucleation or aggregation of crystals. At higher concentrations of calcium and oxalate (>2.5 mM), smaller crystals were formed of which the size was less concentration-dependent (Fig.2). Since crystal size may well affect their interaction with cells, it is crucial that crystals are prepared under defined conditions. In our studies CaOx crystals were generated from 10 mM solutions, resulting in the formation of crystals with an average diameter of about 2 μm (Fig.3).

The method used in this study does not allow discrimination between crystal adherence to the cell surface and cellular uptake of crystals. Our EM studies, however, demonstrated that associated crystals are located inside as well as outside the cells (Fig.5 and 6A). The observation that COM crystals not only bind to renal tubular cells but are also rapidly endocytosed, is in accordance with results obtained by Lieske et al. who described the avid internalization of COM crystals in the renal epithelial African green monkey cell line BSC-1 [29] and the presence of apparent CaOx crystals within tubular epithelial cells of a patient with primary hyperoxaluria [30]. Cheung et al. reported the intracellular solubilization of calcium-containing crystals by cultured human fibroblasts [31]. An ultrastructural study of experimentally induced microliths in the renal tubules of rats, reported previously by our group, also demonstrated the presence of crystal ghosts in the cytoplasm of proximal and distal tubule cells [32] and their removal from the tubuli towards the interstitium [33]. In order to understand the complex process of crystal-cell interaction, not only cell surface binding and uptake characteristics but also putative cellular defence mechanisms should be taken into account. Therefore the fate of endocytosed crystals was studied morphologically.

TEM images showed that initial endocytosed crystals had disappeared from the monolayers within 72 hours (Fig.6A and 6B), which suggests the existence of a regulatory mechanism to eliminate internalized crystals. It is not yet clear whether (a) crystal-containing cells are eliminated from the monolayer and replaced by new cells, (b) crystals are dissolved intracellularly, or (c) these cells are able to eliminate intracellular crystals by exocytosis. Recently, Lieske et al. [38], reported that the internalization of COM crystals by BSC-1 and MDCK cells is a regulated event that can be modified by various signals. In contrast to our results, crystals were still found inside the cells after two weeks. It should be noted, however, that MDCK cells in our experiments are cultured on porous surfaces and are allowed to maturate, whereas the renal cells in Lieske's studies were cultured on solid substrates and in some experiments still proliferating. It is conceivable that cellular response to internalized crystals is determined by the conditions under which these cells are cultured.

Crystal-cell interaction studied at various pH-values, demonstrated that at pH 5.1 significantly more crystals were associated with the cells than at pH 8.1 (Fig.9). From this observation it could be speculated that a relatively low pH of the luminal fluid, predisposes renal tubular epithelium for crystal attachment by altering properties at the cells surface or at the surface of the crystals.

At low temperature (4^0C) the amount of associated crystals was decreased compared to 37^0C, indicating that crystal-cell interaction is an active cellular process (Fig.10).

Recently, evidence was provided that ionic oxalate could injure renal tubular cells [34,35], and also COM crystals can damage renal tubular epithelium [27,32,35]. The possible side-effects of either the CaOx saturated solution and/or the applied COM-crystals in our model system, were investigated using our standard experimental conditions. MDCK monolayers treated with the CaOx saturated buffer with or without crystals demonstrated a release pattern of cellular enzymes (γ-GT, LDH) that was not significantly different from untreated controls. The transepithelial movement of mannitol (P^{Mann}) is a sensitive method to measure the permeability of the tight junctions and inversely correlates with transepithelial electrical resistance in MDCK cells [36]. This method was also used to measure monolayer integrity and sublethal injury in primary cultures of mouse proximal tubular cells [37].

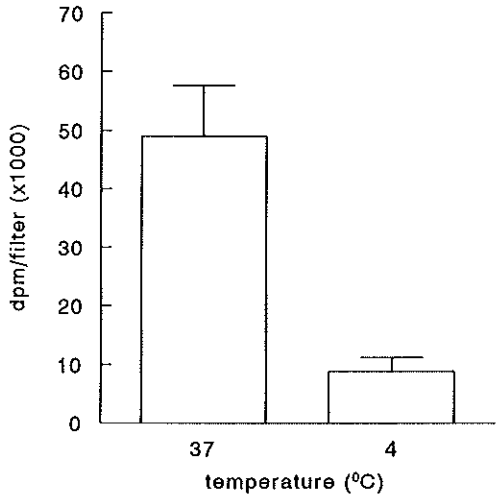

Fig.10. Crystal-cell interaction in buffer B at 4°C and 37°C. (Statistically different analyzed with Student's t-test; means±SD; N=3;P<0.003).

To study the integrity of the monolayers after treatment, P^{Mann} was measured and it was demonstrated that the apical-to-basal flux of [^{3}H]mannitol was unaffected by either treatment (Fig.8B). Finally, compared to untreated controls, the total amount of viable cells, estimated by Trypan Blue exclusion and MTT-conversion, was not decreased in either group within 24 hours (Fig.8A and 8C). Taken together these results indicate that there is no measurable damaging effect on MDCK monolayers induced by either the CaOx saturated solution nor by this solution including COM crystals. Lieske et al. also demonstrated that despite the presence of intracellular crystals, BSC-1 and MDCK cells proliferated normally and no crystal-induced toxicity was observed [38]. Although cell damage induced by CaOx crystals has been observed in many experimental systems, it is conceivable that certain cell types are more vulnerable to these crystals than others. In contrast to the blood, microcrystals are commonly present in the tubular fluid. This could explain why inflammatory responses to crystals, as seen in some systems, are not often observed in the kidney. The fact that the CaOx saturated buffer used in this study was not toxic to the cells is not surprising since damaging effects of oxalic acid to LLC-PK_1 cells were reported to occur at oxalate concentrations $\geq$ 400 μM [34], whereas the final concentration of oxalate in our buffer was lower than 50 μM.

Crystal-cell interaction was further studied using varying amounts of crystals, incubated for various incubation times. It was demonstrated that crystal association with the monolayers reached saturation after about 30 minutes at all crystal concentrations tested. Apparently, a balance was reached between the amount of associated crystals and the amount of free non-associated crystals (Fig.11). When the fraction of non-associated crystals was added to new monolayers, the balance between associated and non-associated crystals was reached again after about 30 minutes, excluding a possible selection of crystals on the basis of their size or other properties (not shown). Furthermore, redistribution of the fraction of non-associated crystals did not lead to a significant increase of crystal association (± 5%) during an additional incubation period of 30 minutes, indicating that during the first incubation there was no irreversible deposition of crystals at unfavorable sites.

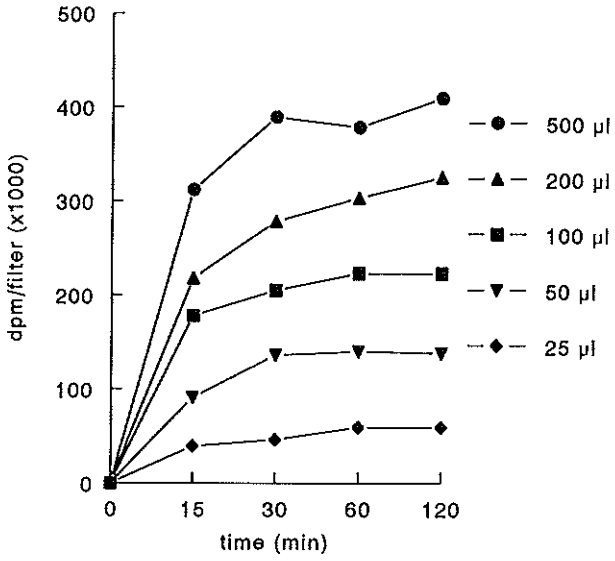

Fig.11. [^{14}C]COM crystal interaction with MDCK cells, varying amounts of crystals (25 to 500 µl crystal suspension) and incubated for varying periods of time (15-120 min). Means from 3 independent measurements (SD values usually less than 10% of means not shown for clarity).

The fact that crystal-cell interaction does not follow classical hyperbolic saturation kinetics has already been recognized by Mandel and Riese et al., who developed a mathematical model to describe the interaction of crystals with renal tubular cells [16,18,19]. In this model, two parameters, $1/\alpha$ and ß, have been defined that were considered to reflect characteristics of the crystals and of the cell cultures, respectively. In primary cultures of IMCD cells exposed to COM crystals, $1/\alpha$ was calculated to be 287 $\mu g/cm^2$ and ß 0.179 [16,18]. In our study, in which MDCK cells were exposed to COM crystals, values of 90 $\mu g/cm^2$ and 0.290 were obtained for $1/\alpha$ and ß, respectively (Fig.12). If ß indeed represents the fraction of cellular area capable of crystal interaction, our data suggest that MDCK cultures have a higher capacity to associate with COM crystals than IMCD cells. In contrast, $1/\alpha$ assumed to reflect the amount of crystals that can interact per unit binding area was considerably higher in IMCD cells than MDCK. It can not be excluded that the COM crystals used by Mandel and Riese et al. had other properties than the crystals applied in our experiments. However, such an apparent difference in "binding" affinity could also be caused by different capacities of the two cell types to endocytose the crystals, a factor that is not explicitely accounted for in the mathematical approach of Mandel and Riese et al.

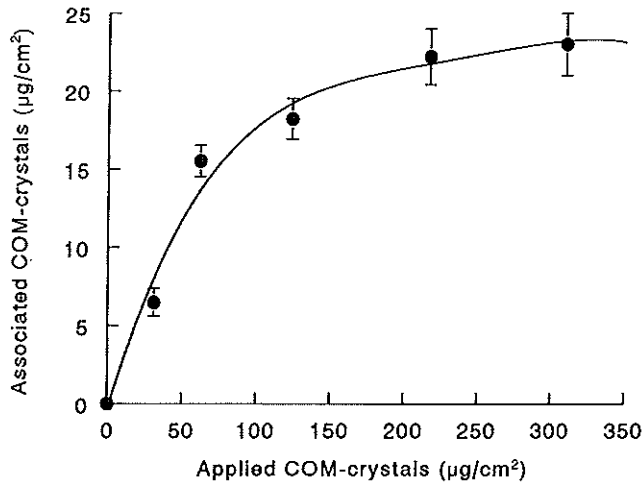

Fig.12. A graphical analysis of concentration-dependent saturation of COM crystals associated with MDCK cells.

In conclusion, the method described in this paper allows the study of subtle cellular events involved in the interaction of COM crystals with maturated MDCK monolayers. Evidence is provided that in an environment that is saturated with calcium oxalate these cells are capable to interact with COM crystals without sustaining measurable injury. Better understanding of the processes involved in crystal-cell interaction in renal tubules could shed some light on the pathophysiology of nephrolithiasis.

The authors wish to thank P van Run, P van Miert, A van der Linden, M van Vliet, WP van Schalkwijk and Mr WJ Visser for technical assistance. Study supported by the Dutch Kidney Foundation (grant C 92.1235).

References

[1] Menon M, Koul H: Calcium oxalate nephrolithiasis. J Clin Endocrin Metab 74:703-707, 1992

[2] Randall A: The origin and growth of renal calculi. Ann Surg 105:1009-1020, 1937

[3] Kahn SR, Hackett RL: Retention of calcium oxalate crystals in renal tubules. Scann Microsc 5:707-712, 1991

[4] Wiessner JH, Mandel GS, Mandel NS: Membrane interactions with calcium oxalate crystals: variation in hemolytic potentials with crystal morphology. J Urol 135:835-839, 1986

[5] Lieske JC, Toback FG: Regulation of renal epithelial cell endocytosis of calcium oxalate monohydrate crystals. Am J Physiol 264:F800-F807, 1993

[6] Elferink JGR: The mechanisms of calcium oxalate crystal-induced haemolysis of human erythrocytes. Br J Exp Path 68:551-557, 1987

[7] Hasselbacher P: Stimulation of synovial fibroblasts by calcium oxalate and monosodium urate monohydrate. J Lab Clin Med 100:977-985, 1982

[8] Elferink JGR, Deierkauf M: Enzyme release from polymorphonuclear leukocytes during interaction with calcium oxalate microcrystals. J Urol 138:164-167, 1987

[9] Elferink JGR: Mode of activation of the metabolic burst in polymorphonuclear leukocytes by calcium oxalate crystals. Agents Actions 22:295-301, 1987

[10] Boogaerts MA, Hammerschmidt DE, Roelant C, Verwilghen RL, Jacob HN: Mechanisms of vascular damage in gout and oxalosis: Crystal induced, granulocyte mediated, endothelial injury. Thromb Haemostas 50:576-580, 1983

[11] Falasca GF, Ramachandrula A, Kelley KA, O'Connor CR, Reginato AJ: Superoxide anion production and phagocytosis of crystals by cultured endothelial cells. Arthr Rheum 36:105-114, 1993

[12] Emmerson BT, Cross M, Osborne JM, Axelsen RA: Ultrastructural studies of the reaction of urate crystals with a cultured renal tubular cell line. Nephron 59:403-408, 1991

[13] Emmerson BT, Cross M, Osborne JM, Axelsen RA: Reaction of MDCK cells to crystals of monosodium urate monohydrate and uric acid. Kidney Int 37:36-43, 1990

[14] Kohri K, Kodama M, Ishikawa Y, Katayama Y, Matsuda H, Imanishi M, Takada M, Katoh Y, Kataoka K, Akiyama T, Iguchi M, Kurita T: Immunofluorescent study on the interaction between collagen and calcium oxalate crystals in the renal tubules. Eur Urol 19:249-252, 1991

[15] Wiessner JH, Kleinman JG, Blumenthal SS, Garancis JC, Mandel GS, Mandel NS: Calcium oxalate crystal interaction with rat renal inner papillary collecting tubule cells. J Urol 138:640-643, 1987

[16] Mandel N, Riese R: Crystal-cell interactions: crystal binding to rat renal papillary tip collecting duct cells in culture. Am J Kid Dis 17:402-406, 1991

[17] Riese RJ, Mandel NS, Wiessner JH, Mandel GS, Becker CG, Kleinman JG: Cell polarity and calcium oxalate crystal adherence to cultured collecting duct cells. Am J Physiol 262:F177-F184, 1992

[18] Riese RJ, Riese JW, Kleinman JG, Wiessner JH, Mandel GS, Mandel NS: Specificity in calcium oxalate adherence to papillary epithelial cells in culture. Am J Physiol 255:F1025-F1032, 1988

[19] Riese RJ, Riese JW, Kleinman JG, Wiessner JH, Mandel GS, Mandel NS: Uric acid crystal binding to renal inner medullary collecting duct cells in primary culture. J Am Soc Nephrol 1:187-192, 1990

[20] Valentich JD: Morphological similarities between the dog kidney cell line MDCK and the mammalian cortical collecting tubule. Ann NY Ac Sci:384-403, 1981

[21] Gausch CR, Hard WL, Smith TF: Characterization of an established line of canine kidney cells (MDCK) Proc Soc Exp Biol Med 122:931-935, 1966

[22] Simons K, Fuller SD: Cell surface polarity in epithelia. Ann Rev Cell Biol 1:243-288, 1985

[23] Romijn JC, Verkoelen CF, Schröder FH: Application of the MTT assay to human prostate cancer cell lines in vitro: establishment of hormone-stimulated growth and drug-induced cytostatic and cytotoxic effects. The Prostate 12:99-110, 1988

[24] Verkoelen CF, Romijn JC, de Bruijn WC, Boevé ER, Cao LC, Schröder FH: Absence of a transcellular transport mechanism in LLC-PK_1 and MDCK cells cultured on porous supports. Scann Microsc 7:1031-1040, 1993

[25] Smith LH: Pathogenesis of renal stones. Min Elect Metab 13:214-219, 1987

[26] Finlayson B, Reid F: The expectation of free and fixed particles in urinary stone disease. Invest Urol 15:442, 1978

[27] Hackett RL, Shevock PN, Kahn SR: Cell injury associated calcium oxalate crystalluria. J Urol 144:1535-1539, 1990

[28] Sepúlveda FV, Burton KA, Pearson JD: The development of γ-glutamyltransferase in a pig renal-epithelial-cell line *in vitro*. Biochem J 208:509-512, 1982

[29] Lieske JC, Walsh-Reitz MM, Toback FG: Calcium oxalate monohydrate crystals are endocytosed by renal epithelial cells and induce proliferation. Am J Physiol 262:F622, 1992

[30] Lieske CL, Spargo BH, Toback FG: Endocytosis of calcium oxalate crystals and proliferation of renal tubular epithelial cells in a patient with type 1 primary hyperoxaluria. J Urol 148:1517-1519, 1992

[31] Cheung HS, McCarty DJ: Mitogenesis induced by calcium-containing crystals. Role of intracellular dissolution. Exp Cell Res 157:63-70, 1985

[32] Boevé ER, Ketelaars GAM, Vermeij M, Cao LC, Schröder FH, de Bruijn WC: An ultrastructural study of experimentally induced microliths in rat proximal and distal tubules. J Urol 149:893-899, 1993

[33] de Bruijn WC, Boevé ER, van Run PRWA, van Miert PPMC, Romijn JC, Verkoelen CF, Cao LC, Schröder FH: Etiology of experimental calcium oxalate monohydrate nephrolithiasis in rat kidneys. Scann Microsc, in press

[34] Menon M, Ayvazian P, Hodapp J, Malhotra R, Renzulli L, Scheid C, Koul H: Oxalate-induced proximal tubular cell damage. J Urol 149:440A, 1993

[35] Kahn SR, Hackett RL: Hyperoxaluria, Enzymuria and Nephrolithiasis. Contrib Nephrol 101:190-193, 1993

[36] Mortell KH, Marmorstein AD, Cramer EB: Fetal bovine and other sera used in tissue culture increase epithelial permeability. In Vitro Cell Dev Biol 29A:235-238, 1993

Chapter 5

CRYSTAL-CELL INTERACTION INHIBITION BY POLYSACCHARIDES

CF Verkoelen, JC Romijn, LC Cao, ER Boevé,
[1]WC de Bruijn, and FH Schröder.

Department of Urology and [1]AEM-Unit Institute of Clinical Pathology Erasmus University Rotterdam, The Netherlands.

Journal of Urology 155:749-752, 1995

Chapter 5

Abstract

Purpose: We studied the effects of polysaccharides on interactions between calcium oxalate monohydrate (COM) crystals and cultured renal cells.
Materials and Methods: Monolayers of MDCK cells were incubated with radiolabelled crystals in the presence of various concentrations of natural glycosaminoglycans (GAGs) and semi-synthetic polysaccharides (SSPs).
Results: While most GAGs were found to have relatively little effect, SSPs (SP54, G871 and G872) were potent inhibitors of crystal-cell association. Pretreatment of crystals, but not of cells, was similarly effective, suggesting polysaccharide-induced modification of crystal surface properties.
Conclusions: This result further supports the idea that SSPs, and especially G872, are of potential interest for treatment of recurrent stone disease.

Introduction

Urinary supersaturation, crystal growth and agglomeration and crystal retention are considered important factors in the pathogenesis of calcium oxalate nephrolithiasis [1,2,3]. Crystal retention could be caused by physical trapment as a result of increased particle size, disturbed urinary flow or adhesion to the brush border of renal tubular cells [4]. Several investigators reported on the attachment and subsequent interaction of calcium oxalate crystals with renal tubular cells in culture [5,6]. The possible role of GAGs in crystal-cell interaction has not yet been fully investigated. Urinary GAGs are found to be potent inhibitors of crystallization [1,2,3]. Metabolic disorders resulting in a modification of the characteristics of urinary GAGs could play a role in renal stone disease. Several GAGs are known to occur in urine including hyaluronic acid (HA), chondroitin-4-sulfate (CS-A), dermatan sulfate (CS-B), chondroitin-6-sulfate (CS-C), heparan sulfate (HS), and keratan sulfate (KS) [1,2]. In addition GAGs are also present at the apical surface of renal tubule cells where they are linked as polysaccharide side-chains to the core proteins of plasma membrane associated proteoglycans [7]. It has been suggested that these cell surface constituents in uroepithelial cells provide a protective layer that prevents retention of crystals [8,9].

Considering the relatively high turn-over of the cell surface coat, shedded GAGs may constitute a major fraction of the urinary GAG pool. Since the inhibitory activity of crystallization in the urine of recurrent stone formers is often decreased [3], it has been suggested that oral administration of synthetic polysaccharides could contribute to the prevention of stone formation by increasing the overall urinary inhibitory activity [1,2,10,11]. In cooperation with the Ocean University of Qindao, China, our institute investigates the potential use of a group of SSPs derived from marine algae [1,10,11,12]. These substances have been shown to be powerful inhibitors of crystal growth and agglomeration. This paper describes the effect of various polysaccharides on COM crystal-cell interaction.

Materials and Methods

Cell culture

MDCK cells, strain II, were obtained from the American Type Culture Collection (ATCC, Rockville, MD, USA) and used between passage numbers 30 and 50. The cells were cultured in Dulbecco's modified MEM supplemented with 10 % fetal calf serum, 20 mM HEPES, 2 mM L-glutamine, 100 IU/ml penicillin and 100 μg/ml streptomycin. The medium was refreshed every two days. The cells were routinely grown in plastic tissue culture flasks (Costar, Badhoevedorp, The Netherlands) at 37°C in a humidified atmosphere of 5% CO_2 in air. Subculturing was performed weekly with 0.05% trypsin/0.02% EDTA (GIBCO-BRL,UK). Cultured in a two compartment culture system on 24 mm porous cell culture inserts with a 0.4 μm pore size (Costar, Badhoevedorp, The Netherlands), MDCK cells form polarized monolayers. Cells were seeded at a density of 1 x 10^6 cells/insert. Although closed monolayers were formed within two days the cells were cultured for an additional period of time to allow full expression of differentiated characteristics. Crystal-cell interaction studies were performed eight days after seeding the cells [13].

Preparation of CaOx crystal suspensions

A solution of radioactive oxalic acid was prepared by adding 1 ml 0.01 mCi/ml (0.37 MBq/ml) [^{14}C]oxalic acid (4.03 GBq/mmol, Amersham International plc., Buckinghamshire, UK) to 0.5 ml 200 mM sodium oxalate. A calcium chloride solution was prepared by adding 0.5 ml 200 mM calcium chloride to 8 ml distilled water. After mixing the two solutions at room temperature, resulting in a final concentration of 10 mM for both calcium and oxalate, [^{14}C]-labeled CaOx crystals with an average size of 2.03 μm [13] were formed immediately. The

suspension was allowed to equilibrate for three days. The crystals were then washed three times with (sodium and chloride-free) CaOx saturated distilled water, resuspended and stored in 5 ml of this solution. The radioactive crystal suspension contained 2.92 mg CaOx crystals/ml. X-ray diffraction of the crystals was studied with an X-ray generator PW 1729/00 connected to an Integrator/Interface PW 1842 (Philips) and demonstrated that they consisted exclusively of calcium oxalate monohydrate (COM).

Crystal-cell interaction studies

We studied crystal-cell interaction in a CaOx saturated buffer (buffer B) that was prepared by the addition of an excess COM crystals (3 mg/ml) to a buffer (pH 6.7) containing (in mM): 118 NaCl, 5.3 KCl, 1.8 $CaCl_2$, 6.6 $NaHCO_3$, 1.3 $MgSO_4$, 2.0 NaH_2PO_4, and 20 HEPES. The cells were washed and preincubated with HEPES buffered serum-free DMEM, added to the apical compartment facing the luminal plasma membrane and the basal compartment facing the contraluminal plasma membrane. After one hour, 1.5 ml buffer B was added to the apical compartment and 2.6 ml fresh serum-free DMEM to the basal compartment. Polysaccharides were added at the apical side of the monolayers. Subsequently, 50 μl of the crystal suspension (146 μg), prepared as described above, was distributed homogeneously on top of the cells. After an incubation period of 60 minutes, the monolayers were rinsed in three successive buffer B baths, to remove non-associated crystals. The filter inserts were cut out with a scalpel and transferred to a scintillation vial. To extract radioactivity, 1 ml 1M perchloric acid was added and the amount of radioactivity was counted in a liquid scintillation counter (Packard, UK). The results were calculated as dpm/filter and expressed as percentage crystal-cell association compared to untreated controls. The inhibitory activity of the various polysaccharides was expressed as IC-50 values which represents the concentration that results in a 50% inhibition compared to untreated controls.

To investigate whether polysaccharides interacted with the cells, the monolayers were incubated with the compound of interest in a volume of 1.5 ml for periods of 5 minutes to 48 hours. After this treatment the monolayers were rinsed three times with PBS and crystal-cell interaction was studied as described. To investigate whether polysaccharides interacted with the crystal surface, the compound of interest was added to the crystal suspension (146 μg crystals in 1.5 ml buffer B). After 5 minutes the suspension was centrifuged, the supernatant removed and the crystals washed three times with fresh buffer B. Washed crystals were resuspended in fresh polysaccharide-free buffer B and crystal-cell interaction studies performed as described.

Polysaccharides

G871 and G872 [11], semi-synthetic sulfated polyguluronic propionates, extracted from marine algae and prepared through physico-chemical modification, were kindly provided by Prof. Guan Hua-Shi, director of the Institute of Food and Drugs, Ocean University of Qingdao, China. Pentosan polysulfate (SP54), a semi synthetic oligosaccharide, obtained after the sulfation of a naturally occurring xylan composed of repeating ß-D-1->4-xylopyranose residues was provided by Bene Artzneimittel GmbH (München, FRG). Glycosaminoglycans are naturally occurring highly negatively charged linear polysaccharides. They are composed of repeating disaccharide units of alternating hexosamine and hexuronic acid residues. Heparin (porcine intestinal mucosa), heparan sulfate (bovine kidney), chondroitin sulfate-A (bovine trachea), CS-B (bovine mucosa), and CS-C (shark cartilage) and hyaluronic acid (human umbilical cord) were obtained from Sigma Chemical Co. (St.Louis, USA).

Statistics

All experiments are performed at least two times. The results are presented as means $\pm$ S.D. of three independent filters. Statistical analysis was performed with a one way analysis of variance (ANOVA) or Student's *t*-test. Differences were considered significant at $P < 0.05$.

Results

Crystal-cell interaction studies are performed in the presence of various polysaccharides. In the group of naturally occurring GAGs, HA and CS-C in concentrations up to 100 μg/ml do not exhibit an inhibitory effect that is significantly different from untreated controls. A concentration-dependent statistically significant inhibitory effect is observed with H, HS, CS-A and CS-B (ANOVA, $P<0.05$). Heparin, the most effective natural polysaccharide, inhibits COM-crystal interaction with MDCK cells for about 90% at a concentration of 25 μg/ml (Fig.1). The SSPs tested exhibit strong inhibitory activity at much lower concentrations. All three semi-synthetic compounds have a statistically significant inhibitory effect (ANOVA, $P<0.05$) on the association of COM-crystals in a range of 0.01-2.0 μg/ml (Fig.2). The IC-50 values derived from the curves shown in Figs.1 and 2, are listed in Table 1. The most potent inhibitor is G872. The inhibitory effect of G872 on crystal-cell interaction at concentrations of 0.5 and 2 μg/ml is significantly stronger compared to G871 and SP54 at these concentrations (Fig.2).

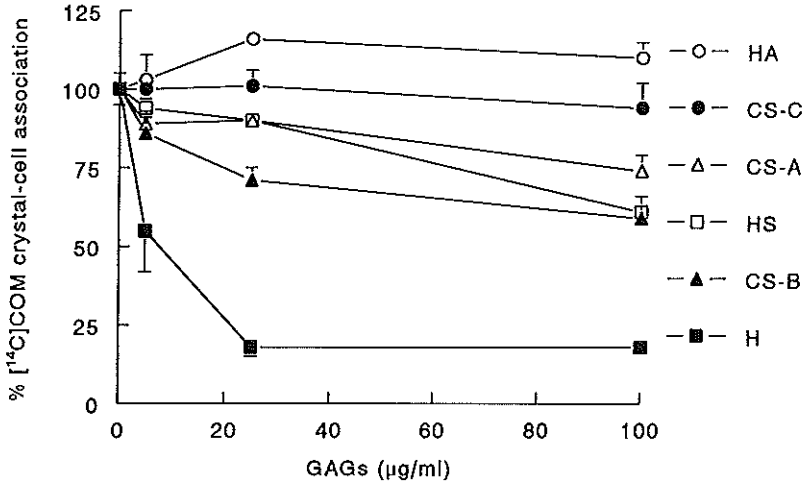

*Fig.1 Effect of glycosaminoglycans on the interaction of COM crystals with MDCK cells (HA: hyaluronic acid; CS-A,B,C: chondroitin sulfate-A,B,C; HS: heparan sulfate; H: heparin). Statistically significant trend is observed with H, HS, CS-A and CS-B (ANOVA, $P<0.05$, $n=3$). *: Significant difference between H and other GAGs (Student's t-test, $P<0.001$, $n=3$).*

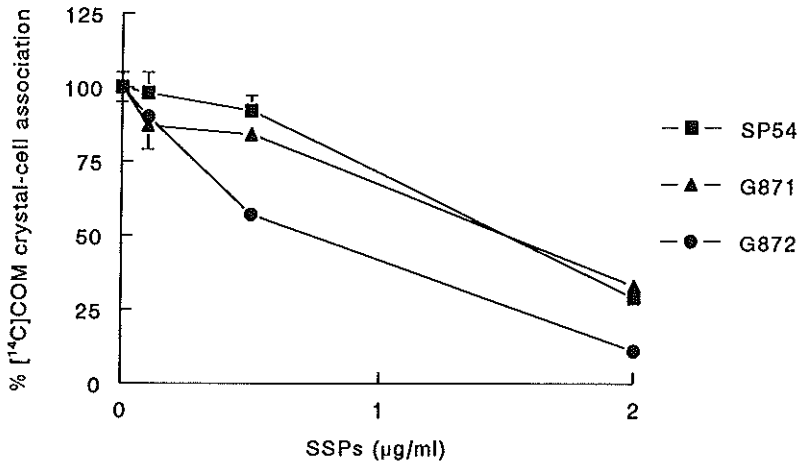

*Fig.2 Effect of semi-synthetic polysaccharides (SP54, G871 and G872) on the interaction of COM crystals with MDCK cells. Statistically significant trend with H, HS, CS-A and CS-B (ANOVA, $P<0.05$, $n=3$). *: Significant difference between G872 and other SSPs (Student's t-test, $P<0.001$, $n=3$).*

Table 1 IC-50 (μg/ml) of polysaccharides in COM crystal-cell interaction inhibition.

polysaccharide	IC50
hyaluronic acid	> 100
heparan sulfate	> 100
chondroitin sulfate-A	> 100
chondroitin sulfate-B	> 100
chondroitin sulfate-C	> 100
heparin	3.1
SP54	2.0
G871	1.8
G872	0.6

Pretreatment

To investigate whether the inhibitory effects of polysaccharides on crystal-cell interaction are caused by alterations of the cell surface, of the crystal surface or of both, cells and crystals are individually treated prior to the determination of their interaction. Based on the data shown in Figs. 1 and 2, concentrations of G872 (2 μg/ml) and heparin (25 μg/ml) are selected with comparable inhibitory effects on crystal-cell interaction (10 ± 2 and 18 ± 3 % of control, see Table 2). Pretreatment of the cells for 5min, 1h, 24h or 48h by either compound, does not cause significant inhibition of interaction with crystals (Table 2). The same result is obtained with CS-B, HS or SP54 (not shown). In contrast, preincubation of the crystal suspension (followed by extensive washing as described in **Materials and Methods** and without subsequent addition of polysaccharides) results in an inhibitory effect that is of the same order of magnitude as the inhibition obtained in the continuous presence of these compounds (23 ± 3 and 15 ± 3 % of control, see Table 2).

Table 2 Effect of continuous exposure with and pre-incubation to polysaccharides on crystal-cell interaction. Data expressed relative to the amount of crystals associated with untreated controls (100%).

	continuous exposure (%)	pretreated cells (%)	pretreated crystals (%)
Heparin, 25 μg/ml	10 ± 2	106 ± 3	23 ± 3
G872, 2 μg/ml	18 ± 3	95 ± 2	15 ± 3

Discussion

The association of CaOx crystals with renal tubular cells could be an early event in the pathogenesis of nephrolithiasis. After the induction of hyperoxaluria and subsequent crystaluria it has been found that crystals are retained in the renal tubules of rats [14,15]. Scanning electron microscopic images demonstrated that CaOx crystals were tightly attached to the luminal surface of renal tubular cells in a patient with hyperoxaluria [16]. In patients with primary hyperoxaluria who received a kidney transplant postoperative biopsies revealed the presence of CaOx crystals within renal tubular cells [17]. We have previously characterized a model system in which the association of CaOx oxalate crystals with MDCK monolayers is investigated using radioactively labeled COM-crystals [13]. Monolayer-associated radioactivity represents crystals attached to the cell surface as well as endocytosed crystals [13]. The present study was initiated to reveal the possible inhibitory effect of naturally occurring and synthetic polysaccharides on crystal-cell association. Having confirmed such an inhibitory activity, it was shown that interaction of polysaccharides with the crystal surface, rather than with the cell surface accounted for the observed effect.

It was demonstrated in a previous study [11] using a constant composition crystallization model and a seeded crystal growth system that G871, G872 and SP54 (10 μg/ml) exhibited strong inhibitory effects on COM-

crystal growth and agglomeration in artificial urine and were capable to shift the COM particle zeta potential in negative direction. G872 had a significantly greater effect than either G871 or SP54 on all the measured parameters [11]. The present study showed that SSPs are also potent inhibitors of crystal-cell interaction with IC-50 values ranging from 0.6-2.0 μg/ml (Table 1). Again G872 was the most effective compound. Naturally occurring GAGs had only limited efficacy in this system (Fig.1). Only relatively high concentrations of HS, CS-A and CS-B (100 μg/ml) resulted in some protection of the cells against the interaction with COM-crystals. The only naturally occurring polysaccharide that exhibits a considerable inhibitory activity was heparin. However, heparin is normally not present in human urine. Although other natural GAGs are excreted in the urine (average amount $\pm$ 25 mg/day) [18] and described to contribute to the overall urinary inhibitory activity [1,2,3] the results from this study indicate that in this concentration these substances do not seem to play an important role in the prevention of crystal retention. Nevertheless, it cannot be excluded that natural GAGs may confer anti-crystal adherence properties on the cell surface. Being the polysaccharide side-chains of membrane-associated proteoglycans, GAGs constitute a negatively charged hydrophyllic layer that binds water molecules and thereby protects the cell membrane against direct contact with circulating material. Free GAGs from the incubation medium, however, will not be readily incorporated into such a structure because the assembly of proteoglycans is a complex intracellular process. Inhibition of crystal-cell interactions by polysaccharides was also reported from studies with rat bladder [8,9]. GAGs at the surface of rat bladder epithelium were found to act as natural barriers against the adherence of crystals. Damage of the mucous layer resulted in increased CaOx crystal retention, which could be reduced by the administration of heparin or SP54 [8]. Gill et al. [9] demonstrated that in contrast to heparin, CS-C and HA could not prevent CaOx crystal adhesion to the chemically injured rat bladder. The presence of cell surface GAGs, mainly located at the apical plasma membrane, was also demonstrated in kidney cells [7], including MDCK cells [19].

The fact that SSPs are effective in inhibiting crystal growth and agglomeration as well as crystal-cell interaction suggests that treatment of recurrent stone formers with these compounds could contribute to the prevention of stone formation. However, in preliminary clinical studies, SP54 proved ineffective as a treatment for recurrent stone formers,

mainly because of its limited urinary excretion after oral administration [20]. Preliminary studies in our institute have suggested that G872 may prove more useful than SP54 since its urinary excretion seems to be higher after oral administration (unpublished observation).
In conclusion, G871 and G872 are potent inhibitors of the interaction of COM crystals with MDCK cells and their inhibitory activity seems to be mediated by their ability to alter crystal properties. Although it can not be excluded that the observed effects of polysaccharides in this study are specific for our model system, it could also reflect a general mechanism of action. To test this hypothesis, animal experiments are currently performed in our laboratory to further investigate the possible value of these compounds in the treatment of recurrent renal CaOx stone disease.

This study was supported by the Dutch Kidney Foundation through grant C 92.1235.

References

[1] Boevé ER, Cao LC, Verkoelen CF, Romijn JC, de Bruijn WC, Schröder FH (1994) Glycosaminoglycans and other sulphated polysaccharides in calculogenesis of urinary stones. World J Urol 12:43,

[2] Sallis JD (1987) Glycosaminoglycans as inhibitors of stone formation. Mineral Electrolyte Metab.13:273

[3] Menon M, Koul H (1992) Calcium oxalate nephrolithiasis. J Clin Endocrin Metab 74:703

[4] Kok DJ, Khan SR (1994) Calcium oxalate nephrolithiasis, a free or fixed partcle disease. Kidney Int 46:847

[5] Riese RJ, Mandel NS, Wiessner JH, Mandel GS, Becker CG, Kleinman JG (1992) Cell polarity and calcium oxalate crystal adherence to cultured collecting duct cells. Am J Physiol 262:F177

[6] Lieske JC, Toback FG (1993) Regulation of renal epithelial cell endocytosis of calcium oxalate monohydrate crystals. Am J Physiol 264:F800

[7] Spicer SS, Baron DA, Sato A, Schulte BA (1981) Variability of cell surface glycoconjugates. J Histochem Cytochem 29:994

[8] Parsons CL, Stauffer C, Schmidt JD (1980) Bladder-surface glycosaminoglycans: an efficient mechanism of environmental adaptation. Science 208:605

[9] Gill WB, Jones KW, Ruggiero KJ (1981) Protective effects of heparin and other sulfated glycosaminoglycans on crystal adhesion to injured urothelium. J Urol 127:152

[10] Cao LC, Boevé ER, Schröder FH (1991) The mechanisms of action of glycosaminoglycans (GAGs) in calcium oxalate stone prevention:a review. J Lithotr Stone Dis 3:324

[11] Cao LC, Boevé ER, Schröder FH, Robertson WG, Ketelaars GAM, de Bruijn WC (1992) The effect of two new semi-synthetic glycosaminoglycans (G871,G872) on the zeta potential of calcium oxalate crystals and on growth and agglomeration. J Urol 147:1643

[12] Boevé ER, Cao LC, Schröder FH, Ketelaars GAM, Vermey M, de Bruijn WC (1990) The influence of 3 exogeneous glycosaminoglycans on the experimental induction of microliths in rats. Urol Res 18:62

[13] Verkoelen CF, Romijn JC, de Bruijn WC, Boevé ER, Cao LC, Schröder FH (1995) Association of calcium oxalate monohydrate crystals with MDCK cells. Kidney Int 48:129

[14] Kahn SR, Hackett RL (1991) Retention of calcium oxalate crystals in renal tubules. Scann Microsc 5:707

[15] de Bruijn WC, Boevé ER, van Run PRWA, van Miert PPMC, Romijn JC, Verkoelen CF, Cao LC, Schröder FH (1994) Etiology of experimental calcium oxalate monohydrate nephrolithiasis in rats. Scann Microsc 8:541

[16] Morgenroth K, Backmann R, Blaschke R (1968) On the formation of deposits of calcium oxalate in the human kidney in oxalosis. Beitr Path Anat 136:454

[17] Lieske CL, Spargo BH, Toback FG (1992) Endocytosis of calcium oxalate crystals and proliferation of renal tubular epithelial cells in a patient with type 1 primary hyperoxaluria. J Urol 148:1517

[18] Hwang TIS, Preminger GM, Poindexter J, Pak YC (1988) Urinary glycosaminoglycans in normal subjects and patients with stones. J Urol 139:995

[19] Takeuchi J, Mitsuko S, Mikihiro S, Masahiko Y, Emiko S, Leighton J (1977) Cell surface glycosaminoglycans of cell line MDCK derived from canine kidney. Cancer Res 37:1507

[20] Hesse A, Wuzel H, Vahlensieck W (1991) Significance of glycosaminoglycans for the formation of calcium oxalate stones. Am J kidney Dis 17:414

Chapter 6

INCREASED CALCIUM OXALATE MONOHYDRATE CRYSTAL BINDING TO INJURED RENAL TUBULAR EPITHELIAL CELLS IN CULTURE

CF Verkoelen, BG van der Boom,
[1]AB Houtsmuller, FH Schröder, and JC Romijn.

Department of Urology and [1]Pathology, Erasmus University Rotterdam, The Netherlands.

American Journal Physiology 274:F958-F965, 1998

Abstract

The retention of crystals in the kidney is considered to be a crucial step in the development of a renal stone. This study demonstrates the time-dependent alterations in the extent of calcium oxalate monohydrate (COM) crystal binding to Madin-Darby canine kidney (MDCK) cells during their growth to confluency and during the healing of wounds made in confluent monolayers. As determined by radiolabeled COM crystal binding studies and confirmed by confocal scanning laser microscopy (CSLM), relatively large amounts of crystals (10.4 ± 0.4 $\mu g/cm^2$) bound to subconfluent cultures that still exhibited a low transepithelial electrical resistance (TER < 400 $\Omega.cm^2$). The development of junctional integrity, indicated by a high resistance (TER > 1500 $\Omega.cm^2$), was followed by a decrease of the crystal binding capacity to almost undetectable low levels (0.13 ± 0.03 $\mu g/cm^2$). Epithelial injury resulted in increased crystal adherence. The highest level of crystal binding was observed 2 days post-injury when the wounds were already morphologically closed but TER was still low. Confocal images showed that during the repair process, crystals selectively adhered to migrating cells at the wound border and to stacked cells at sites where the wounds were closed. After the barrier integrity was restored, crystal binding decreased again to the same low levels as in undamaged controls. These results indicate that whereas functional MDCK monolayers are largely protected against COM crystal adherence, epithelial injury and the subsequent process of wound healing lead to increased crystal binding.

Introduction

Renal stones are composed of crystals that are generated in the tubular fluid as the result of calcium salt supersaturation. Intratubular retention of crystals is considered a pathological step that ultimately leads to stone formation in the kidney. Various mechanisms have been proposed to explain crystal retention (17). Due to crystal growth and agglomeration, particles may be formed that are too large to freely pass the renal tubules. Alternatively, relatively small crystals could be retained by adhering to the surface of the urothelial lining and then increase in size (17,24). The latter possibility is supported by electron microscopic data showing small crystals attached to the luminal surface of renal tubular

epithelium of stone formers (25). The association of crystals with renal tubule cells has also been observed in patients with disorders in intestinal oxalate absorption or in oxalate metabolism (20,33). Crystal-cell interaction studies in cell culture demonstrated that calcium oxalate crystals have affinity for the renal epithelial cell surface, most likely by interacting with negatively charged membrane components (5,21).
In the present study we examined the impact of epithelial injury on crystal-cell interaction. The idea that renal tubular cell injury might play a role in urolithiasis is supported by several lines of evidence: (a) In clinical studies it was found that idiopathic calcium oxalate stone formers excrete high amounts of brush border and lysosomal enzymes of renal epithelial origin in their urine (1), (b) increased urinary enzyme levels and renal tubular apical membranes were also found in experimental models of stone disease (11,16), and (c) calcium oxalate crystals are able to adhere to injured urothelium of the rat urinary bladder (10,15). Although it is generally assumed that tubule cell damage also increases the risk for crystal retention in the kidney, evidence for this assumption has not yet been provided. Using an established experimental model in which cultured MDCK cells are confronted with preformed COM crystals (30), we studied the effect of epithelial injury on crystal binding. For the first time experimental evidence is provided that renal epithelial damage can lead to increased crystal attachment.

Materials and Methods

Cell culture
High resistance MDCK cell strain I (9) was kindly provided by Prof. G van Meer, Laboratory for Cell Biology and Histology, AMC Amsterdam, The Netherlands. Cells were seeded at a high plating density (2.2×10^5 cells/cm^2) on 24 mm polycarbonate porous filter inserts (Transwells, 0.4 μm pore size, Costar, Badhoevedorp, The Netherlands), and cultured in Dulbecco's modified minimal essential medium (DMEM) supplemented with 10 % fetal calf serum. Medium was refreshed every other day. Cultures were routinely checked for mycoplasma contamination and found to be negative in all experiments described here. In order to reduce variability of the results caused by differences in seeding density, plating efficiency, size of the inflicted wounds, etc., the different parameters were measured with the same filter inserts whenever possible. In some experiments parallel inserts were used with cells that originated from the same population and that were plated at an identical density.

Preparation of CaOx crystal suspensions
The method to generate calcium oxalate monohydrate crystals is a slight modification of the method that has been described previously (30). Briefly, a solution of radioactive sodium oxalate was prepared by adding 1 ml 0.37 MBq/ml [^{14}C]oxalic acid (Amersham Int.plc., Buckinghamshire, UK) to 0.25 ml 200 mM sodium oxalate. A calcium chloride solution was prepared by adding 0.25 ml 200 mM calcium chloride to 8.5 ml distilled water. After mixing the two solutions at room temperature (final concentration of 5 mM for both calcium and oxalate), radiolabeled CaOx crystals were formed immediately. The crystal suspension was allowed to equilibrate for three days, then washed three times with (sodium and chloride-free) CaOx saturated water and resuspended in 5 ml of this solution (1.46 mg CaOx crystals/ml).

Crystal binding
The assay used to measure COM crystal binding is a modification of the method described previously (30). The composition of the incubation buffer in the present study more closely resembled the conditions found *in vivo* in the renal collecting duct. The apical compartment received a buffer (CCD-A) representative for the tubular fluid and contained (in mM): 140 NaCl, 5 KCl, 1.5 $CaCl_2$, 0.5 $MgCl_2$, 50 ureum, pH 6.6, 310-320 mosmol/kg H_2O. This solution was saturated with CaOx. To the basal compartment, representative for renal peritubular capillary plasma, a buffer (CCD-B) was added that contained (in mM): 124 NaCl, 25 $NaHCO_3$, 2 Na_2HPO_4, 5 KCl, 1.5 $CaCl_2$, 0.5 $MgCl_2$, 8.3 D-glucose, 4 L-alanine, 5 Na-acetate, 6 ureum, and 10 mg/ml bovine albumin, pH 7.4, 310-320 mosmol/kg H_2O. Both solutions were equilibrated for 20 min. with 5% CO_2 in air at 37^{0}C and adjusted to pH 6.7 (CCD-A), or pH 7.4 (CCD-B). The cells were washed and preincubated for 10 min with calcium-containing PBS, to be replaced by CCD-A in the apical compartment and CCD-B in the basal compartment. Subsequently, the crystal suspension was vigorously pipetted and 50 μl was distributed homogeneously on top of the cells (16 μg/cm^2). After an incubation period of 60 minutes the monolayers were rinsed extensively to remove all non-associated crystals. The filter inserts were cut out with a scalpel and transferred to a scintillation vial. To extract radioactivity, 1 ml 1M perchloric acid was added and the amount of radioactivity was counted in a liquid scintillation counter (Packard, UK). The amount of associated crystals was calculated from the dpm/filter and the results were usually expressed in μg/cm^2.

[^{3}H]Thymidine incorporation
Culture medium was replaced by fresh medium containing 3.7 KBq/ml [methyl-^{3}H]thymidine (Amersham). After an incubation period of 5 h, the cultures were washed 3 times with PBS, and counted in a liquid-scintillation counter.

Epithelial barrier integrity

The permeability of the monolayers for mannitol (P_{mann}) and the transepithelial electrical resistance (TER) were measured to assess the functional intactness of the epithelial barrier. D-[^{3}H]mannitol (5.6 KBq) was applied to buffer CCD-A and the time-dependent appearance of radiolabeled mannitol at the basolateral side of the monolayers was measured in 200 μl aliquots after 0, 20, 40 and 60 minutes. The clearance of mannitol (C_{mann}) was calculated from the equation V_L.B/A, in which V_L is the volume in the basal compartment (in μl), and A and B the amount of radioactivity (in dpm/μl), measured in the apical and basal compartment, respectively. $P_{mann}=C_{mann}$/min.

The electrical resistance across the epithelium was measured through KCl-agar bridges which connected the bathing solutions to matched calomel electrodes (K401, Radiometer, Copenhagen, Denmark), that in turn were connected to a voltage-clamp amplifier (Qualitron, Amsterdam, The Netherlands). The resistance (in Ω.cm^2), corrected for the fluid resistance between the potential sensing electrodes, was calculated from the change in potential difference while passing a current of 1 μA through the epithelium.

Wounds made in confluent monolayers

To study the effect of epithelial damage on crystal adherence, MDCK monolayers were injured 5 days post-seeding. Strips of cells were scraped off from the monolayer, using the tip of a sterile 10 ml tissue culture pipette. Two perpendicular scratches created a relatively large cross-shaped wound with an approximate area of 100-150 mm^2, equal to about one third of the total filter area. After injury, the process of wound healing was monitored by a number of parameters, including P_{mann}, TER, thymidine incorporation, light and confocal microscopy.

Confocal Laser Scanning Microscopy

After incubation with COM-crystals the cultures were washed extensively with CaOx-saturated PBS to remove all non-adhered crystals. The cells were fixed in 3.7% formaldehyde for 15 min. and then permeabilized for 15 min. with 70% ethanol. Subsequently, the inserts were washed with PBS, cut out and incubated for 15 min. with 5 μg/ml fluorescein isothiocyanate conjugated phalloidin (FITC-phalloidin) at the apical site, washed 2x3 min. with PBS and mounted in Vectashield (Vector Laboratories, USA). After processing as described above, the wounded areas were marked at the bottom of the glass slide and images were made with a Zeiss LSM 410 laser scanning confocal microscope (Zeiss, Oberkochen, FRD). A 488 nm Ar-laser was used to excitate the FITC-phalloidin. COM crystals were detected by their reflection of the 633 nm (red) Kr-laser. The FITC-emission signal and the 633 nm signal reflected by the crystals were separated by a 560 nm beam splitter. The FITC-signal was passed

through a 510-540 nm band-pass filter to block reflection from the 488 nm laser. No blocking filter was used for the reflection signal. To make sure that observed reflections were from the crystals and not from any other materials in the preparation, images were taken from preparations with and without crystals. These studies showed that only the glass-slides and the filter insert reflected in the absence of crystals, whereas the reflecting particles were observed only after the addition of crystals. To study the localization of crystals in the various experiments described above, two types of images were recorded: (a) XY-scans of 512x512 pixels in a focal plane (horizontal scans), and (b) cross-sectional XZ-scans of 512x256 pixels perpendicular to the monolayer (vertical scans).

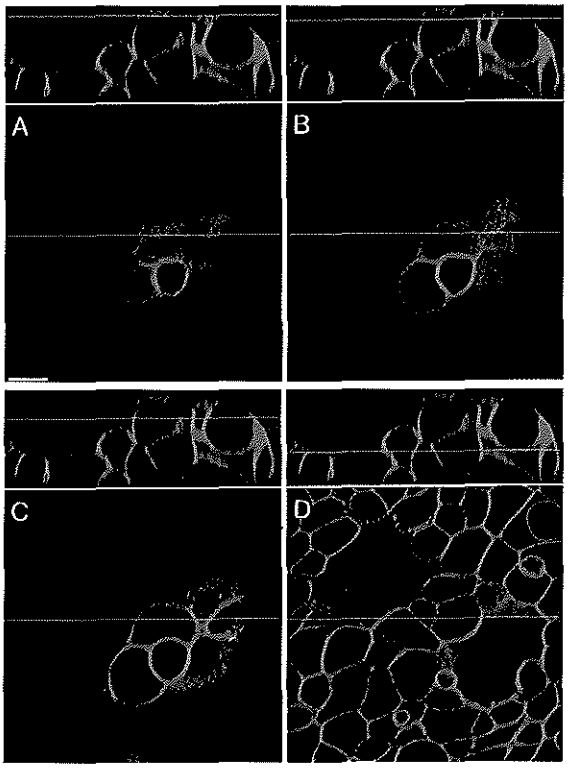

Fig.1. Digital images obtained by confocal microscopy of crystal adherence to stacked cells at various distances form the epithelial surface. The lines in the vertical scans indicate at which height the horizontal scans were taken. After the cells were fixed and permeabilized, F-actin is labeled by fluorescent phalloidin (green), whereas the COM crystals and the polycarbonate inserts are visualized by light reflection (red). Crystal binding is observed at various heights (A, B and C), but can no longer be seen when XY-scans are taken (in this case) >5 μm from the top (D). This series of optical sections demonstrates how the various confocal images presented in this paper were obtained. Bar, 10μm.

The method used for screening crystal binding to cells is shown in Fig.1. A series of XY scans at various heights was performed to detect and localize adherent crystals. Only representative images were selected for the figures that are included in this paper.

Results

Proliferation of MDCK cells to confluent monolayers with a functional epithelial barrier integrity

Freely proliferating MDCK cells double their population relatively fast (population doubling time of approximately 24 h), but cells seeded at high density increased in number more slowly, probably due to cell-cell contact inhibition. After plating $1.0x10^6$ cells per insert, the total number of cells gradually increased to $3.39x10^6$ in 7 days (not shown). In parallel, the total amount of protein increased from 0.16 to 0.65 mg per insert within this time-period (not shown). The permeability of developing monolayers for molecules and ions, monitored by measuring P_{mann} and TER, concomittantly decreased in time. P_{mann} was reduced from approx. 8.5 μl/min directly after seeding to a minimum level of about 0.2 μl/min within three days (Fig.2). TER remained relatively low (<400 $\Omega.cm^2$) during the first three days after seeding, but rapidly increased one day later to high values (1500-4000 $\Omega.cm^2$) to be maintained during the days thereafter (Fig.2).

COM crystal binding during the development of confluent monolayers

The crystal binding capacity of MDCK cells during the development of confluent monolayers was determined in time-course experiments (Fig.2). Relatively large amounts of crystals (approx.10 $\mu g/cm^2$) associated with the cultures during the first 3 days post-seeding. After 4 days in culture a steep decrease in crystal binding was observed (3.72 ± 0.81 $\mu g/cm^2$), followed by a more gradual further decrease to a level as low as 0.16 ± 0.02 $\mu g/cm^2$ after 9 days of culture (Fig.2). These results were confirmed by confocal microscopical images that showed many crystals being firmly attached to the cell surface two days post-seeding (Fig.3A), whereas crystals were not observed on monolayers that had been maintained in for six days (Fig.3B).

Wound healing

The removal of cell strips from the monolayers immediately destroyed the epithelial barrier integrity, indicated by a 15-20 fold increase in the permeability for mannitol and a fall in the electrical resistance (Fig.4). Staining with hematoxylin after epithelial damage showed that the wounds healed rapidly and were already closed within 2 days (Fig.5). During wound healing, P_{mann} gradually decreased to re-obtain low control levels after 2-3 days (Fig.4). The electrical resistance remained at a relatively low level during this time period, but increased rapidly 3-4 days post-injury (Fig.4).

A proliterative response to injury was shown by the transient increase of [^{3}H]thymidine incorporation. There was a two-fold rise one day after damaging the monolayers and then the level gradually decreased again to low control values (Table 1). The observation that confluent monolayers still incorporated baseline levels of [^{3}H]thymidine, suggests that the cells continued to divide at low frequency, most likely reflecting normal cell turnover in confluent monolayers. The migration of MDCK cells into the denuded areas during the wound healing process was visualized 24 h post-injury by confocal microscopy (Fig.6). These images showed flattened cells located at the wound border (Fig.6A,B), intermediately high cells located more distal from the wound border (Fig.6C,D) and relatively high cells in undamaged areas on the same inserts (Fig.6E,F).

COM crystal binding during wound healing

Immediately after the damage was applied, the level of crystal binding increased from 0.2 ± 0.03 to 2.33 ± 0.26 $\mu g/cm^2$. Whereas identical or somewhat lower levels were found one day post-injury (2.14 ± 0.04 $\mu g/cm^2$), crystal binding was maximal (3.90 ± 0.35 $\mu g/cm^2$) at wound closure (Fig.5), two days after inflicting the wounds (Fig.4, Table 1). Crystal binding decreased to low control levels (0.16 ± 0.02 $\mu g/cm^2$) after the monolayers re-obtained high TER values (Fig.4). From these results it was speculated that the crystals preferentially adhered to the cells that were closing the wounds. To test this hypothesis, confluent monolayers were damaged and after a recovery period of 2 days, the cross-shaped area of the former wound was separated from the remaining part of the filter insert after incubation with radiolabeled crystals. Radioactivity counting of the two parts indicated that $>90\%$ of the adhered crystals became associated with the re-epithelialized former wound area.

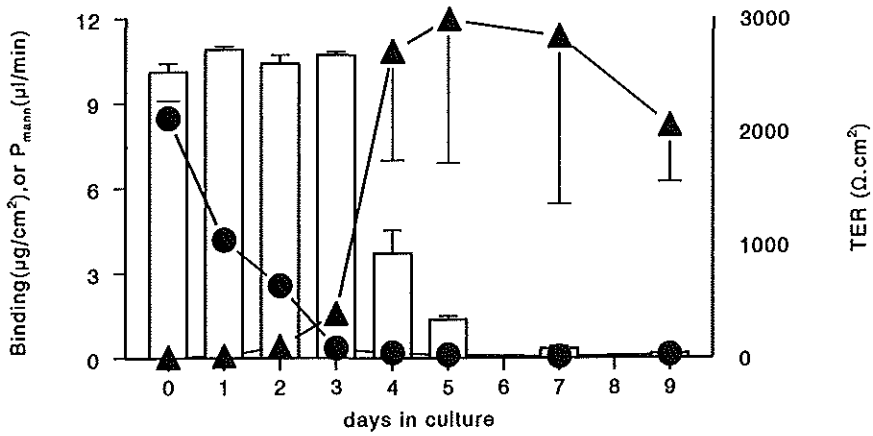

Fig.2. [^{14}C]COM crystal binding in $\mu g/cm^2$ (bars) to MDCK cells during their growth into confluent monolayers. The development of the epithelial barrier to the diffusion of molecules and ions is assessed by P_{mann} in $\mu l/min$ (circles) and TER in $\Omega.cm^2$ (triangles). Crystal binding decreases to almost undetectable levels 6-7 days post-seeding.

Confocal microscopy of crystal binding during wound healing

Crystal binding to damaged MDCK monolayers was studied in more detail by confocal microscopy (Fig.7). Directly after the removal of epithelial strips from an intact monolayer (5 days post-seeding), no crystals were found attached to cells but instead they were found adhered to the growth substrate (Fig.7A). Although attachment of radiolabeled crystals to inserts prior to cell seeding was negligible (<0.3%), a significant amount of radiolabeled crystals (appr. 20%) bound to inserts from which the monolayer was scraped completely. One day post-injury, crystals were observed at the surface of cells that were migrating from the wound border into the denuded area (Fig.7B). In addition, crystals were able to adhere to the remaining open area of the growth substrate (not shown).

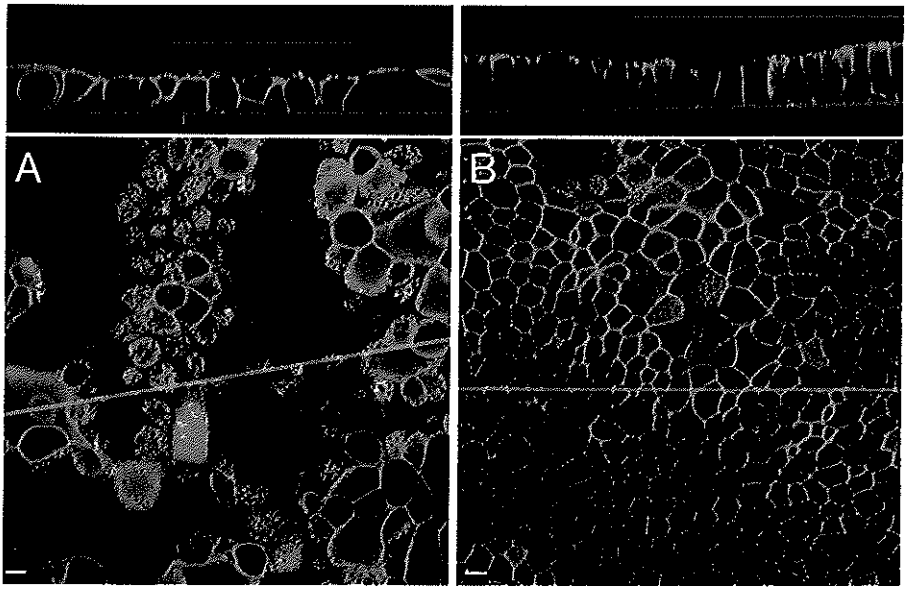

Fig.3. *Confocal microscopic images of MDCK monolayers incubated with COM crystals, two (A) and six (B) days post-seeding. Cells are visualized by Phalloidin-FITC labeled F-actin (green). The growth substrate, the glass-slide placed on top of the cells and the COM crystals are shown by light reflection (red). The lines in the horizontal scans (bottom panels) indicate the location of the vertical scans (top panels). These images clearly show that crystals adhere at the surface of two days cultured MDCK cells, but not to monolayers cultured for six days. Bar, 10μm.*

It should be noticed, however, that binding to the growth substrate is already greatly reduced considering the limited area that is still available for crystal binding at this time (see Fig.5). Crystal binding to cells was not observed in undamaged areas (not shown). At two days post-injury, crystals were found attached to the surface of migrating cells at sites where wound borders almost or just contacted (Fig.7C). At other sites, where wound borders had already contacted and cells that continued to migrate had piled-up to form a "scar", relatively large amounts of crystals were found to be attached to the upper surface of stacked cells (Fig.1 and Fig.7D). Underneath the scar the epithelium regained its differentiated morphology and during the following two days the majority

of the stacked cells were released and probably removed with the next culture medium change. Three days post-injury, crystals were only found attached to remaining areas of stacked cells in the center of the former wound (Fig.7E), whereas one day later the monolayers morphologically resembled undamaged controls and crystals were no longer found attached to the monolayer surface (Fig.7F).

Discussion

The results from the present study show that COM crystal adherence to cultured renal cells is greatly influenced by the developmental stage of the culture. Whereas relatively large amounts of crystals bound to subconfluent monolayers, crystal adherence to confluent cultures with an established barrier function was nearly undetectable.

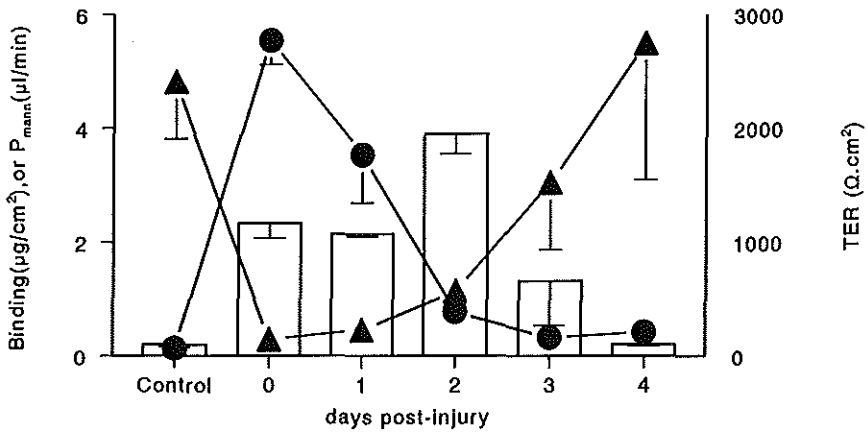

Fig.4. [^{14}C]COM crystal binding in µg/cm² to undamaged confluent monolayers and during the restoration of cultures that were mechanically wounded (bars) into monolayers with a functional barrier integrity, assessed by P_{mann} in µl/min (circles) and TER in Ω.cm² (triangles).

The results obtained with radiolabeled crystals were examined more in detail by confocal microscopy. With this novel technique to study crystal-cell interaction the cells are visualized by fluorescence (phalloidin-FITC) and the crystals by light reflection. These images clearly showed the adherence of crystals to the apical side of monolayers in which TER was still low, whereas crystal binding to functional monolayers was not observed (Fig.3). The apical side of a renal epithelium should protect the cells against harsh conditions in the external environment such as acidity, hydrolases, high and low ionic strength and particles in the tubular fluid including bacteria, parasites, viruses (27), and most likely also crystalline material. To provide such a protective barrier, the apical membrane is stabilized by intermolecular interactions between specific membrane components (6,29). The observed reduction of crystal binding during the development of a functional MDCK monolayer in the present study seems to reflect the establishment of such a protective layer. A steep increase of the electrical resistance was always paralleled by a marked decrease in crystal binding. It is well documented that the establishment of the epithelial barrier integrity reflects the formation of tight junctions (7). These structures function as a barrier for transepithelial diffusion of molecules and ions through the paracellular pathway. Moreover, tight junctions form a fence that prevents mobile proteins and lipids in the exoplasmatic leaflet of the lipid bilayer from diffusing across this boundary between the apical and basolateral membrane (2,27,29). It has been reported earlier that calcium chelation-induced disruption of tight junctions in primary cultured rat inner medullary collecting duct cells resulted in the appearance of a basolateral marker at the apical membrane, concomittant with the enhancement of the level of crystal binding. These effects could be reversed by readdition of calcium. The authors speculated that potential crystal binding molecules normally residing in the basolateral membrane of polarized cells may appear at the luminal cell surface as a result of lateral diffusion of membrane components (26). Also our data suggest that an inverse relationship exists between cell polarity, established after the assembly of tight junctions, and crystal binding. The reduction in crystal binding to polarized MDCK cells could be explained by the disappearance of potential binding molecules from the cell surface. Alternatively, it is possible that the accessibility of the binding sites is reduced by alterations in their molecular conformation or because they become masked by other components such as extracellular surface-associated glycoconjugates. The

polarization process is not completed directly after the tight junctions are formed but apical and basolateral domains are further enriched in specific membrane constituents. Newly synthesized proteins and lipids are delivered to the appropiate destination and some of the components that had been trapped earlier are removed and redistributed (27). This may explain why in the present study, the binding of crystals to MDCK cells continues to decline after the tight junctions are formed (Fig.2). The establishment and maintenance of functional cellular polarity is particularly important in the kidney, where vectorial transepithelial transport depends on the polarized insertion of specific transporters in the plasma membranes of renal tubular cells (2,7). Abnormal intracellular delivery and polarization of membrane proteins can lead to serious diseases, such as cystic fibrosis or autosomal dominant polycystic kidney disease (34). On the basis of the present results it is conceivable that in renal stone disease a faulty polarization of membrane components not only could affect vectorial reabsorption and secretion but also could predispose the tissue for crystal retention.

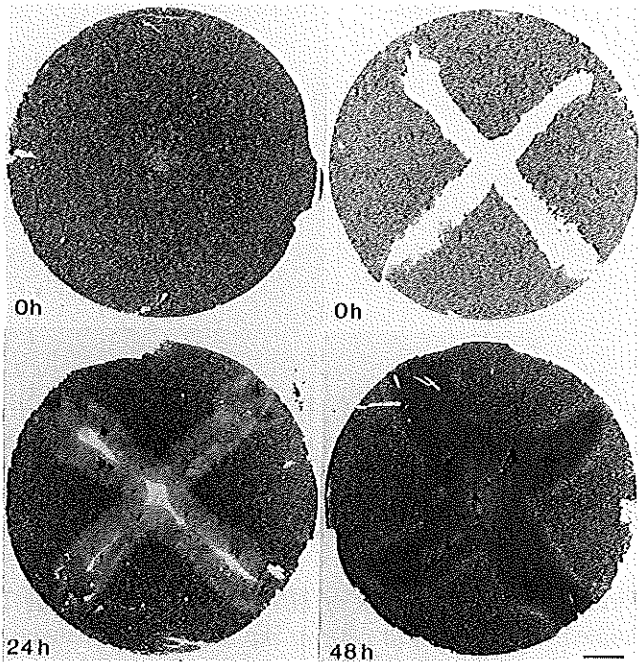

Fig.5. Light microscopic images of the healing of wounds made in intact MDCK monolayers, showing that 48 h post-injury the wounds are morphologically closed. Bar, 3mm.

From the observation that monolayers with an intact barrier function are largely protected from COM crystal binding and from earlier observations that negatively charged molecules in the tubular fluid inhibit crystal-cell interactions (22,31), it can be derived that the renal tubular epithelium is protected from crystal binding by at least two different defence mechanisms: (a) the composition of the apical membranes of polarized renal tubular cells is unfavorable for crystal attachment (b) negatively charged molecules in the tubular fluid prevent crystal retention by covering potential binding sites at the crystal surface. According to this idea, crystal retention will only occur when both putative defence mechanisms are compromised.

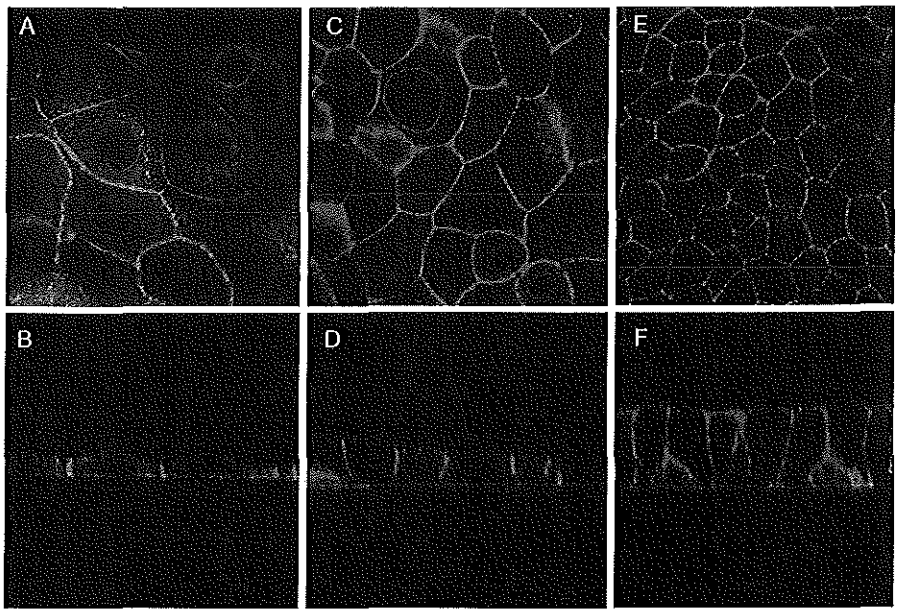

Fig. 6. *Confocal microscopic images of MDCK cells on the same inserts, 24 h post-injury, showing relatively flat cells at the border of the wound (A and B), cells with intermediate height in repopulated zones more distal from the wound border (C and D) and relatively high cells in areas that had not been damaged (E and F). The lines in the horizontal scans (A,C,E) indicate the location of the vertical scans (B,D,F). Bar, 10μm.*

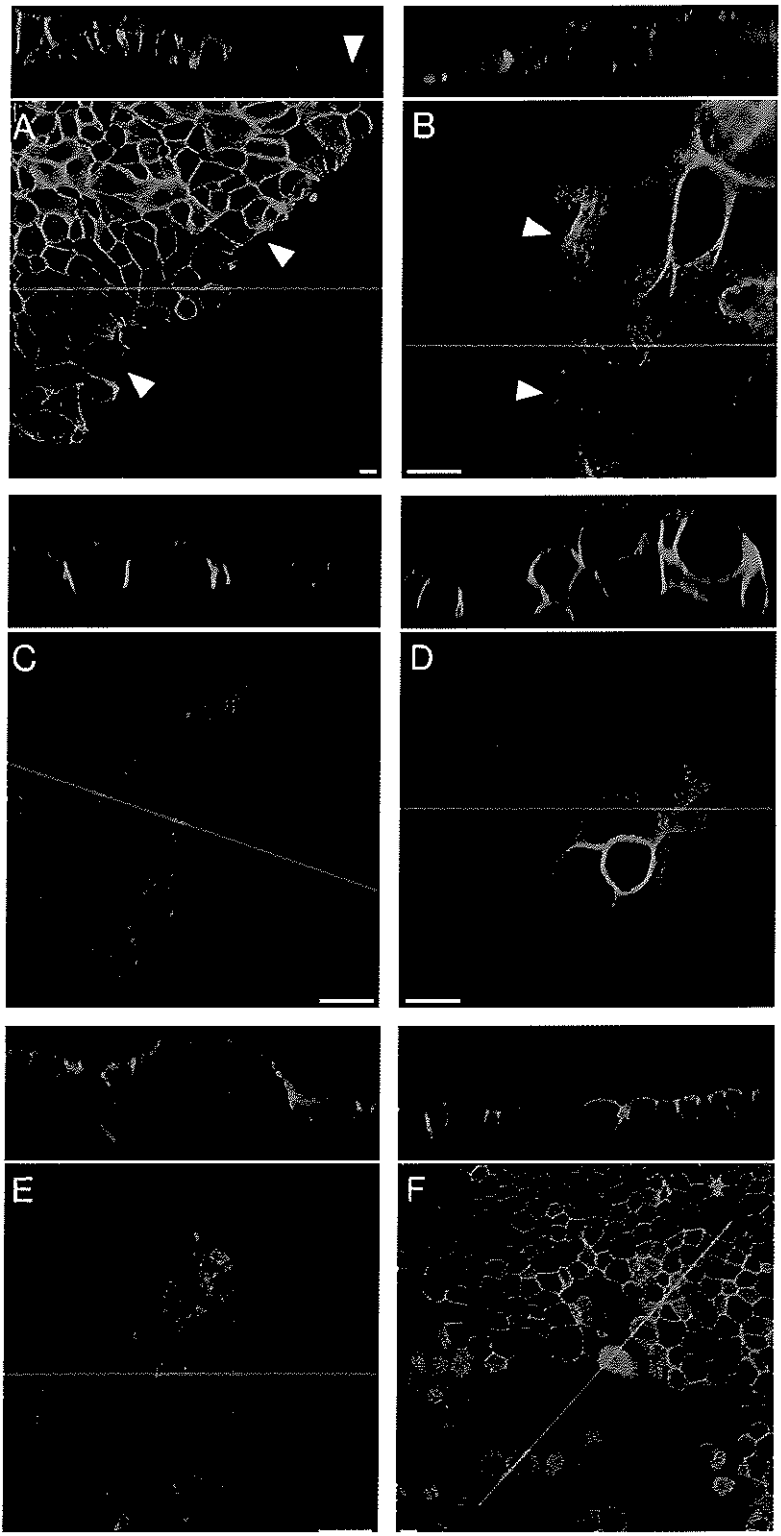
A
B
C
D
E
F

Fig. 7. *(see previous page) Localization of COM crystals after injury and during repair visualized by confocal microscopy. Cells are visualized by Phalloidin-FITC labeled F-actin (green). The growth substrate, the glass-slide placed on top of the cells and the COM crystals are shown by light reflection (red). Functional monolayers (five days post-seeding) cultured on permeable inserts were damaged and immediately or 1-4 days post-injury incubated for one hour with COM crystals. After the removal of all non-adhered crystals, the inserts were prepared for confocal microscopy, as described in Materials and Methods. The lines in the horizontal scans indicate the location of the vertical optical sections through the cell layer. (A) Directly after damage, crystals were not observed at either the cell surface or at the border of the fresh wound (wound border indicated by arrow head in the horizontal scan). The elevated level of crystal binding at this time appeared to be caused by the adherence of crystals to cellular remainings on the newly exposed growth substrate (arrow head in the vertical scan). The presence of crystals on the surface of the bare insert was observed when the horizontal images were inspected more closely to the growth substrate (not shown), which was further confirmed by [^{14}C]COM binding studies (see text). (B) One day post-injury the crystals selectively adhered to migrating cells at the border of the wound (arrow heads). (C) Two days post-injury the wounds were morphologically closed and crystal binding was observed to migrating cells at sites where two wound borders most likely just contacted each other and (D) to cells piling-up from the cell-layer at sites where the wounds were closed. (E) Three days after damaging the cultures, crystals bound only to remaining stacked cells in the center of the former wound. (F) After 4 days practically all stacked cells were released again into the apical medium and crystal binding was no longer observed to cells in the former wound or anywhere else in the culture. Bar, 10μm.*

The results from the present study also show that damaging intact monolayers increases the risk for crystal adherence. Elevated levels of [^{14}C]COM crystal binding were observed immediately after damage was inflicted, but confocal images showed that this initial rise was caused by crystal binding to the newly exposed growth substrate rather than to the remaining cells. This was surprising since we found that crystals had only little affinity for bare inserts. With the use of radiolabeled crystals, however, it was demonstrated that crystals could adhere to inserts from which the cells were scraped. Probably, after scraping cells from the growth substrate typical wound proteins like fibrin, laminin, and fibronectin or other epithelial remainings acted as a glue to which crystals were able to adhere. It is therefore conceivable that the loss of tubular cells can also contribute to crystal retention in the kidney by the

adherence of crystals to components of the exposed basement membrane. The observation that crystal binding is still enhanced while the incorporation of [^{3}H]thymidine already returned to low control levels indicates that cell proliferation is not an absolute requirement for crystal binding. The wound healing process, which proceeds as the combined result of proliferation and migration of cells bordering the wound, entails flattening and dedifferentiation of migrating cells, accompanied by local and temporary disruption of polarity (3,14). During this process crystal binding to cells increased. Confocal microscopy showed that crystals adhered to the surface of cells at the wound border that were migrating into the denuded areas (Fig.7B,C) but not to cells in undamaged areas on the same inserts (not shown). This indicates that during repair crystals preferentially bind to the surface of the dedifferentiated and unpolarized cells. The highest level of crystal binding was observed when wounds were already closed, as judged by morphological criteria, but when TER was still low. Confocal cross sections revealed that at this point crystals also adhered to the surface of stacked cells (Fig.7D,E and Fig.1), that had piled-up at sites where two wound borders contacted each other. The relatively high level of crystal binding that was measured two days post-injury therefore was the combined result of crystals attached to migrating and to stacked cells. During the next days, the repair process was completed as indicated by the disappearance of the stacked cells (Fig.7F) and the re-establishment of a high TER (Fig.4). At this time, the level of crystal binding was reduced again to the low values found in undamaged controls (Fig.4), and crystals were no longer found attached to cells (Fig.7F).

The question that remains to be answered is to which sites at the cell surface crystals become attached in developing monolayers or during repair from injury. Interactions between epithelial cell surfaces and components in the external environment has also been investigated in other fields. The association of cationic proteins with the epithelium was explored to extend the understanding of events at sites of inflammation, and molecular aspects of the attachment of microbes to animal cell surfaces were investigated to obtain more knowledge of infectious processes. Negatively charged membrane phospholipids were proposed as major binding sites for protaminesulfate (19), whereas glycoconjugates were identified as the dominating part of cell surface receptors for the attachment of bacteria and viruses (13).

Table 1. Incorporation of [^{3}H]thymidine and binding of [^{14}C]COM crystals to MDCK monolayers during their recovery from mechanically induced injury.

days post-injury	[^{3}H]thymidine incorporation (dpm/insert)		COM crystal binding (μg/cm^2)	
	undamaged controls	wounded monolayers	undamaged controls	wounded monolayers
0	16636 ±3407	15746 ±1254	0.17 ±0.04	1.99* ±0.31
1	17132 ±3701	35306* ±3757	0.11 ±0.01	0.79** ±0.30
2	17350 ±2192	27742* ±895	0.13 ±0.02	3.90* ±0.74
3	18826 ±2128	11872** ±1869	0.15 ±0.02	0.94 ±1.12
4	17182 ±1956	12691** ±1079	0.10 ±0.04	0.11 ±0.02

*Results from a representative experiment, values are means±SD of three independent measurements. *,** Significantly different from undamaged controls, analyzed with Student's t-test, $P<0.01$ and $P<0.02$, respectively.*

Calcium oxalate crystal binding seems to be less specific, e.g. based on electrostatic interactions between the calcium ions at the crystal surface and negatively charged sites at the cell surface. Negatively charged membrane phospholipids, such as sphingomyelin, phosphatidylinositol and phosphatidylserine (4,5) as well as cell surface glycoconjugates, including sialic acid residues of glycoproteins and glycolipids (21,23) and heparansulfate moieties of membrane associated proteoglycans (32), all have been proposed as candidates for crystal binding sites. If so, these sites apparantly are less available for crystal adherence in a well polarized monolayer of MDCK-I cells. Although it is conceivable that the appearance of potential binding molecules at the apical plasma membrane or that an enhanced accessibility of such sites could predispose the cell surface for crystal retention, the condition(s) under which the renal tissue

may acquire an enhanced affinity for crystals (is) are presently unknown. The results from this study suggest that the regeneration of the injured nephron represents a pathological condition under which the renal epithelium is susceptible for crystal binding. It is not clear which mechanisms are responsible for the epithelial injury that is often observed in stone disease. It could be speculated that a reduction in the amount or quality of the inhibitors of crystallization in the tubular fluid allows enhanced crystal growth and agglomeration leading to the formation of larger particles. During their transit through the nephron these enlarged particles could then injure the epithelium simply by abrasion. On the other hand, it is possible that damage is caused by other forms of epithelial injury such as ischemia (18), crystal attachment (12), inflammatory mediators (8), or high concentrations of xenobiotics such as oxalate (28). Whatever the mechanism of injury may be, the results from the present study suggest that in the kidney increased adherence of crystals may occur after injury and during the repair of wounds.

This study was supported by the Dutch Kidney Foundation through grant C95.1494.

References

[1] Baggio B, G Gambaro, E Ossi, S Favaro, A Borsatti (1983) Increased urinary excretion of renal enzymes in idiopathic calcium oxalate nephrolithiasis. J Urol 129:1161

[2] Balcorava-Ständer J, SE Pfeiffer, SD Fuller, K Simons (1984) Development of cell surface polarity in the epithelial MDCK cell line. EMBO J 11:2687

[3] Bement WM, P Forscher, MS Mooseker (1993) A novel cytoskeletal structure involved in purse string wound closure and cell polarity maintenance. J Cell Biol 121:565

[4] Bigelow MW, JH Wiessner, JG Kleinman, NS Mandel (1996) Calcium oxalate crystal membrane interactions: Dependence on membrane lipid composition. J Urol 155:1094

[5] Bigelow MW, JH Wiessner, JG Kleinman, NS Mandel (1997) Surface exposure of phosphatidylserine increases calcium oxalate crystal attachmant to IMCD cells. Am J Physiol 272:F55

[6] Boggs JM (1987) Lipid intermolecular hydrogen bonding: influence on structural organization and membrane function. Biochim Biophys Acta 906:353

[7] Cereijido ML, Gonzalez-Mariscal, RG Contreras (1988) Epithelial tight junctions. Am Rev Respir Dis 138:S17

[8] Conyers G, L Milks, M Conklyn, H Showell, E Cramer (1990) A factor in serum lowers resistance and opens tight junctions of MDCK cells. Am J Physiol 259:C577

[9] Fuller S, C-H Von Bonsdorf, K Simons (1984) Vescicular stomatitis virus infects and matures only through the basolateral surface of the polarized epithelial cell line, MDCK. Cell 38:65

[10] Gill WB, KW Jones, KJ Ruggiero (1981) Protective effects of heparin and other sulfated glycosaminoglycans on crystal adhesion to injured urothelium. J Urol 127:152

[11] Hackett RL, PN Shevock, SR Kahn (1990) Cell injury associated calcium oxalate crystalluria. J Urol 144:1535

[12] Hackett RL, PN Shevock, SR Khan (1994) Madin-Darby canine kidney cells are injured by exposure to oxalate and to calcium oxalate crystals. Urol Res 22:197

[13] Karlsson K-A (1989) Animal glycosphingolipids as membrane attachment sites for bacteria. Annu Rev Biochem 58:309

[14] Kartha S, FG Toback (1992) Adenine nucleotides stimulate migration in wounded cultures of kidney epithelial cells. J Clin Invest 90:288

[15] Khan SR, CA Cockrell, B Finlayson, RL Hackett (1984) Crystal retention by injured urothelium of the rat urinary bladder. J Urol 132:153

[16] Khan SR, PN Shevock, RL Hackett (1989) Urinary enzymes and calcium oxalate urolithiasis. J Urol 142:846

[17] Kok DJ, SR Khan (1994) Calcium oxalate nephrolithiasis, a free or fixed particle disease. Kidney Int 46:847

[18] Leiser J, BA Molitoris (1993) Disease processes in epithelia: the role of the actin cytoskeleton and altered surface membrane polarity. Biochim Biophys Acta 1225:1

[19] Lewis SA, JR Berg, TJ Kleine (1995) Modulation of epithelial permeability by extracellular macromolecules. Physiol Rev 75:561

[20] Lieske JC, BH Spargo, FG Toback (1992) Endocytosis of calcium oxalate crystals and proliferation of renal tubular epithelial cells in a patient with type 1 primary hyperoxaluria. J Urol 148:1517

[21] Lieske JC, R Leonard, H Swift, G Toback (1996) Adhesion of calcium oxalate monohydrate crystals to anionic sites on the surface of epithelial cells. Am J Physiol 270:F192

[22] Lieske JC, R Leonard, FG Toback (1995) Adhesion of calcium oxalate monohydrate crystals to renal epithelial cells is inhibited by specific anions. Am J Physiol 268:F604

[23] Lieske JC, R Norris, FG Toback (1997) Adhesion of hydroxyapatite crystals to anionic sites on the surface of renal epithelial cells. Am J Physiol 273:F224

[24] Menon M, H Koul (1992) Calcium oxalate nephrolithiasis. J Clin Endocrin Metab 74:703

[25] Morgenroth K, R Backmann, R Blaschke (1968) On the formation of deposits of calcium oxalate in the human kidney in oxalosis. Beitr Path Anat 136:454

[26] Riese RJ, NS Mandel, JH Wiessner, GS Mandel, CG Becker, JG Kleinman (1992) Cell polarity and calcium oxalate crystal adherence to collecting duct cells. Am J Physiol 262:F177

[27] Rodriguez-Boulan E, WJ Nelson (1989) Morphogenesis of the polarized epithelial cell phenotype. Science 245:718

[28] Scheid C, H Koul, WA Hill, J Luber-Narod, L Kennington, T Honeyman, J Jonassen, M Menon (1996) Oxalate toxicity in LLC-PK_1 cells: Role of free radicals. Kidney Int 49:413

[29] Simons K, G van Meer (1988) Lipid sorting in epithelial cells. Biochem 27:6197

[30] Verkoelen CF, JC Romijn, WC de Bruijn, ER Boevé, LC Cao, FH Schröder (1995) Association of calcium oxalate monohydrate crystals with MDCK cells. Kidney Int 48:129

[31] Verkoelen CF, JC Romijn, LC Cao, ER Boevé, WC de Bruijn, FH Schröder (1996) Crystal-cell interaction inhibition by polysaccharides. J Urol 155:749

[32] Verkoelen CF, BG van der Boom, JC Romijn, FH Schröder (1996) Cell density dependent calcium oxalate crystal binding to sulphated proteins at the surface of MDCK cells. In: CYC Pak, MI Resnick, GM Preminger (eds) Urolithiasis, Dallas, Texas, pp 208

[33] Wharton R, VD'agati, AM Magun, R Whitlock, CL Kunis, GB Appel (1990) Acute detoriation of renal function associated with enteric hyperoxaluria. Clin Nephrol 34:116

[34] Wilson PD (1997) Epithelial cell polarity and disease. Am J Physiol 272:F434

Chapter 7

CELL TYPE-SPECIFIC ACQUIRED PROTECTION FROM CRYSTAL ADHERENCE BY RENAL TUBULE CELLS IN CULTURE

CF Verkoelen, BG van der Boom, DJ Kok,
AB Houtsmuller[1], P Visser[2], FH Schröder and JC Romijn

Departments of Urology, [1]Pathology and [2]Cell Biology,
Erasmus University Rotterdam, The Netherlands

submitted

Abstract

Background The adherence of crystals to the surface of renal tubule epithelial cells is considered an important step in the development of nephrolithiasis. Previously, we demonstrated that functional monolayers formed by the renal tubule cell line MDCK acquire protection against the adherence of calcium oxalate monohydrate (COM) crystals. We now studied whether this property is cell type-specific. The susceptibility of the cells to crystal binding was further studied under different culture conditions.
Methods Cell type specificity and the influence of the growth substrate was tested by comparing COM crystal binding to LLC-PK_1 cells and to two MDCK strains cultured on either permeable or impermeable supports. These cell lines are representative for the renal proximal tubule (LLC-PK_1) and distal tubule/collecting ducts (MDCK) segments of the nephron where crystals are expected to be absent and present, respectively.
Results Whereas relatively large amounts of crystals adhered to subconfluent MDCK cultures, the level of crystal binding to confluent monolayers was reduced for both MDCK strains. On permeable supports MDCK cells not only obtained a higher level of morphological differentiation but also acquired a higher degree of protection than on impermeable surfaces. Crystals avidly adhered to LLC-PK_1 cells, irrespective of their developmental stage or growth substrate used.
Conclusions These results show that the prevention of crystal binding is cell type-specific and expressed only by differentiated MDCK cells. The anti-adherence properties acquired by MDCK cells may mirror a specific functional characteristic of its *in situ* equivalent, the renal distal tubule/collecting ducts.

Introduction

Renal stones are largely composed of calcium salts that are precipitated from the tubular fluid. The crystallization of stone salts results from the ability of the kidney to concentrate the tubular fluid [1]. The selective reabsorption of water and solutes takes place in distinct segments of the nephron [2]. The distribution of these reabsorptive capacities is reflected in different risks for crystallization at the various sites in the nephron [3-9]. The first nucleation risk, for example, is encountered in the loop of Henle which disappears as the fluid becomes diluted in the ascending limb and distal tubule [3-9].

During antidiuresis, extensive net water reabsorption leads to an increased risk for crystal formation in the collecting duct towards the papillary tip [4-9]. Crystals formed in the tubular fluid are not necessarily harmful as long as they are eliminated with the urine. Crystal growth and agglomeration, however, could create particles which are too large to freely pass the renal tubules [10-12]. In addition, cell culture studies [13-15] have indicated that crystals can bind to the surface of the renal tubule epithelium. Indeed, crystal deposits with a size smaller than the diameter of the tubules have been found attached to the luminal surface of renal tubular cells in hyperoxaluric patients [16,17] and rats [18].

Previously, we showed that the affinity of the luminal surface of MDCK-I cells for COM crystals highly depends on the developmental stage of the cultures. Relatively large amounts of crystals could adhere to subconfluent cultures, whereas intact and functional monolayers were largely protected from crystal binding [19]. It was speculated that the anti-adherence capacity of functional MDCK cultures may reflect a physiologically relevant property. If so, we expect anti-adherence properties to be present in cell types that are frequently confronted with crystals and absent in cells that normally do not encounter crystals. Indeed, calcium oxalate crystals did not adhere to the surface of the transitional epithelium of the bladder [20], but were found to bind avidly to the surface of red blood cells [21], leukocytes [22], endothelial cells [23] and fibroblasts [24], which are normally not exposed to such crystals. Based on information from the literature, calcium oxalate crystals will be frequently present in the tubular fluid of the renal collecting duct, but not in that passing the proximal tubule. To further test this hypothesis, we now extended the crystal binding studies to include another cell line with characteristics of the renal collecting duct (MDCK-II), as well as a cell line that closely resembles the renal proximal tubule (LLC-PK_1). Since the development of cultured cells is influenced by the substrate on which they are grown, these experiments were performed with cells grown on permeable and impermeable surfaces, to study more closely the relationship between the developmental stage of the cells and crystal binding.

Materials and Methods

Cell culture

MDCK-I [25] and MDCK-II [26] were kindly provided by Prof. G van Meer, Laboratory for Cell Biology and Histology, Amsterdam Medical Center, Amsterdam, The Netherlands. LLC-PK_1 cells were obtained from the American Type Culture Collection (ATCC). The cells were routinely seeded at a plating density of 2.2 x 10^5 cells/cm^2, on either polycarbonate porous filter inserts (Transwells, 24 mm, 0.4 μm pore size), or on tissue culture plates (12 wells, 24 mm, both obtained from Corning Costar, Badhoevedorp, The Netherlands). The cells were cultured in Dulbecco's modified minimal essential medium (DMEM) supplemented with 10% fetal calf serum (FCS). Culture medium was refreshed every other day. The cell lines were routinely checked for mycoplasma contamination and found to be negative in all experiments described in this study. Transepithelial electrical resistances (TER) were measured with an EVOM-G connected to an Endohm-24 (World Precision Instruments, Sarasota, Fl, USA).

Preparation of calcium oxalate crystal suspension

A solution of radioactive sodium oxalate was prepared by adding 1 ml 0.37 MBq/ml [^{14}C]oxalic acid (Amersham Int.plc., Buckinghamshire, UK) to 0.25 ml 200 mM sodium oxalate. A calcium chloride solution was prepared by adding 0.25 ml 200 mM calcium chloride to 8.5 ml distilled water. After mixing the two solutions at room temperature, COM crystals formed immediately. The suspension was allowed to equilibrate for three days and after washing resuspended in 5 ml CaOx saturated distilled water. Crystal suspensions were kept at room temperature and freshly prepared every other week.

COM crystal binding

The assay to measure COM crystal binding was described previously (30). The filters were cut out and the culture dishes were scraped. The level of crystal binding was calculated from the amount of associated dpm's and expressed in $\mu g/cm^2$.

Brush border enzyme measurements

Cell monolayers were washed with PBS, scraped in 1 ml 50 mM Tris-HCl (pH 7.4) and sonicated for 30 s. on ice. After centrifugation for 10 min. at 2000 g the supernatant was used to measure enzyme activity. Gamma-glutamyl transpeptidase (γ-GT, EC 2.3.2.2) activity was determined spectrophotometrically, using L-γ-glutamyl-3-carboxy-4-nitroanilide as substrate and alkaline phosphatase (AP, EC 3.1.3.1) activity was assayed with sodium p-nitrophenylphosphate as substrate.

Na^+,K^+-ATPase polarization

[^{3}H]ouabain (NEN, specific activity 20.5 Ci/mmol) was used to quantify the number of apical and basolateral membrane binding sites [27]. Since the basolateral membrane of cells grown on solid substrates is not accessible, these studies were limited to cells cultured on permeable supports. Total [^{3}H]ouabain binding (0.05 μM) and non-specific binding in an excess of cold ouabain (50 μM) was measured in a binding buffer containing 1 μCi/ml [^{3}H]ouabain in K^+-free Ringer buffer that consisted of (in mM): 140 NaCl, 1.8 $CaCl_2$, 5 D-glucose and 10 tris(hydroxymethyl)aminomethane (Tris).HCl, pH 7.4. The cells were washed twice with PBS and then 1.0 ml binding buffer (37^{0}C) was added at the apical or basolateral side of the monolayers. After 20 min the binding buffer was removed, the cells were washed 10 times in ice-cold Ringer buffer to which 100 mM $MgCl_2$ was added, the filters were cut out with a scalpel and radioactivity was counted in a scintillation counter. The nonspecific binding of radiolabeled ouabain was generally lower than 1%. The amount of ouabain binding was calculated and expressed as fmol/10^6 cells.

Confocal Laser Scanning Microscopy

The cells were fixed in 3.7% formaldehyde for 15 min. and then permeabilized for 15 min. with 70% ethanol. Subsequently, the cells were washed with PBS, and incubated for 15 min with 1 μg/ml fluorescein isothiocyanate conjugated phalloidin (FITC-phalloidin) at the apical site, washed 2x3 min. with PBS and mounted in Vectashield (Vector Laboratories, USA). Images were made with a Zeiss LSM 410 laser scanning confocal microscope (Zeiss, Oberkochen, FRD). A 488 nm Ar-laser was used to excitate the FITC-phalloidin. COM crystals were detected by their reflection of the 633 nm (red) Kr-laser. The FITC-emission signal and the 633 nm signal reflected by the crystals were separated by a 560 nm beam splitter. The FITC-signal was passed through a 510-540 nm band-pass filter to block reflection from the 488 nm laser. No blocking filter was used for the reflection signal.

Scanning electron microscopy

To perform scanning electron microscopy, the cells were fixed in 2.5% glutaraldehyde in cacodylate buffer. After washing, the samples were postfixed in OsO_4 in cacodylate buffer, washed again in cacodylate buffer, dehydrated in a graded serie of ethanol and finally critical point dried. After mounting on stubs a conductive layer was sputtercoated on the samples and examined in a JEOL JSM 25 scanning electron microscope

Results

Cell culture characteristics

When cells were grown to confluence on 24 mm permeable filter inserts or 24 mm solid plastic wells, the monolayers always reached a higher cell density on the porous supports. On inserts, MDCK-I, MDCK-II and LLC-PK_1 became confluent at 3.3 ± 0.3, 3.9 ± 0.4 and 3.9 ± 0.2 $x10^6$ cells, respectively, whereas confluency on plastic wells was reached at respectively, 2.4 ± 0.4, 3.3 ± 0.2 and 1.9 ± 0.4 $x10^6$ cells. Thus, apparently the cells are more densely packed on permeable growth substrates. The transepithelial electrical resistances (TER) of confluent monolayers of MDCK-I, MDCK-II and LLC-PK_1 cells grown on porous supports were, respectively, 8200 ± 3500, 70 ± 15 and 98 ± 15 $\Omega.cm^2$. To determine whether the cell lines formed polarized monolayers on permeable substrates, the binding of [^{3}H]ouabain to Na^+,K^+-ATPase was measured at the apical and basolateral plasma membrane of confluent monolayers. These studies demonstrated an asymmetrical distribution of Na^+,K^+-ATPase with a predominant localization at the basolateral membrane in all three cell lines (Fig.1). The level of proximal tubule brush border enzyme (γ-GT and AP) activities was very high in LLC-PK_1 cells, but almost undetectable low in MDCK-I cells. MDCK-II cells expressed low but measurable AP activities, whereas this cell line expressed intermediately high levels of γ-GT activity (Table 1).

Table 1. *γ-glutamyl transpeptidase (γ-GT) and alkaline phosphatase (AP) enzyme activity (U/mg protein) in homogenates of filter-grown confluent monolayers of MDCK-I, MDCK-II and LLC-PK_1 cells.*

	MDCK-I	MDCK-II	LLC-PK_1
γ-GT	2.0 ± 1.5	323 ± 10	993 ± 45
AP	0.2 ± 0.2	3.7 ± 0.2	331 ± 12

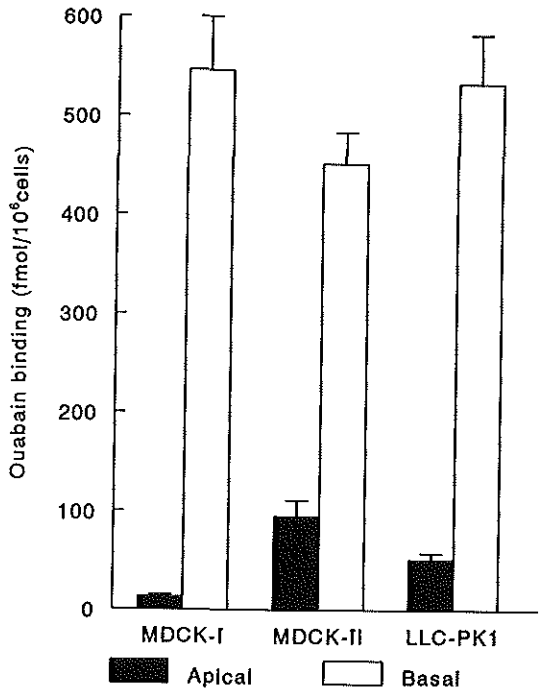

Fig.1. *Plasma membrane distribution of ouabain binding sites. The apical or basolateral membranes of cells grown on pairs of filters for 7 days were incubated with radiolabeled ouabain. The amount of specific binding was determined and expressed in fmoles/10^6 cells. The results show that all three cell lines formed polarized monolayers. Little ouabain binding was detected on the apical membrane, whereas substantial amounts of binding were detected at the basolateral membrane. The results are representative for three experiments.*

COM crystal binding

The binding of COM crystals to cells cultured on permeable and impermeable supports is depicted in Fig.2. Two days post-seeding the level of crystal binding to MDCK-I, MDCK-II as well as to LLC-PK_1 cells, is relatively high, irrespective of the growth substrate on which they were cultured. After MDCK-I cells had formed confluent monolayers the level of crystal binding decreased. Compared to cells grown on impermeable surfaces, the reduction of the crystal binding capacity was substantially

greater in cultures on permeable supports, and in fact, crystal binding was nearly undetectable. A time-dependent decrease in crystal binding was also observed with monolayers formed by MDCK-II cells. On porous supports, these levels did not become as low as those to MDCK-I cells and relatively high levels of crystal binding were measured to confluent MDCK-II monolayers on impermeable supports. There was no significant decrease in crystal binding to LLC-PK_1 cells cultured on either growth substrate during their growth to confluencey (Fig.2).

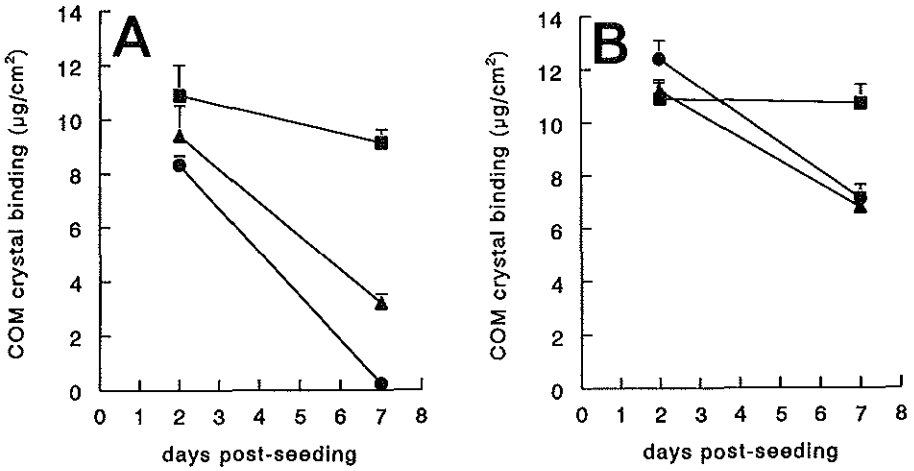

Fig.2. *Binding of COM crystals at the surface of cells cultured on permeable or impermeable growth substrates. Crystal binding was studied 2 and 7 days post-seeding. The apical membrane received radiolabeled COM crystals (16 µg/cm2) that were allowed to adhere for one hour. The level of crystal adherence was calculated from the amount of surface associated dpm and expressed in µg/cm². The results, representative for five experiments, show that both MDCK cell strains cultured on either substrate, acquire protection from the adherence of crystals in time. Strongest anti-adherence properties are obtained by MDCK cells cultured on permeable supports. On permeable supports, MDCK-I cells acquire higher levels of protection than MDCK-II cells. Monolayers formed by LLC-PK_1 cells on either growth substrate acquire no or hardly any protection against the adherence of crystals.*

Morphological studies

The adherence of COM crystals to confluent monolayers, as well as the morphology of the cells, was visualized by confocal microscopy. These studies revealed that there was a remarkable difference in the morphology of MDCK cells cultured on permeable or impermeable supports (Fig.3). On

permeable substrates, the cells formed a tight row of cuboidal cell (Fig.3D,F), resembling the morphology of its in situ equivalent, the collecting duct [28], whereas cells cultured on a solid substrate had a more slender, less differentiated appearance (Fig.3C,E). Morphological differences between LLC-PK_1 cells cultured on either substrate were less conspicuous. On both substrates the cells were rather flat (Fig.3A,B), which is in agreement with the morphology of the epithelium in the renal proximal tubule [28].

These images further showed that COM crystal adherence is abundant to the surface of LLC-PK_1 cells cultured on permeable or impermeable growth substrates (Fig.3A,B), usually less abundant to MDCK-II cells on either substrate (Fig.3C,D), limited to MDCK-I cells cultured on a solid substrate (Fig.3F) and absent at the surface of MDCK-I cells cultured on a permeable surface (Fig.3E).Scanning microscopy images of filter-grown confluent monolayers showed that LLC-PK_1 cells had tall microvilli and single cilea forming the brush border (Fig.4A). COM crystals were found abundantly attached to their surface (Fig.4A). The surface of MDCK-II cells was covered with microvilli that were less tall and with some cilea that seemed to have affinity for the crystals (Fig.4B). The surface of MDCK-I cells was characterized by the presence of many small and stubby microvilli, apparently without affinity for COM crystals (Fig.4C).

Discussion

Previously, we reported that the affinity of the cell surface of high resistance MDCK cells for COM crystals depended on the developmental stage of the cultures [19,29]. Crystal binding decreased during the growth of unpolarized precursor cells into confluent and functional monolayers. The level of crystal binding increased during the repair of wounds made in intact monolayers, to decrease again after the wounds were healed [19]. During this process crystals were found to adhere preferentially to migrating cells at the border of the wound. From these observations it was speculated that the protection against crystal adherence acquired by intact monolayers might reflect a functional property of cells with characteristics of the renal collecting duct. In the present study, this idea was further investigated using cell lines with characteristics from different regions of the nephron. The results show that the level of crystal binding to high resistance MDCK-I and low resistance MDCK-II cells decreased during their growth to confluency.

In contrast, LLC-PK_1 cells were unable to avoid crystal adherence, irrespective of their stage of development. As far as we know, there is one other report in which the binding of COM crystals was studied to epithelial cells during their growth to confluency. These studies showed that the level of crystal binding decreased to confluent monolayers of rat IMCD cells, but not to MDCK cells [30]. Although this seems to be in contrast with our results, it should be mentioned that in the latter study MDCK cells did not form monolayers, but piled up into multilayers. We also found that crystals preferentially adhered to stacked MDCK cells at sites where wound borders contacted [19]. Nevertheless, the results obtained with IMCD cells are largely comparable to those obtained in this study with MDCK cells cultured on solid substrates (Fig.2).

It is often assumed that LLC-PK_1 cells originate from the renal proximal tubule [31] and MDCK cells from the renal collecting duct [32-35]. The observation that the proximal tubule brush border marker enzymes γ-GT and AP were abundantly expressed in LLC-PK_1 but virtually absent in MDCK-I cells is in agreement with their supposed origin. Substantial γ-GT and AP enzyme activities, however, were also detectable in MDCK-II cells. The original MDCK cell line was established from the whole kidney of a dog, and although it exhibits many morphological and functional similarities with the mammalian cortical collecting duct, it has been recognized that this cell line is not homogeneous. Typical characteristics of intercalated cells of the collecting duct (ICC) such as the binding of peanut agglutinin (PNA) as well as the presence of carbonic anhydrase (CA) activity were expressed in 30-50% of the MDCK cells [32]. Over the years, a number of relatively stable MDCK strains were isolated, including low resistance strains [26,32-35] with characteristics of collecting duct α-and ß-ICC [34], and high resistance strains [25,33-36], with characteristics of collecting duct principal cells [34] and ß-ICC [36]. The presence of γ-GT and AP enzyme activities in MDCK-II cells in this study confirms earlier findings [33] and suggests that its brush border shows some resemblance with the proximal tubule. This may explain why the level of crystal binding to MDCK-II cells does not become as low as that observed to MDCK-I cells.

Scanning electron microscopy images revealed an impressive difference in cell surface architecture between the various cell lines. In agreement with the renal proximal tubule, LLC-PK_1 cells have abundant tall microvilli, whereas the villi are much shorter on MDCK-II cells, and distinct short and stubby on the surface of MDCK-I cells. In general, the apical membrane should protect the cell from the harsh conditions in the outside world.

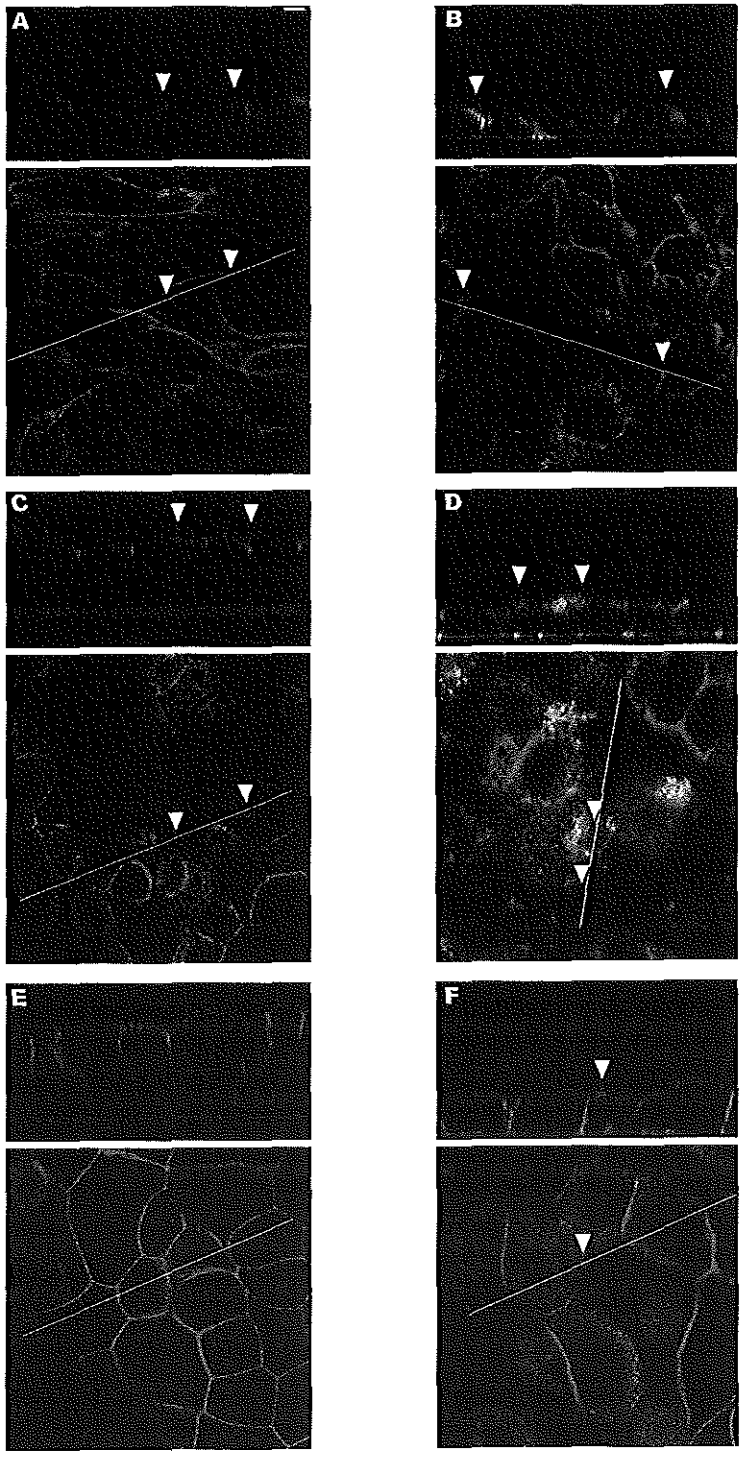
A
B
C
D
E
F

Fig.3. *(see previous page). Confocal microscopy images of the adherence of COM crystals to the surface of confluent monolayers of LLC-PK$_1$ (A,B), MDCK-II (C,D) and MDCK-I (E,F) cells, cultured on permeable (A,C,E) and impermeable (B,D,F) growth substrates. The location of COM crystals is indicated with arrows. The lines in the horizontal scans (bottom panels) indicate the location of the vertical scans (top panels). These images show that MDCK cells cultured on a permeable surface (C,E) are much taller and thus more differentiated compared to cells cultured on a impermeable surface (D,F). This difference in morphological differentiation is less clear in LLC-PK$_1$ cells that have a rather slender appearance cultured on either growth substrate (A,B). Furthermore, these images show the adherence of crystals at the surface of LLC-PK$_1$ (A,B) and MDCK-II (C,D) cells cultured on either growth substrate, whereas crystals are observed at the surface of MDCK-I cells cultured on a solid surface (F), but not to those cultured on a permeable support (E). Bar=10μm.*

One of these harse conditions is the physical contact with calcium oxalate crystals which can inflict severe damage to tissues [37]. In the bladder, polysaccharide side-chains of cell surface associated glycoconjugates were proposed as primary defensive barrier to the adhesion of microbes and microliths [20]. The possiblity that such a protective cell surface coat also explains the repulsion of crystals by functional MDCK cells warrents further investigation. The epithelium lining the renal tubules is composed of a single layer of polarized cells. The apical surface faces the lumen whereas the basolateral side faces the basement membrane. These two plasma membrane domains have different protein and lipid compositions. Each cell in the layer is linked to its neighbors by tight junctions that not only form the permeability barrier between the cells but also inhibit the lateral diffusion of lipids and proteins between the two plasma membrane domains.

We showed that the ability of crystals to become associated with the cell surface decreased rapidly after the tight junctions were formed [19]. Since the polarity of the cell surface increases sharply after tight junction formation [38], we and others [39] suggested that the establishment of epithelial polarity might protect the cell surface from crystal adherence. In the present paper, we studied the possible relationship between the development of the differentiated polarized epithelial cell phenotype and COM crystal binding in more detail.

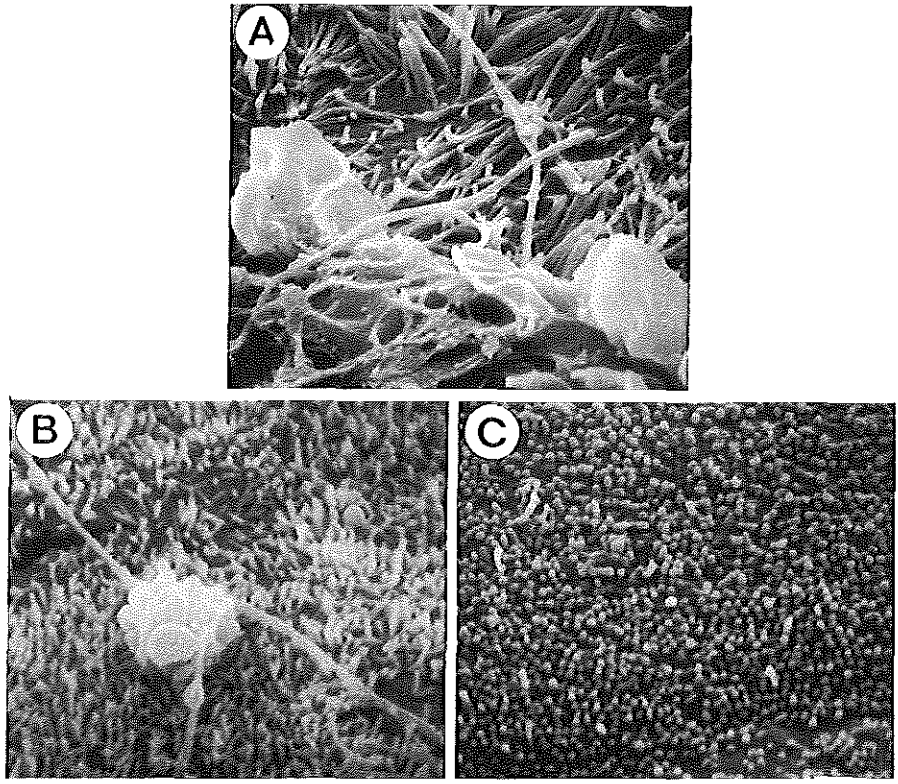

Fig. 4. Scanning electron microscopy images of COM crystal binding to the apical surface of functional monolayers formed by LLC-PK$_1$ (A), MDCK-II (B), or MDCK-I (C) cells, cultured on permeable growth substrates. LLC-PK$_1$ cells have tall microvilli and cilea forming the brush border and COM crystals are found abundantly attached to the cell surface (A). Microvilli of intermediate length and cilea with apparent affinity for COM crystals are seen at the surface of MDCK-II cells (B), whereas the surface of MDCK-I cells is covered by small and stubby microvilli and no crystals are found attached to its brush border (C). Bar=1μm.

It was demonstrated that ouabain, which binds specifically to an extracellular domain of the α subunit of active Na^+,K^+,ATPase [40], predominantly binds at the basolateral membrane of confluent filter-grown monolayers formed by MDCK-I, MDCK-II, as well as by LLC-PK$_1$ cells, indicating that all three cell types formed highly polarized monolayers. Since the degree of epithelial differentiation and polarization also depends on the surface on which the cells are grown [41], we also studied cell morphology and crystal binding to cells cultured on different growth supports. These studies showed that, compared to cells grown on a solid substrate, MDCK

cells grown on permeable surfaces not only achieved a higher degree of morphological differentiation (Fig.3), but also obtained higher levels of protection (Fig.2). These results further support the idea that the ability of crystals to adhere to the MDCK cell surface depends on their stage of differentiation and polarization. Since MDCK-I cells obtained a higher level of polarization than MDCK-II cells (Fig.1), this could explain the differences in susceptibility to crystal binding between these two strains. On the other hand, polarized monolayers formed by LLC-PK_1 cells appeared to be unable to avoid crystal binding, indicating that epithelial polarization certainly is not a general mechanism to protect the cell surface from crystal binding. It should be emphasized, however, that differentiated epithelial cell phenotypes express only those characteristics that are functionally indispensable and that protection from crystal binding could be expressed only in those segments of the nephron where such protection is required.
From the literature on micropuncture and transport studies a reasonable impression can be derived on how factors relevant to calcium-salt precipitation change throughout the nephron. Based on these data several groups have studied the question whether crystallization can start inside the nephron and, if so, in which segments it will most likely start [3-9]. It appears that under normal intratubular conditions calcium-salt crystallization can occur within the time that tubular fluid normally spends in the nephron [4,7]. It starts with a calcium-phosphate phase under conditions found in the thin limbs. This crystallization phase then (partly) dissolves when collecting duct conditions are approached, thereby inducing formation of calcium oxalates [4,7-9]. The relevance of this heterogeneous nucleation is especially clear considering that without these dissolving particles under exactly the same conditions, calcium oxalate formation does not occur within the passage time of fluid through these segments [7]. In the distal tubules and collecting ducts the crystals may increase in size by crystal growth, but never approach sizes in the range of the tubule diameter [10,42]. In the collecting ducts, where crystals emerging from numerous nephrons meet, particle size may increase dramatically by crystal aggregation [10]. These data indicate that starting somewhere in the Loop of Henle, the presence of crystals will be a normal event. Retention of these particles can only take place by adhesion to the tubular epithelium. In the collecting ducts, particles can be retained by adhesion and because of formation of aggregates which are too large to pass freely. This being so, it is reasonable to expect that in the collecting ducts additional protection can be expected from controlling the aggregation process [11,12].

Here, we found that indeed cells with distal/collecting duct characteristics have the ability to prevent crystal adhesion. In contrast, in the proximal tubule crystallization will not take place unless the oxalate concentrations reach the extreme levels as found in e.g. hereditary hyperoxaluria, ethylene glycol intoxication, or animal models of hyperoxaluria [4,7]. This puts our present findings that cells of proximal tubule origin cannot prevent crystal adherence into a functional perspective. It also adds a dimension to the risk posed by high oxalate levels. Namely, crystals are formed at sites which are not prepared to avoid their adherence (Fig.5).

	PT	DlH	AlH	DT	CD
Retention by	Adhesion	Adhesion	Adhesion	Adhesion	Size/adhesion
Anti-adhesion	no	?	?	yes	yes
Crystals present					
Low oxalate	no	starting	yes	yes	yes
High oxalate	yes	yes	yes	yes	yes

Fig.5. The site of calcium oxalate crystal formation and crystal retention in the various segments of the nephron, as well as epithelial surfaces that may be protected from crystal adhesion. PT; proximal tubule, DLH; descending Limb of Henle, ALH; ascending Limb of Henle, DT; distal tubule, CD; collecting duct. Low oxlate; <1000 μmoles/24h, High oxalate; >1000 μmoles/24h.

Taken together, the results from this study show that the binding of COM crystals is reduced to functional and polarized monolayers formed by MDCK cells, but not to those formed by LLC-PK_1 cells. MDCK cells obtain a higher degree of morphological differentiation on permeable supports and are more protected from crystal binding than cells cultured on impermeable growth substrates. These results further support the idea that anti-adhesion properties acquired by differentiated MDCK cells reflects a functional characteristic of its *in situ* equivalent, the renal collecting duct.

Literature

[1] Wexler A, Kalaba RE, Marsh DJ (1991) Three-dimensional anatomy and renal concentrating mechanisms. I. Modeling results. Am J Physiol 260:F368

[2] Berry CA (1982) Heterogeneity of tubular transport processes in the nephron. Ann Rev Physiol 44:181

[3] Asplin JR, Mandel NS, Coe FL (1996) Evidence for calcium phosphate supersaturation in the loop of Henle. Am J Physiol 270:F604

[4] Kok DJ (1997) Intratubular crystallization events. World J Urol 15:219

[5] Lupak I, Bek-Jensen H, Fornander AM, Hojgaard I, Nilsson MA, Tiselius HG (1994) Crystallization of calcium oxalate and calcium phosphate at supersaturation levels corresponding to those in different parts of the nephron. Scanning Microsc 8:47

[6] Deganello S, Asplin J, Coe FL (1990) Evidence that tubule fluid in the thin segment of the Loop of Henle normally is supersaturated and forms a poorly crystallized hydroxyapatite that can initiate renal stones. Kidney Int 37:472 (abstract)

[7] Kok DJ (1996) Crystallization and stone formation inside the nephron. Scanning Microsc 10:471

[8] Tiselius HG, Hojgaard I, Fornander AM, Nilsson MA (1996) Is calcium phosphate the natural promotor of calcium oxalate crystallization? In: Pak CYC, Resnick MI, Preminger GM (eds) Urolithiasis, proceedings VIIIth Int Symp on Urolithiasis. Millett Inc, Dallas pp 238

[9] Tiselius HG, Fornander AM, Nilsson MA (1998) Studies on the crystallization process following addition of calcium phosphate crystals to solutions with a composition corresponding to that in the collecting duct. Scanning Microsc, in press

[10] Kok DJ, Khan SR (1994) Calcium oxalate nephrolithiasis, a free or fixed particle disease. Kidney Int 46:847

[11] Kok DJ, Papapoulos SE, Bijvoet OLM (1990) Crystal agglomeration is a major element in calcium oxalate urinary stone formation. Kidney Int 37:51

[12] Kok DJ, Papapoulos SE, Bijvoet OLM (1986) Excessive crystal agglomeration with low citrate excretion in recurrent stone formers. The Lancet i:1056

[13] Lieske JC, Leonard R, Swift H, Toback G (1996) Adhesion of calcium oxalate monohydrate crystals to anionic sites on the surface of epithelial cells. Am J Physiol 270:F192

[14] Bigelow MW, Wiessner JH, Kleinman JG, Mandel NS (1997) Surface exposure of phosphatidylserine increases calcium oxalate crystal attachmant to IMCD cells. Am J Physiol 272:F55

[15] Verkoelen CF, Romijn JC, de Bruijn WC, Boevé ER, Cao LC, Schröder FH (1995) Association of calcium oxalate monohydrate crystals with MDCK cells. Kidney Int 48:129

[16] Wharton R, V D'agati, Magun AM, Whitlock R, Kunis CL, Appel GB (1990) Acute detoriation of renal function associated with enteric hyperoxaluria. Clin Nephrol 34:116

[17] Morgenroth K, Backmann R, Blaschke R: On the formation of deposits of calcium oxalate in the human kidney in oxalosis (1968) Beitr Path Anat 136:454

[18] de Bruijn WC, Boevé ER, van Run PRWA, van Miert PPMC, Romijn JC, Verkoelen CF, Cao LC, Schröder FH (1994) Etiology of experimental calcium oxalate monohydrate nephrolithiasis in rat kidneys. Scann Microsc 8:541

[19] Verkoelen CF, van der Boom BG, Houtsmuller AB, Schröder FH, Romijn JC (1998) Increased calcium oxalate monohydrate crystal binding to injured renal tubular epithelial cells in culture. Am J Physiol 274:F958

[20] Gill WB, Jones KW, Ruggiero KJ (1981) Protective effects of heparin and other sulfated glycosaminoglycans on crystal adhesion to injured urothelium. J Urol 127:152

[21] Elferink JGR (1987) The mechanisms of calcium oxalate crystal-induced haemolysis of human erythrocytes. Br J Exp Path 68:551

[22] Elferink JGR, Deierkauf M (1987) Enzyme release from polymorphonuclear leukocytes during interaction with calcium oxalate microcrystals. J Urol 138:164

[23] Falasca GF, Ramachandrula A, Kelley KA, O'Connor CR, Reginato AJ (1993) Superoxide anion production and phagocytosis of crystals by cultured endothelial cells. Arthr Rheum 36:105

[24] Hasselbacher P (1982) Stimulation of synovial fibroblasts by calcium oxalate and monosodium urate monohydrate. J Lab Clin Med 100:977

[25] Fuller S, Von Bonsdorf C-H, Simons K (1984) Vescicular stomatitis virus infects and matures only through the basolateral surface of the polarized epithelial cell line, MDCK. Cell 38:65

[26] Louvard D (1980) Apical membrane aminopeptidase appears at site of cell-cell contact in cultured kidney cells. Proc Natl Acad Sci, USA 77:4132

[27] Molitoris BA (1993) Na^+-K^+-ATPase that redistributes to apical membrane during ATP depletion remains functional. Am J Physiol 265:F693

[28] Seldin DW and Giebisch G (eds), The kidney (1992), Physiology and Pathophysiology, Second Edition, Raven Press, New York

[29] Verkoelen CF, van der Boom BG, Schröder FH, Romijn JC (1997) Cell cultures and nephrolithiasis. World J Urol 15:229

[30] Bigelow MW, Wiessner JH, Kleinman JG, Mandel NS (1997) The dependence on membrane fluidity of calcium oxalate crystal attachment to IMCD membranes. Calcif Tissue Int 60:375

[31] Hull RN, Cherry WR and Weaver GW (1976) The origin and characteristics of a pig kidney cell strain, LLC-PK_1. In Vitro 10:670

[32] Pfaller W, Gstraunthaler G, Kersting U and Oberleitner H (1989) Carbonic anhydrase activity in Madin Darby canine kidney cells. Renal Physiol Biochem 12:328

[33] Richardson JCW, Scalera V, Simmons NL (1981) Identification of two strains of MDCK cells which resemble separate nephron tubule segments. Biochim Biophys Acta, 673:26

[34] Gekle M, Wunsch S, Oberleitner H, Sibernagel S (1994) Characterization of two MDCK-cell substypes as a model system to study principal cell and intercalated cell properties. Pflugers Arch 428, 157

[35] Devuyst O, Beauwens R, Denef J-F, Crabbé J, Abramov M (1994) Subtypes of Madin-Darby canine kidney (MDCK) cells defined by immunocytochemistry: Further evidence for properties of renal collecting duct cells. Cell Tissue Res 277:231

[36] Ebner S, Marin-Grez M (1996) Video-imaging micro-fluormetric assessment of luminal chloride/bicarbonate exchange activity in Madin-Darby Canine kidney cells: Influence of cell density 4,4'-diisothiocyano-2,2'-disulfonic stilbene and acetazolamide. Biol Chem Hoppe-Seyler, 377:275

[37] Broyer M, Jouvet P, Niaudet P, Daudon M, Revillon Y (1996) Management of oxalosis. Kidney Int 49:S93

[38] Balcarova-Ständer J, Pfeiffer SE, Fuller S, Simons K (1984) Development of cell surface polarity in the epithelial Madin Darby canine kidney (MDCK) cell line. EMBO J 3:2687

[39] Riese RJ, Mandel NS, Wiessner JH, Mandel GS, Becker CG, Kleinman JG (1992) Cell polarity and calcium oxalate crystal adherence to collecting duct cells. Am J Physiol 262:F177

[40] Hammerton RW, Krzeminski KA, Mays RW, Ryan TA, Wollner DA, Nelson WJ (1991) Mechanism for regulating cell surface distribution of Na+,K+-ATPase in polarized epithelial cells. Science 254:847

[41] Steele RE, Preston AS, Johnson JP, Handler JS (1986) Porous-bottom dishes for culture of polarized cells. Am J Physiol 251:C136

[42] Finlayson B, Reid F (1978) The expectation of free and fixed particles in urinary stone disease. Invest Urol 15:442

Study supported by the Dutch Kidney Foundation (grant C95.1494).

Chapter 8

GENERAL DISCUSSION

Chapter 8

General discussion

8.1 Urinary excretion of oxalate

Renal elimination of metabolic breakdown products of exogenous and endogenous compounds is a major way of clearing the internal milieu from potentially dangerous substances. A great number of endogenous substances are secreted by the organic anion pathway. This active secretory system is nonspecific and may handle substances of widely different structures. Secretion is mediated by membrane transport proteins that carry organic anions against an electrochemical gradient from the peritubular side into the lumen of the proximal tubule. The renal elimination of the organic anion oxalate is an important risk factor for the formation of stones in the kidney [1-8]. Oxalate is extremely poorly soluble in the presence of calcium and in biological fluids the oxalate and calcium concentration product easily exceeds the value needed for spontaneous crystal formation. Although crystals by themselves are not necessarily harmful, their retention in the kidney ultimately leads to stone formation. Oxalate is a much more important determinant of supersaturation than calcium. Many stone formers tend to excrete slightly elevated amounts of oxalate in their urine. Mild hyperoxaluria, characterized by an excretion above 0.56 mmoles/day, the upper limit of normal, but usually amounting to less than 1 mmol/day, has been reported in up to 30% of idiopathic calcium stone formers. The question whether cellular transport mechanisms in the kidney are actively involved in the generation of hyperoxaluria is a major issue in calcium stone disease research [9-11]. The physiological aspects of renal oxalate transport are still poorly understood [1-8]. Plasma oxalate is freely filtered into Bowman's space and like any other substance entering the tubules, oxalate could be secreted and/or reabsorbed across the epithelium. The renal excretion of xenobiotics can follow different patterns [12]: (1) Excretion depending on filtration only, as is the case for the osmotic diuretic mannitol. (2) Excretion depending on filtration and active secretion, with little reabsorption, as is seen for example for PAH and tetraethylammonium. (3) Renal excretion depending on filtration and passive reabsorption, with no secretory movement, as has been described for paracetamol. (4) Renal excretion depending on filtration, active secretion and passive reabsorption, as is the case for the organic anions phenybutazon and nitofurantoin. (5) Renal excretion after filtration, active secretion, and passive as well as active reabsorption, as found for ascorbate and pyrazonoate. It is not known which of these pathways is followed during the excretion of oxalate.

8.2 Transport studies in cell culture

The development of cell culture techniques has offered advantages for the study of transcellular transport of solutes across renal epithelial monolayers. The experiments described in *Chapter 1* were performed to disclose possible oxalate transport mechanisms in cell culture. Most studies were performed with the proximal tubule cell line, LLC-PK_1 [13]. We measured unidirectional oxalate fluxes and oxalate uptake at both plasma membranes. The experimental design of these studies was initially based on that of several other studies on Na^+-dependent transport mechanisms in this cell line [14,15]. The functional integrity and correct polarization of the cultured epithelial monolayer was indicated by the development of tight junctions (TER) and the polarized expression of the Na^+-dependent hexose carrier (apical) and Na^+,K^+-ATPase (basolateral). Under the experimental conditions used, however, we were unable to detect a net directed flux of oxalate across these monolayers and in addition there was no difference in initial uptake rates at either plasma membrane. Also when these studies were repeated under short-circuited conditions in Ussing-chambers, oxalate was not preferentially transported to either side of the monolayer.

Oxalate has been proposed to enter the cell at the basolateral membrane in exchange for sulfate and/or bicarbonate [16-23]. This process is energetically driven by the Na^+/K^+-ATPase pump system which provides the Na^+-gradient by which sulfate and bicarbonate are reabsorbed from the tubular fluid. Chloride/oxalate exchange is one of the proposed mechanisms for the cellular exit of oxalate at the apical membrane [5,6,23-26]. It is therefore conceivable that oxalate secretion only takes place when the physiological conditions are favorable for chloride absorption. Confluent monolayers of LLC-PK_1 cells cultured on a solid substrate form cyst-like structures called "domes" which accumulate between the cells and the growth substrate [28]. It has been recognized that dome formation represents active reabsorption of NaCl and fluid. When LLC-PK_1 cells are cultured on a permeable support, dome formation is not observed since the fluid will be transported across the epithelium to the basal compartment. We speculated that the transport buffers used in the initial transport studies may have contained anions that inhibited the transcellular movement of oxalate by competing for sites at the anion-exchange proteins. Therefore, in *Chapter 2*, an alternative approach was used to study oxalate transport. In these experiments an ultrafiltrate-like buffer was applied to the apical compartment, whereas a buffer resembling the composition of peritubular plasma was applied at the opposite side of the monolayers. The monolayers

were subsequently allowed to process the various components in time. The rationale for this experimental approach was that in this more natural way the cells themselves may create the conditions that are favorable for active oxalate transport. This study showed that the luminal concentration of oxalate gradually increased in time to reach values after two days that were at least 3-fold higher than those in the basal compartment. Although this increase in apical oxalate seemed to suggest oxalate secretion, it appeared to match the increase in apical inulin concentrations, indicating that the observed increase in luminal oxalate is the passive consequence of water reabsorption. These results emphasize the important role that water reabsorption has on the concentration of oxalate in the tubules and thus on the level of urinary saturation. This issue is of particular interest in relation to the recent findings that oxalate (and formate) may participate in the reabsorption of NaCl in the mammalian proximal tubule. Electroneutral transcellular NaCl reabsorption seems to be effected by the action of two parallel exchangers at the apical membrane: Na^+/H^+ and Cl^-/base, in which the counter anion for chloride could be OH^-, HCO_3^-, formate or oxalate. Recycling of oxalate across the luminal membrane via oxalate/OH^- exchange would produce the net thermodynamic effect of electroneutral NaCl uptake since the OH^- secreted during oxalate recycling would neutralize the proton secreted by the luminal Na^+/H^+ antiporter [29-34]. Therefore, these relatively specific exchange mechanisms for oxalate transport in the plasma membranes of renal tubular cells may subserve functions, such as NaCl reabsorption, that are not directly related to oxalate homeostasis. In *Chapter 2* we show that functional monolayers of LLC-PK_1 cells process an ultrafiltrate-like solution in a strikingly similar way as that described in the mammalian renal proximal tubule [35]. Bicarbonate, glucose, and phosphate are transported rapidly from the apical to basolateral side of the monolayer. Sodium and chloride are reabsorbed without major consequences for the osmolality in the apical and basal fluid. Calcium and potassium are also reabsorbed, but to a smaller extent than sodium. Also this study shows that under normal conditions there is no net directed transport of oxalate but an equilibrium in its bidirectional transepithelial movement.

The first event in stone development probably is the precipitation of calcium phosphate crystals in the Limb of Henle. This is followed by calcium oxalate crystallization in the distal tubule and collecting ducts, whereby previously formed calcium phosphate crystals may act as a heterogenous nucleator [36-38]. The first crystallization step is sensitive to variations in the concentration of calcium and phosphate at the end of the proximal

tubule, the latter is sensitive to calcium and oxalate concentrations and pH in the distal tubule and collecting ducts [36-42]. Most filtered phosphate is actively reabsorbed in the proximal tubule. Factors that influence phosphate reabsorption include the amount of filtered phosphate, dietary intake, the level of ionized calcium and acid-base status [35]. Also the bulk of filtered calcium is reabsorbed in the proximal tubule. Calcium transport is primarily passive in this segment of the nephron and is influenced by the amount of filtered calcium, dietary calcium and phosphate intake, calcium complexation in the tubular fluid, defects in sodium and water reabsorption, and acid-base status [43]. Proximal tubular handling of water, calcium, phosphate and oxalate therefore is an important variable determining the risk of crystal formation in the nephron. It is conceivable that abnormalities in proximal tubule transport explains the formation of too many and too large particles as witnessed in recurrent stone former urines. In view of these data, transport functions of the proximal tubule are of interest for idiopathic calcium stone formation. LLC-PK_1 cells may prove useful to study the regulation of NaCl and water transport in the proximal tubule, the effect of different calcium concentrations on the transport of phosphate, as well as the effect of metabolic acidosis on the cellular handling of compounds that are involved in renal stone disease. This information may provide new insights in processes that take place in the renal proximal tubule and that may influence the risk for crystallization and stone formation in later segments of the nephron.

In the meantime, also other investigators studied oxalate transport in LLC-PK_1 cells. Wandzilak et al. reported that oxalate uptake was inhibited in the presence of sulfate, chloride, bicarbonate or anion-exchange inhibitors [44]. Koul et al. performed short-term oxalate influx and efflux studies in LLC-PK_1 cells [45]. Their results indicated the presence of an oxalate/chloride exchanger at the apical and an oxalate/sulfate (bicarbonate) exchanger at the basolateral surface. Although these results suggest that the basic elements for oxalate transport are present in the membranes of these cells, these experiments do not appreciably extend our knowledge beyond the level gained from isolated membranes and do not demonstrate the occurrence of net directed oxalate transport. The advantage of an intact and functional epithelium in culture is that it allows the measurement of secretory or absorptive tracer fluxes across the epithelium. The absence of net oxalate transport in our studies suggested to us that the presence of these membrane anion-exchange mechanisms are not sufficient to mediate directed transcellular fluxes of oxalate. Although tissue culture techniques have been

available for several years, the number of studies addressing the transport of classical organic cations or anions is surprisingly small. Transport of organic anions such as PAH has also been examined in LLC-PK_1 cells and found to be negligible or nonexistent. It is possible that the absence of organic anion transport in cell culture reflects the loss of this ability due to the long term culture conditions. On the other hand, the number of cell lines available for these studies is relatively small and it cannot be excluded that LLC-PK_1 cells are derived from a part of the proximal tubule that is not involved in organic anion secretion.

8.3 Renal handling of oxalate in animals

As early as in 1962, clearance studies in dogs by Cattel et al. showed that the amount of oxalate excreted into the urine was greater than the quantity that was filtered at the glomerulus, indicating active tubular secretion of oxalate [46]. In addition, stopped-flow analysis indicated that the tubular secretion of oxalate is localized at the proximal tubule, whereas there was no evidence for active reabsorption of oxalate [46]. In the late seventies and early eighties a number of investigators studied the renal handling of oxalate in rats by clearance, micropuncture and microperfusion techniques [47-52]. Greger et al. [52] suggested that bidirectional movement of oxalate takes place in the rat proximal convoluted tubule (PCT) and net oxalate secretion in the straight segment of the proximal nephron. Weinman et al. however proposed that oxalate is secreted in early portions of the rat PCT and undergoes bidirectional transport in later segments [51]. Later the same group suggested the existence of more than one oxalate secretory system in early and late segments of the rat PCT [48,49]. Clearance and microperfusion experiments in rabbits confirmed that oxalate undergoes net renal secretion in the proximal tubule and showed that this secretion is more extensive in early and late segments than in the straight segment of the PCT. Moreover, these authors found a significant internephronal heterogeneity for oxalate secretion reflected by the observation that superficial nephrons showed a greater rate of secretion than juxtamedullary nephrons [50]. Based on results from microperfusion experiments Tremaine et al. suggested that the transport system for oxalate in the chicken kidney is separate from those handling PAH and uric acid [47]. Taken together, these results seem to indicate that oxalate can be secreted in the mammalian proximal tubule, although the exact location is still unclear. Such a heterogeneous distribution of organic anion transporters along the proximal tubule was also reported for PAH. In the rabbit, PAH is generally transported most efficiently by the

S2 segment, in the rat predominantly in the pars recta (S3), and in the pig organic anion transport appears to be more efficient in the S1 segment. It is of interest to notice in this respect that although LLC-PK_1 cells are derived from the kidney of a pig, it is possible that they originate from a part of the proximal tubule distinct from S1.

8.4 Renal handling of oxalate in man

Most information concerning the renal handling of oxalate in humans has been obtained from renal clearance studies. This required the measurement of both plasma and urine oxalate concentrations from samples collected within the same time frame. Until recently, however, the issue of oxalate clearance has been difficult to approach because a reliable determination of plasma oxalate was not available. Classical oxalate clearance studies employing [^{14}C]oxalate methods have shown that the clearance of oxalate exceeds the clearance of extracellular markers such as inulin or creatinine, thus indicating net tubular secretion [53]. Results of isotope dilution methods, however, may have been influenced by the difficulty in obtaining steady state values of [^{14}C]oxalate in plasma [54,55]. Reported estimates of oxalate renal clearance were significantly higher, for example, in single injections than in continuous infusion studies [56]. More recently, reliable enzymatic and ion-chromatographic methods that permit a standard renal clearance determination have shown that in healthy subjects the renal clearance of oxalate is close to unity, indicating an equilibrium between oxalate reabsorption and secretion in the tubules [3,54-60]. There is still conflicting information, however, about the handling of oxalate in kidneys of calcium oxalate stone formers. Schwille et al. [58] found a fractional oxalate clearance above 1.0 in male idiopathic hypercalciuric stone formers. Gambaro et al. [55] reported that a selected group of stone formers with a higher than normal erythrocyte oxalate flux rate, had a fractional oxalate clearance of 1.84, whereas this value was 1.08 in controls. An interesting observation in the latter study was that the 24 hour excretion of oxalate was not significantly different between the two groups. Earlier, these investigators found that when challenged with an oxalate load, stone formers had higher peaks of oxaluria and a faster excretion of the oxalate load. It was suggested that in stone formers, normal meals already might trigger urinary oxalate peaks sufficiently high to induce the stone forming process. In contrast, Hatch [57] recently reported the results of a study in which she examined renal oxalate handling in 35 patients with mild hyperoxaluria. In 22 patients, oxalate clearance was decreased relative to creatinine while

serum oxalate was increased. In these patients hyperoxaluria was felt to be absorptive. In 13 patients in whom hyperoxaluria was present during fasting, renal clearance was normal and hyperoxaluria was felt to arise from increased endogeneous oxalate production. In this study there was no evidence for a renal oxalate leak in hyperoxaluric stone formers. Moreover, Sutton et al reported [3] that in rather large populations, the fractional clearance of oxalate in idiopathic calcium stone formers was not different from normals. Mean plasma oxalate also was not significantly different between the two groups. These authors concluded that the mild hyperoxaluria observed in the idiopathic calcium stone formers resulted in part from dietary factors and/or enhanced intestinal oxalate absorption. The observation that in healthy subjects the amount of oxalate excreted in the urine does not exceed the amount filtered is, according to Hatch, also supported by the oxalate/creatinine clearance ratio calculated from plasma and urine oxalate concentrations determined by sensitive and reliable assays [57]. Considering an average urine flow rate of 1.04 ml/min (1.5 l/24h), an average oxalate urinary excretion of 280 μmoles/24 hours, and a plasma oxalate concentration ranging from 1.5-2.5 μM, then the renal oxalate clearance is 129-78 ml/min., as calculated by the formula: $C_{ox}=U_{ox}.V/P_{ox}$, in which C_{ox} is the oxalate clearance, U_{ox} is the oxalate concentration in urine, V is urine flow rate and P_{ox} is plasma oxalate. When creatinine clearance is around the normal value of 120 ml/min, the estimated fractional clearance indeed is around 1.0 (0.64-1.08). It should further be noticed that when oxalate would be secreted at a higher than normal rate, this would deplete oxalate in the blood resulting in decreased plasma oxalate concentrations. At normal plasma oxalate an increase in renal oxalate secretion can only lead to sustained hyperoxaluria when plasma oxalate is continuously replenished by other sources. This seems to rule out a renal leak as sole explanation for hyperoxaluria. As mentioned ealier, the amount of oxalate that reaches the final urine is the net result of filtration, tubular secretion and reabsorption. It is well documented that clearance techniques cannot definitively separate reabsorption or secretion for substances that undergo both [61]. Transport can occur in one direction in one nephron segment and in the opposite direction in another, or it can be bidirectional within a given segment. In general, tubular secretion of organic anions is considered an active carrier mediated process, whereas reabsorption is passive and induced by the urine to blood concentration gradient [12,62]. It is possible that, after glomerular filtration and subsequent tubular secretion, the amount of oxalate that ultimately reaches the urine entirely

depends on the amount that leaks back and thus on the oxalate permeability of the tubular epithelium. The apical to basolateral directed oxalate concentration gradient generated and sustained by monolayers of LLC-PK_1 cells as described in *Chapter 2*, indicates that oxalate does not easily diffuse through the paracellular pathway. The tubular fluid to blood oxalate concentration gradient *in vivo* is probably much larger, considering an oxalate concentration at the end of the collecting duct comparable to that in the final urine (200 μmoles/l) and normal plasma oxalate (2.5 μmoles/l). Although the junctional complexes are much tighter in this segment of the nephron, it is conceivable that under these conditions some passive back diffusion will occur. It has been reported that the urinary excretion of oxalate in normal males was increased after intravaneous infusion with acetazolamides, which o.a. inhibits fluid transport in the proximal tubule. These authors speculated that the rise in urinary oxalate was caused by an effect of this diuretic on oxalate back diffusion in the distal nephron [63]. Taken together, since oxalate is filtered freely and oxalate secretion and reabsorption are in equilibrium in healthy subjects, urinary oxalate concentrations normally depend entirely on plasma oxalate. This implies that oxalate certainly is not eliminated as effectively as PAH and thus presumably by another pathway. The renal handling of oxalate in idiopathic calcium stone formers is less clear. Most likely there are subgroups of patients that excrete more oxalate into the urine due to enhanced intestinal absorption and/or increased endogeneous production. In these patients renal oxalate secretion does not seem to play an important role. In another subgroup, urinary oxalate could be increased due to increased tubular secretion or decreased tubular back diffusion. The latter group might be identified by their relatively low plasma oxalate concentrations. Although our cell culture studies were not succesfull in revealing the mechanisms involved in the transcellular movement of oxalate, knowledge of these mechanisms is essential for the development of new therapies. A model of cultured renal tubular cells exhibiting organic anion transport would be a valuable tool to obtain such detailed information.

8.5 Crystal-cell interaction

The retention of crystals in the urinary tract is considered an important factor in the effective growth of renal calculi. It is not entirely clear, though, how crystals become trapped inside the kidney. The fixed particle theory was first proposed in 1978 by Finlayson, who stated that given urinary flow rates, anatomical dimensions, and crystallization mechanisms,

it is extremely unlikely that kidney stones could form without sites of attachment [64]. Recently, Kok and Khan addressed the same issue and essentially came to the same conclusions but added the possibility that crystal agglomeration could contribute to this process [65]. From this theoretical model it appears that agglomeration within the tubule could lead to crystal masses that are large enough to become stuck inside the renal tubules. Although there is some evidence favoring this nonspecific retention of crystals over the fixed particle theory, these two hypotheses are not mutually exclusive. The deposition of crystalline material in the body is the cause of a number of disease entities, such as gouty arthritis, oxalosis, synovitis, vasculitis, bone disease, and silicosis [66-69]. The cellular response to crystals has been studied with several cell types, including red blood cells, leukocytes, endothelial cells, and fibroblasts, and with various crystals, such as monosodium urate (MSU), calcium pyrophosphate dihydrate (CPPD), calcium oxalate monohydrate (COM), calcium oxalate dihydrate (COD), and hydroxyapatite (HA) [66-69]. These studies demonstrated that the physical interaction of crystals with cells generally leads to injury caused by rupture of the phospholipid bilayer and acute inflammatory responses. The interaction of crystals with renal tubule cells has also been studied. These studies are still relatively recent and the results obtained by the various investigators should be interpreted with caution since they are complicated by a number of factors. In the first place, these studies are performed with cells that exhibit characteristics of different segments of the nephron including, the proximal tubule (BSC-1, LLC-PK_1 and OK1), the collecting duct (MDCK-ATCC, MDCK-I, MDCK-II), and inner medullary collecting duct (IMCD, cIMCD). Furthermore, cells are grown on different growth substrates, either solid or permeable, which may influence their cell surface properties. Studies are performed with proliferating cells or confluent cultures. In addition, crystals are generated using various protocols, which may influence their binding properties. It is therefore not surprising that the results obtained are not always comparable. Nevertheless, these investigations may provide new insights in one of the fundamental biologic processes underlying renal stone disease.

8.6 Cell culture models

A number of permanent growing cell lines with characteristics of different segments of the nephron has been developed over the years. Some investigators prefer to use primary cultures from freshly isolated material. The advantages and disadvantages of both methods have been discussed

earlier. The conditions under which cells are cultured can influence their characteristics. Cell growth on permeable supports has the advantage of inducing the correct polarization and allows separate access to apical and basolateral domains of the plasma membrane [27,28,70-72]. MDCK cells seeded at high densities on permeable filters form columnar shaped cells with apical tight junctions and numerous microvilli at the apical plasma membrane, whereas cells cultured on conventional solid growth substrates remain rather slender in architecture [*Chapter 7*,73]. Furthermore, monolayers cultured on porous supports can be maintained in culture for weeks without loosing their barrier integrity and viability, whereas cells grown on solid substrates begin to detach already after about 8-10 days (unpublished observations). The transport of the glucose analog α-MG was used to study the functional differentiation of the brush border in LLC-PK_1 cells cultured on permeable substrates. It was demonstrated that maximum directed transport activity was achieved after 9-10 days in culture [*Chapter 2*]. In addition, it was found that LLC-PK_1 as well as low resistance MDCK cells seeded at high densities, express their highest brush border γ-GT and AP enzyme activities 7-8 days post-seeding [73]. Taken together, a number of conclusions can be drawn from these observations. In the first place, it is clear that cells grown on porous supports obtain higher levels of morphological and functional differentiation compared to cells cultured on solid substrates. Furthermore, functional studies should be conducted with confluent monolayers that are sufficiently maturated to express the relevant specialized characteristics.

As discussed earlier, calcium oxalate crystals normally are not expected to be formed early after filtration. The concentration of oxalate in ultrafiltrate is assumed to be comparable to that in plasma. This implies that, as a result of renal fluid reabsorption, the concentration of oxalate will rise passively along the length of the nephron to reach levels of supersaturation high enough for spontaneous nucleation in segments around or beyond the thin limbs. Crystal formation presumably can only be expected at earlier sites of the nephron when oxalate concentrations are raised to unphysiologically high levels, for instance after acute ethylene glycol poisoning, during severe primary hyperoxaluria or in rats fed a crystal inducing diet. Cells with properties of the renal proximal tubule, to our opinion, therefore are not the first choice to study crystal-cell interaction. For most of our studies, we selected MDCK cells, a cell line with characteristics of the renal collecting duct. To study the influence of the stage of cell development on crystal-cell interaction, crystal binding was studied during the proliferation of MDCK

cells to confluency on permeable and impermeable growth substrates. The level of binding was measured on a daily basis during a total period of 10 days. It was found that the amount of crystals that could adhere to the surface of cells cultured on permeable supports declined as soon as the tight junctions were formed. Soon after the barrier integrity was completely installed, crystals practically did no longer adhere to the cell surface. Although the level of crystal binding to cells grown on solid growth substrates decreased also, these levels never became as low as those to monolayers cultured on permeable supports [*Chapter 7*]. These observations indicate that crystal binding is highly influenced by the developmental stage of the cultures.

8.7 Binding sites

An obvious question is: how do crystals become associated with the cell suface? The interaction between macromolecules and the epithelial cell surface has been investigated in other fields. The association of cationic proteins with the epithelium was explored to extend the understanding of events at sites of inflammation, and molecular aspects of the attachment of microbes to animal cell surfaces were investigated to obtain more knowledge of infectious processes. Negatively charged membrane phospholipids were proposed as major binding sites for protamine sulfate [74], whereas cell surface glycoconjugates were identified as the dominating part of receptors for the attachment of bacteria and viruses [75]. Crystals composed of calcium salts have a positive surface charge (zeta potential) [76,77] and in the tubular fluid they behave as cationic macromolecules. The surface of epithelial cells is negatively charged due to the anionic sites in the carbohydrate-rich peripheral zone. Calcium oxalate crystal binding most likely is not very specific and based on electrostatic interactions between the positively charged calcium ions at the crystal surface and the negatively charged sites at the cell surface. Crystal attachment requires that the attractive forces involved are large enough to counteract the shear forces caused by the rapidly flowing tubule fluid. Negatively charged membrane phospholipids, such as sphingomyelin, phosphatidylinositol and phosphatidylserine [78-81] as well as cell surface glycoconjugates, including N-acetyl neuraminic acid (sialic acid) residues of glycoproteins and glycolipids [82-85] and heparan sulfate moieties of membrane associated proteoglycans [85], all have been proposed as candidates for crystal binding sites. Although crystals are found occasionally in anyones urine, stones are encountered in only a subset of the population. Therefore, crystals probably

normally are washed-out harmlessly with the urine, whereas they are retained in the kidneys of stone formers. Crystal adherence could be caused by an enhanced affinity of crystals for the cell surface, an enhanced cell surface affinity for crystals, or an increase in their mutual attraction.

8.8 Cell surface protection

If the adherence of crystals to the urothelium is considered an unwanted incident, than it is reasonable to assume that physiological mechanisms exist to prevent crystal binding. COM crystals indeed do not adhere to the surface of functional MDCK cells [*Chapters 6 and 7*]. To investigate if this property is specific for this cell line, crystal binding was studied to LLC-PK_1 and different strains of MDCK cells. These studies confirmed that crystals were repulsed by functional monolayers of MDCK cells, but not by those formed by LLC-PK_1 cells. Irrespective of the developmental stage or growth substrate used, LLC-PK_1 cells were unable to avoid the adherence of COM crystals [*Chapter 7*]. These results suggest that the apical plasma membrane of collecting duct cells, in contrast to that of proximal tubule cells, is constructed such that the adherence of microliths is avoided. Recently, it has been suggested that bacteria are involved in nephrolithiasis. It was found that nanobacteria were present in 30 randomly selected human kidney stones, indicating that most likely all human kidney stone contain these microorganism. From this observation and from the fact that under serum free conditions nanobacteria produce calcium phosphate, it was speculated that nanobacteria may play an important role in pathological calcification conditions including renal stone formation [122]. Bacterial adhesion to the host epithelium is the initial event of the infectious process and is followed by host membrane penetration and tissue invasion. Healthy tissues normally are resistant to infection and some form of compromise of host defence must be necessary for bacteria to adhere to the cell surface. The apical membrane of the renal tubule epithelium protects the cells from pathogens in the outside world. We provided evidence that an intact epithelium formed by MDCK cells is also protected from the adherence of CaOx crystals and that crystal binding only takes place after wounding the epithelium. Tissues also become susceptible to infection with bacteria after overt injury [123]. It is therefore conceivable that some form of epithelial injury leads to the adherence of crystals as well as bacteria, which might explain the presence of microbes in renal stones. This scenario does not exclude the possibility that apatite producing nanobacteria contribute to the process of stone formation.

As far as we know, there is one other report in which the binding of COM crystals was studied to epithelial cells during their growth to confluency. These studies, performed by Bigelow and coworkers [86], showed that the level of crystal binding decreased during the formation of confluent monolayers of IMCD cells. A similar effect, however, was not seen in this study with MDCK cells [86]. Although this seem to be in contrast with our results, it should be mentioned that the MDCK cells in the study of Bigelow et al. did not form monolayers, but continued to proliferate and piled up into multilayers. The observation that substantial amounts of crystals still could bind to confluent IMCD monolayers is possibly explained by the fact that these cells were cultured on solid surfaces. It is likely that much lower amounts of crystals will adhere to confluent IMCD monolayers on permeable substrates. Nevertheless, the observation that IMCD cells acquired some protection against crystal binding supports the idea that crystal binding is reduced as much as possible in late segments of the nephron. Earlier it was found that also the surface of the transitional epithelium of the bladder is able to withstand the adherence of bacteria, viruses and crystals [87,88]. Polysaccharide side chains of cell surface associated proteoglycans were identified as primary defensive barrier. Calcium oxalate crystal binding was increased after the bladder urothelium was chemically injured. Since this effect could be reversed by heparin, it was suggested that glycosaminoglycans in the cell surface coat form a protective hydrophilic layer. Bennett has stated already in 1963 that the extracellular polysaccharide-rich coating of the cell can be viewed as a filter, retarding the passage of particles, molecules or ions above a certain size. Polysaccharides can bind large quantities of water by the hydrogen binding capabilities of its numerous hydroxyl groups. A feature that, according to this author, applies in every day life in the use of cellulose-coated cotton towels and washcloths [89]. The presence of a protective polysaccharide layer might also explain the repulsion of crystals at the surface of MDCK cells. If so, one would expect that the enzymatical removal of parts of the coat should result in an increased affinity of the cell surface for crystals. Treatment with neuraminidase [82,84,85], heparinase [85] or trypsin [82,85], however, never resulted in enhanced levels of crystal binding, but in lower levels of binding, suggesting that membrane associated glycoconjugates do not protect the cell surface from crystals but rather attract them. Perhaps the attraction or repulsion of crystals depends on the configuration of the carbohydrates at the cell surface. Another conclusion that can be drawn from the observation that the enzymatic

removal of cell surface moieties decreased crystal binding, is that this seems to deny the presence of crystal binding molecules beneath the cell surface coat. Nevertheless, Mandel and coworkers reported that crystal binding predominantly depends on the lipid composition of the lipid bilayer [78-81]. They found that the interaction of red blood cells with COM was increased when the membranes were enriched with anionic phospholipids [78]. In addition, treatment of IMCD cells with calcium-ionophore A-23187 which resulted in an enrichment of anionic phophatidylserine (PS) in the external leaflet of the apical plasma membrane enhanced the level of crystal binding [79]. The increase in crystal binding following PS exposure could be blocked by preincubating the cells with the PS-specific binding protein annexin V. On the basis of these results it was proposed that exposure of anionic phospholipid headgroups on the papillary urothelial surface may have a major impact on the magnitude of stone crystal attachment to kidney tubule epithelium. Identification of a particular cell surface molecule, or multiple cell surface molecules, as binding site for crystals must be based on evidence satisfying at least two criteria. First, presence of a receptor should be prerequisite for binding. Conversely, absence of the putative receptor should prevent specific binding. Second, it should be possible to show that the crystals actually interact physically with the cell surface molecule(s) in question. Whereas the first two criteria were satisfactorially adressed by Mandel's group, it was not demonstrated that the crystals actually became associated with PS. It cannot be excluded that the enrichment of the apical membrane with PS influenced the conformation of the oligosaccharide side-chains of cell surface glycocunjugates and thus possibly their availability for crystal attachment and the reduction of crystal binding after preincubating PS enriched membranes with anexin V could, for example, be caused by stearic hindrance. PS normally is restricted to the inner leaflet of the lipid bilayer, whereas the outer leaflet hardly contains any aminophospholipids. PS is exposed at the outer leaflet during apoptosis, which is a well-organized process of cell-suicide used to eliminate unwanted or damaged cells from multicellular organisms. Although enhanced apoptotic decay of cells is a participant in a number of disease states, including certain forms of infection, ischemia-reperfusion damage, infarction, neuro-degenerative and neuromuscular diseases and AIDS, there is no evidence available that programmed renal cell death is increased in nephrolithiasis. In *Chapter 6*, we showed that the binding of COM crystals decreased during the growth of MDCK cells to confluency. FITC labeled annexin V binding studies demonstrated that subconfluent MDCK cultures did not contain more

apoptotic cells than confluent monolayers which does not support a possible role for PS under these conditions (unpublished observations). It cannot be excluded, however, that there are more than one type of cell surface receptors for crystals and the identity of putative binding sites expressed in the kidneys of stone formers has not yet been revealed.

8.9 Inhibition

In vitro studies on crystallization showed that in the presence of glycoproteins [76] or polysaccharides [77] the zeta potential of COM crystals shifts from positive into a negative direction, indicating the association of these compounds with the crystal surface. Perhaps these substances not only influence crystal-crystal interaction but also crystal-cell interaction. It was found that crystal binding indeed is decreased by most of the polyanionic macromolecular inhibitors of crystallization, including nephrocalcin, uropontin and members of the polysaccharide-family of sulphated glycosaminoglycans (GAGs) [83]. We investigated the inhibitory effect of polysaccharides on crystal binding to low resistance MDCK cells and found that GAGs in concentrations normally present in human urine are not very potent inhibitors of crystal adherence [*Chapter 4*]. Only relatively high concentrations of heparan sulphate and chondroitin sulphate-A and-B resulted in some inhibition. Lieske et al. [83] found that chondroitin sulfates, heparan sulfate and hyaluronic acid effectively prevented COM crystal binding to BSC-1 cells. Since the GAG concentrations in that and our study were expressed in moles and grams, respectively, and molecular size (distribution) data are not available, it is unclear whether the conditions in these two studies were comparable, but probably higher concentrations were applied by Lieske et al. [83]. To our opinion, GAG concentrations should not be expressed in moles because GAG molecules are not identical in length. It should be realized that GAG concentrations in the tubular fluid must be lower than those in the final urine because GAGs derived from bladder tissue contribute to urinary GAGs [37]. In contrast to GAGs, semi-synthetic polysaccharides (SP54, G871, G872) were found to be very strong inhibitors of crystal binding. Since they are also strong inhibitors of crystal growth and agglomeration, these substances are considered potential drugs for the treatment of recurrent calcium stone disease [77,90,91]. Lieske and Toback [83] as well as we [*Chapter 4*] found that polysaccharides exert their inhibitory effects by modifying the crystal surface rather than the cell surface. In conclusion, negatively charged molecules that enter the tubular fluid at the glomerulus or that are synthesized by the renal cells themselves

are able to neutralize potential binding sites at the crystal surface thereby facilitating crystal elimination with the urine.

8.10 Epithelial polarity

Polarity is a steady state situation resulting from molecular sorting of the traffic between the cell surface and internal organelles. The establishment and maintenance of functional cellular polarity is particularly important in the kidney, where vectorial transepithelial solute transport depends on the polarized insertion of specific pumps, channels and carriers in the apical or basolateral plasma membrane of renal tubular cells [70,71]. A possible relationship between epithelial polarization and crystal binding was first proposed by Riese and coworkers [92]. They found that calcium chelation-induced disruption of tight junctions in primary cultures of rat IMCD cells resulted in increased levels of crystal binding accompanied by the appearance of a basolateral marker at the apical membrane, which could be reversed by the readdition of calcium. The authors speculated that potential crystal binding molecules normally residing in the basolateral membrane of polarized cells may appear at the luminal cell surface as a result of lateral diffusion of membrane components. Also our results described in *Chapter 6* suggest that an inverse relationship exists between MDCK cell polarity, established after the assembly of tight junctions, and crystal binding. It was speculated that the reduction in crystal binding to polarized MDCK cells could be explained by the disappearance of potential binding molecules from the cell surface, from a reduced accessibility of the binding sites by alterations in their molecular conformation or because they become masked by extracellular surface-associated glycoconjugates. Bigelow et al reported that the growth of IMCD cells into confluent monolayers not only resulted in reduced levels of crystal binding but also in a decreased membrane fluidity [86]. From this observation it was hypothesized that the ability to form a crystal attachment region on the cell surface may be related to the fluidity of the membrane. Membrane fluidity refers to the physical state of the membrane and is determined by structural and dynamic factors, including the packing of individual fatty acyl chains within the bilayer, phospholipids, cholesterol and glycoproteins [93]. The dynamic component of membrane fluidity reflects its microviscosity which may be important in determing lateral mobility and intramembranous protein coupling interactions. A change in the physical state of the membrane can influence its architecture and possibly the exposure of potential crystal binding molecules.

8.11 Internalization

Once crystals become attached to the cell surface, part of them are subsequently taken up by the cells [94-97, *Chapter 3*], which could be the next step in the development of a stone. Alternatively, this could represent a protective mechanism to remove potential stone growth sites from the cell surface. Once inside the cell, crystals were found to stimulate cell proliferation which could expose new membrane domains for additional crystal binding [94]. Crystal endocytosis is affected in cell culture by compounds that are normally present in the tubular fluid such as EGF, ADP, THP, fibronectin, and TGF-ß [95], suggesting that structural alterations of these molecules *in vivo* may influence this process. The fate of the crystals once they are inside the cells is presently unknown. Ultrastructural studies showed that initially endocytosed crystals had disappeared from low resistance MDCK cell interior within 3 days, suggesting a regulatory mechanism to eliminate internalized crystals [*Chapter 3*]. It is not yet clear whether the crystals are exocytosed, dissolved intracellularly, or that crystal-containing cells are eliminated and replaced by new cells. It should be emphasized, however, that most of the crystal endocytosis studies were performed with cells that exhibit properties of the renal proximal tubule [94-96,98], a site of the nephron that is specialized in taking up macromolecules from the tubular fluid. Since sialic acid residues have been proposed as possible binding molecule at the surface of renal tubule cells it is interesting to note that the labeling of the various segments of the nephron with the lectin limax flavus which binds specifically to sialic acid residues revealed that the proximal tubule stained much more intense than any other part of the nephron [99]. Studies on crystal endocytosis therefore should be repeated using cells with properties of renal segments where crystals are to be expected (e.g. high resistance MDCK or IMCD cells). These studies can be performed under conditions during which the cells are susceptible for crystal adherence, for example after mechanical injury. In hyperoxaluric patients [97,100-103] and in animals treated with hyperoxaluria inducing agents [104,105], crystals were found in the tubular lumen as well as in the interstitium. In rats supplied for nine days with a crystal inducing diet, large crystal agglomerates partially overgrown by the epithelium were seen inside the tubule lumen [105]. The overgrowth of relatively large particles by cells lining the renal tubules might explain the translocation of crystalline material from the tubular lumen towards the interstitium and perhaps only relatively small crystals are internalized by the tubular cells. It has also been reported that COM crystals stimulate

interstitial cell growth and it was proposed that enhanced growth of these cells may affect the extracellular matrix, which in turn could stimulate the growth of epithelial cells thereby predisposing the tissue for additional crystal binding [98,105].

8.12 Pathological conditions

Nephrolithiasis is frequently associated with renal cell damage. Already in 1937, Randall concluded from examining more than 400 pairs of human kidneys at necropsy, that the papillary calcium plaques which he found in about 20% of the kidneys were the end stage of renal tubular damage [87]. More recently, the relationship between cellular injury and urolithiasis was supported by the excretion of cellular enzymes and blood in the urine of stone formers, the observation that the organic stone matrix contains components derived from extrarenal sources and by the attachment of calcium oxalate crystals to the damaged epithelium of the bladder [87,88,107-110]. It is not clear, however, if the process of stone formation itselve is damaging to the urothelium or that epithelial damage precedes stone formation. We tackled this problem that intrigued stone research for such a long time by studying crystal binding to intact and damaged confluent monolayers of MDCK cells. These studies clearly demonstrated that crystal binding is increased after epithelial damage and during the subsequent repair process. Although the physical contact between cells and crystals often leads to cell damage, we found that MDCK monolayers were not significantly injured by COM crystals (*Chapter 4*). During their transit through the tubules and under the force of rapidly flowing fluid, crystals could injure the epithelium by abrasion. Alternatively, epithelial damage could be caused under several other conditions: (1) Ischemia: Recently, a vascular related etiology for the origin of urolithiasis has been proposed after the identification of calcified vessels near the tip of the papillae. Tissue ischemia occurs when a reduction in regional blood flow decreases delivery of oxygen and substrates to levels inadequate to maintain cellular energy status finally leading to cellular damage [111]. (2) Inflammation: An inflammatory response induced by interstitial crystals has been reported in urolithiasis. At such sites of inflammation the tissue could be injured by the release of various agents from neutrophils [112]. (3) Crystals: Although calcium oxalate crystals were not injurious to MDCK cells in our studies, Hackett et al. found that exposure of renal tubule cells to COM resulted in the loss of cells from the cultures [113,114]. (4) Oxalate: It was also suggested that oxalate not only promotes stone disease by influencing the level of

supersaturation, but that the ion itself may affect the renal epithelium to predispose the tissue for crystal retention [115-119]. Finally, the cell surface could be altered by mechanisms that are not necessarily pathological. For example, it has been reported that during metabolic acidosis the plasma membrane of collecting duct cells is rearranged by alterations in cell polarity leading to the secretion of H^+ ions into the tubular fluid [120,121]. These processes are accompanied by an increase in the surface area of the apical membrane, induced by the transfer of membrane from tubulovesicles to the cell surface. Thus, it is conceivable that adaptive reponses to physiological stimuli, such as an acid load, can contribute to the risk for crystal retention in the renal collecting duct.

8.13 Conclusions

From the observation that monolayers with an intact barrier function are largely protected from COM crystal binding and from earlier observations that negatively charged molecules in the tubular fluid inhibit crystal-cell interactions (22,31), it can be derived that the renal tubular epithelium is protected from crystal binding by at least two different defence mechanisms: (a) the composition of the apical membranes of polarized renal tubular cells is unfavorable for crystal attachment (b) negatively charged molecules in the tubular fluid prevent crystal retention by covering potential binding sites at the crystal surface. According to this idea, crystal retention will only occur when both putative defence mechanisms are compromised. The advantage of renal cell culture models is that biological processes can be studied in detail in isolated cells from defined segments of the nephron. In a multifaced and complex disease such as urolithiasis this can also be a disadvantage because cellular abnormalities that are observed in one segment can result from cellular disfunctions in another. It is therefore impossible to mimic the complete pathophysiology of stone formation in cell culture. Nevertheless, since the inventory of many of the symptoms (risk factors) of inborn or acquired disorders is meanwhile made up we can now study them more in detail. Renal cells in culture could provide a tool in the study of some of the fundamental biological processes influencing renal stone disease.

References

[1] Robertson WG, Peacock M (1980) The cause of idiopathic calcium stone disease: Hypercalciuria or hyperoxaluria? Nephron 26:105

[2] Robertson WG, Peacock M, Heyburn PJ, Marshal DH, Clark PB (1978) Risk factors in calcium stone disease of the urinary tract. Brit J Urol 50:449

[3] Sutton RAL, Walker VR (1994) Enteric and mild hyperoxaluria. Miner electrol Metab 20:352

[4] Williams AW, Wilson DM (1990) Dietary intake, absorption, metabolism and excretion of oxalate. Sem Nephrol 10:2

[5] Wandzilak TR, Williams HE (1990) The hyperoxaluric syndromes. Endocr Metab Clin N Am 19:851

[6] Williams HE, Wandzilak TR (1989) Oxalate synthesis, transport and the hyperoxaluric syndromes. J Urol 141:742

[7] Larsson L, Tiselius HG (1987) Hyperoxaluria. Min Electr Metab 13:242

[8] Menon M, Mahle CJ (1982) Oxalate metabolism and renal calculi. J Urol 127:148

[9] Baggio B, Gambaro G, Marchini F, Cicerello E, Borsatti A (1984) Raised transmembrane oxalate flux in red blood cells in idiopathic calcium oxalate nephrolithiasis. The Lancet 2:12

[10] Gambaro G, Baggio B (1992) Idiopathic calcium oxalate nephrolithiasis: a cellular disease. Scanning Microscopy 6:247

[11] Borsatti A (1991) Calcium Oxalate nephrolithiasis: defective oxalate transport. Kidney Int 39:1283

[12] Besseghir K, Roch-Ramel F (1987) Renal excretion of drugs and other xenobiotics. Renal Physiol 10:221

[13] Hull RN, Cherry WR, Weaver GW (1976) The origin and characteristics of a pig kidney cell strain, LLC-PK_1. In Vitro 10:670

[14] Rabito CA (1986) Sodium cotransport processes in renal epithelial cell lines. Min Electr Metab 12:32

[15] Mullin JM, Fluk L, Kleinzeller A (1986) Basal-lateral transport flux of methyl α-D-glucoside across LLC-PK_1 renal epithelial cells. Biochim Biophys Acta 885:233

[16] Aronson PS (1989) The renal proximal tubule: A model for diversity of anion exchangers and stilbene-sensitive anion transporters. Annu Rev Physiol 51:419

[17] David C, Ullrich KJ (1992) Substrate specificity of the luminal Na^+-dependent sulphate transport system in the proximal renal tubule as compared to the contraluminal sulphate exchange system. Pflügers Arch 421:45

[18] Fritz G, Rumrich G, Ullrich KJ (1989) Anion transport through the contraluminal cell membrane of renal proximal tubule. The influence of hydrophobicity and molecular charge distribution on the inhibitory activity of organic anions. Biochim Biophys Acta 978:249

[19] Kuo SM, Aronson PS (1988) Oxalate transport via the sulfate/HCO_3 exchanger in rabbit renal basolateral membrane vesicles. J Biol Chem 263:97

[20] Löw I, Friedrich T, Burckhardt G (1984) Properties of an anion exchanger in rat renal basolateral membrane vesicles. Am J Physiol 246:F334

[21] Ullrich KJ, Rumrich G, Klöss S (1984) Contraluminal sulfate transport in the proximal tubule of the rat kidney. Pflügers Arch 402:264

[22] Ullrich KJ, Rumrich G (1988) Contraluminal transport systems in the proximal renal tubule involved in secretion of organic anions. Am J Physiol 254:F453

[23] Ullrich KJ (1994) Specificity of transporters for 'organic anions' and 'organic cations'in the kidney. Biochem Biophys Acta 1197:45

[24] Yamakawa K, Kawamura J (1990) Oxalate:OH exchange across rat renal cortical brush border membrane. Kidney Int 37:1105

[25] Karniski LP, Aronson PS (1987) Anion exchange pathways for Cl^- transport in rabbit renal microvillus membranes. Am J Physiol 253:F513

[26] McConnel KR, Aronson PS (1994) Effects of inhibitors on anion exchangers in rabbit renal brush border membrane vesicles. J Biol Chem 269:21489

[27] Handler JS, Perkins FM, Johnson JP (1980) Studies of renal cell function using cell culture techniques. Am J Physiol 238:F1

[28] Mullin JM and O'Brien T (1987) Spontaneous reversal of polarity of the voltage across LLC-PK_1 renal epithelial cell sheets. J Cell Physiol 133:515

[29] Berry C, Rector F (1989) Electroneutral NaCl absorption in the proximal tubule: Mechanisms of apical Na-coupled transport. Kidney Int 36:403

[30] Wang T, Giebisch G, Aronson PS (1992) Effects of formate and oxalate on volume absorption in rat proximal tubule. Am J Physiol 263:F37

[31] Wang T, Agulian SK, Giebisch G, Aronson P (1993) Effects of formate and oxalate on chloride absorption in rat distal tubule. Am J Physiol 264:F730

[32] Wang T, Egbert AL, Abbiati T, Aronson PS, Giebisch G (1996) Mechanisms of stimulation of proximal tubule chloride transport by formate and oxalate. Am J Physiol 271:F446

[33] Wareing M, Green R (1994) Effects of formate and oxalate on fluid reabsorption from the proximal convoluted tubule of the anaesthesized rat. J Physiol 447:347

[34] Aronson PS (1996) Role of ion exchangers in mediating NaCl transport in the proximal tubule. Kidney Int 49:1665

[35] Berry CA (1982) Heterogeneity of tubular transport processes in the nephron. Ann Rev Physiol 44:181

[36] Asplin JR, Mandel NS, Coe FL (1996) Evidence for calcium phosphate supersaturation in the loop of Henle. Am J Physiol 270:F604

[37] Kok DJ (1997) Intratubular crystallization events. World J Urol 15:219

[38] Tiselius HG, Fornander AM, Nilsson MA (1998) Studies on the crystallization process following addition of calcium phosphate crystals to solutions with a composition corresponding to that in the collecting duct. Scanning Microsc, in press

[39] Lupak I, Bek-Jensen H, Fornander AM, Hojgaard I, Nilsson MA, Tiselius HG (1994) Crystallization of calcium oxalate and calcium phosphate at supersaturation levels corresponding to those in different parts of the nephron. Scanning Microsc 8:47

[40] Deganello S, Asplin J, Coe FL (1990) Evidence that tubule fluid in the thin segment of the Loop of Henle normally is supersaturated and forms a poorly crystallized hydroxyapatite that can initiate renal stones. Kidney Int 37:472 (abstract)

[41] Kok DJ (1996) Crystallization and stone formation inside the nephron. Scanning Microsc 10:471

[42] Tiselius HG, Hojgaard I, Fornander AM, Nilsson MA (1996) Is calcium phosphate the natural promotor of calcium oxalate crystallization? In: Pak CYC, Resnick MI, Preminger GM (eds) Urolithiasis, proceedings VIIIth Int Symp on Urolithiasis. Millett Inc, Dallas. pp 238-239

[43] Seldin DW, Giebisch G (eds) (1992) The Kidney, Physiology and Pathophysiology, Second Edition, Raven Press, New York

[44] Wandzilak TR, Calo L, Borsatti, Williams HE (1992) Oxalate transport in cultured porcine renal epithelial cells. Urol Res 20:341

[45] Koul H, Ebisuno S, Renzulli (1994) Polarized distribution of oxalate transport systems in LLC-PK_1 cells, a line of renal epithelial cells. Am J Physiol 266:F266

[46] Cattell WR, Spencer AG, Taylor GW, Watts RWE (1962) The mechanism of the renal excretion of oxalate in the dog. Clin Sci 22:43

[47] Tremaine LM, Bird JE, Quebbemann AJ (1985) Renal tubular excretory transport of oxalate in the chicken. J Pharm Exp Ther 233:7

[48] Knight FK, Senekjian HO and Weinman EJ (1979) Effect of para-aminohippurate on renal transport of oxalate. Kidney Int 15:38

[49] Knight TF, Sansom SC, Senekjian HO, Weinman EJ (1981) Oxalate secretion in the rat proximal tubule. Am J Physiol 240:F295

[50] Senekjian HO, Weinman EJ (1982) Oxalate transport by proximal tubule of the rabbit kidney. Am J Physiol 243:F271

[51] Weinman EJ, Frankfurt SJ, Ince A, Sansom S (1978) Renal tubular transport of organic acids. Studies with oxalate and para-aminohippurate in the rat. J Clin Invest 61:801

[52] Greger R, Lang F, Oberleithner H, Deetjen P (1978) Handling of oxalate by the rat kidney. Pflügers Arch 374:243

[53] Oswald H, Hautman R (1979) Renal elimination kinetics and plasma half-life of oxalate in man. Urol Int 34:440

[54] Kasidas GP, Nemat S, Rose GA (1990) Plasma oxalate and creatinine and oxalate/creatinine clearance ratios in normal subjects and in primary hyperoxaluria. Evidence for renal hyperoxaluria. Clin Chim Acta 191:67

[55] Gambaro G, Petrarulo M, Nardelotto A, Marangella M, Baggio B (1995) Erythrocyte transmembrane flux and renal clearance of oxalate in idiopathic calcium nephrolithiasis. Kidney Int. 48:1549

[56] Prenen JAC, Boer P, Dorhout Mees EJ, Endeman HJ, Spoor SM, Oei HY (1982) Renal clearance of [^{14}C]oxalate:comparison of constant infusion with single-injection techniques. Clin Sci 63:47

[57] Hatch M (1993) Oxalate status in stone-formers. Two distinct hyperoxaluric entities. Urol Res 21:55

[58] Schwille PO, Manoharan M, Rumenapf G, Wölfel G, Berens H (1989) Oxalate measurements in the picomol range by ion chromatography: Values in fasting plasma and urine of controls and patients with idiopathic calcium urolithiasis. J Clin Chem Clin Biochem 27:87

[59] Barratt TM, Kasidas GP, Murdoch I, Rose GA (1991) Urinary oxalate and glycolate excretion and plasma oxalate concentrations. Arch Dis Childhood 66:501

[60] Hagen L, Walker VR, Sutton RAL (1993) Plasma and urinary oxalate and glycolate in healthy subjects. Clin Chem 39:134

[61] Schuster VL, Seldin DW (1992) Renal clearance. In: The kidney, Brenner BM and Rector FC (eds), Chapter 28, 943

[62] Craig Brater D, Sokol PP, Hall SD, McKinney TD (1992) Renal elimination of drugs:Methods and Determinants. In:The kidney, Brenner BM and Rector FC (eds), Chapter 107, 3597

[63] Boer P, Beutler JJ, van Rijn HJM, Berckmans RJ, Koomans HA, Dorhout Mees EJ. Urinary oxalate excretion during intravenous infusion of diuretics in man. Nephron 54:187

[64] Finlayson B, Reid F (1978) The expectation of free and fixed particles in urinary stone disease. Invest Urol 15:442

[65] Kok DJ, Khan SR (1994) Calcium oxalate nephrolithiasis, a free or fixed particle disease. Kidney Int 46:847

[66] Elferink JGR (1987) The mechanisms of calcium oxalate crystal-induced haemolysis of human erythrocytes. Br J Exp Path 68:551

[67] Elferink JGR, Deierkauf M (1987) Enzyme release from polymorphonuclear leukocytes during interaction with calcium oxalate microcrystals. J Urol 138:164

[68] Falasca GF, Ramachandrula A, Kelley KA, O'Connor CR, Reginato AJ (1993) Superoxide anion production and phagocytosis of crystals by cultured endothelial cells. Arthr Rheum 36:105

[69] Hasselbacher P (1982) Stimulation of synovial fibroblasts by calcium oxalate and monosodium urate monohydrate. J Lab Clin Med 100:977

[70] Simons K, Fuller SD (1985) Cell surface polarity in epithelia. Ann Rev Cell Biol 1:243

[71] Handler JS (1989) Overview of epithelial polarity. Annu Rev Physiol 51:729

[72] Kreiberg JL, Wilson PD (1988) Renal cell culture. J Electron Microsc Tech 9:235

[73] Verkoelen CF, Romijn JC, Boevé ER, Schröder FH (1996) Cell cultures as a model in the study of nephrolithiasis. Ital J Mineral Electrolyte Metab 10:57

[74] Lewis SA, Berg JR, Kleine TJ (1995) Modulation of epithelial permeability by extracellular macromolecules. Physiol Rev 75:561

[75] Karlsson K-A (1989) Animal glycosphingolipids as membrane attachment sites for bacteria. Ann Rev Biochem 58:309

[76] Hess B, Nakagawa Y, Coe FL (1989) Inhibition of calcium oxalate monohydrate crystal aggregation by urine proteins. Am J Physiol 257:F99

[77] Cao LC, Boevé ER, Schröder FH, Robertson WG, Ketelaars GA, de Bruijn WC (1992) The effect of two new semi-synthetic glycosaminoglycans (G871 and G872) on the zeta potential of calcium oxalate crystals and on growth and agglomeration. J Urol 147:1643

[78] Bigelow MW, Wiessner JH, Kleinman JG, Mandel NS (1996) Calcium oxalate-crystal membrane interactions: Dependence on membrane lipid composition. J Urol 155:1094

[79] Bigelow MW, Wiessner JH, Kleinman JG, Mandel NS (1997) Surface exposure of phosphatidylserine increases calcium oxalate crystal attachment to IMCD cells. Am J Physiol 272:F55

[80] Mandel N (1994) Crystal-membrane interaction in kidney stone disease. J Am Soc Nephrol 5:S37

[81] Mandel N (1996) Mechanisms of stone formation. Sem Nephrol 16:364

[82] Lieske JC, R Leonard, H Swift, G Toback (1996) Adhesion of calcium oxalate monohydrate crystals to anionic sites on the surface of epithelial cells. Am J Physiol 270:F192

[83] Lieske JC, Leonard R, Toback FG (1995) Adhesion of calcium oxalate monohydrate crystals to renal epithelial cells is inhibited by specific anions. Am J Physiol 268:F604

[84] Lieske JC, Norris R, Toback FG (1997) Adhesion of hydroxyapatide crystals to anionic sites on the surface of renal epithelial cells. Am J Physiol 273:F233

[85] Verkoelen CF, van der Boom BG, Romijn JC, Schröder FH (1996) Cell density dependent calcium oxalate crystal binding to sulphated proteins at the surface of MDCK cells. In: CYC Pak, MI Resnick, GM Preminger (eds) Urolithiasis, Dallas, Texas, 208

[86] Bigelow MW, Wiessner JH, Kleinman JG, Mandel NS (1997) The dependence on membrane fluidity of calcium oxalate crystal attachment to IMCD membranes. Calcif Tissue Int 60:375

[87] Gill WB, KW Jones, KJ Ruggiero (1981) Protective effects of heparin and other sulfated glycosaminoglycans on crystal adhesion to injured urothelium. J Urol 127:152

[88] Khan SR, CA Cockrell, B Finlayson, RL Hackett (1984) Crystal retention by injured urothelium of the rat urinary bladder. J Urol 132:153

[89] Bennett HS (1962) Morphological aspects of extracellular polysaccharides. J Histochem Cytochem 11:14

[90] Boevé ER, Cao LC, Schröder FH, Ketelaars GAM, Vermey M, Bruijn WC de (1990) The influence of 3 exogeneous glycosaminoglycans on the experimental induction of microliths in rats. Urol Res 18:62

[91] Boevé ER, Cao LC, Verkoelen CF, Romijn JC, de Bruijn WC, Schröder FH (1994) Glycosaminoglycans and other sulphated polysaccharides in calculogenesis of urinary stones. World J Urol 12:43

[92] Riese RJ, Mandel NS, Wiessner JH, Mandel GS, Becker CG, Kleinman JG (1992) Cell polarity and calcium oxalate crystal adherence to collecting duct cells. Am J Physiol 262:F177

[93] Molitoris BA, Hoilien C (1987) Static and dynamic componenets of renal cortical brush border and basolateral membrane fluidity: Role of cholesterol. J Membrane Biol 99:165

[94] Lieske JC, Walsh-Reitz MM, Toback FG (1992) Calcium oxalate monohydrate crystals are endocytosed by renal epithelial cells and induce proliferation. Am J Physiol 262:F622

[95] Lieske JC, Toback FG (1993) Regulation of renal epithelial cell endocytosis of calcium oxalate monohydrate crystals. Am J Physiol 264:F800

[96] Lieske JC, Swift H, Martin T, Patterson B, Toback FG (1994) Renal epithelial cells rapidly bind and internalize calcium oxalate monohydrate crystals. Proc Natl Acad Sci USA 91:6987

[97] Lieske CL, Spargo BH, Toback FG (1992) Endocytosis of calcium oxalate crystals and proliferation of renal tubular epithelial cells in a patient with type 1 primary hyperoxaluria. J Urol 148:1517

[98] Goswami A, Singhal PC, Wagner JD, Urivetzki M, Valderrama E, Smith AD (1995) Matrix modulates uptake of calcium oxalate crystals and cell growth of renal epithelial cells. J Urol 152:206

[99] Roth J, Taatjes DJ (1985) Glycocalyx heterogeneity of rat kidney urinary tubule: demonstration with a lectin-gold technique specific for sialic acid. Eur J Cell Biol, 39:449

[100] Mandell I, Krauss E, Millan JC (1980) Oxalate-induced acute renal failure in Crohn's disease. Am J Med 69:628

[101] Morgenroth K, Backmann R, Blaschke R (1968) On the formation of deposits of calcium oxalate in the human kidney in oxalosis. Beitr Path Anat 136:454

[102] Saxon A, Busch GJ, Merrill JP, Franco V, Wilson RE (1974) Renal transplantation in primary hyperoxaluria. Arch Intern Med 133:464

[103] Wharton R, D'Agati V, magun AM, Whitlock R, Kunis CL, Appel GB (1990) Acute detoriation of renal function associated with enteric hyperoxaluria. Clin Nephrol 34:116

[104] Kahn SR, Hackett RL (1991) Retention of calcium oxalate crystals in renal tubules. Scann Microsc 5:707

[105] Bruijn WC de, Boevé ER, van Run PRWA, van Miert PPMC, Romijn JC, Verkoelen CF, Cao LC, Schröder FH (1994) Etiology of experimental calcium oxalate monohydrate nephrolithiasis in rats. Scanning Micr 3:541

[106] Randall A (1937) The origin and growth of renal calculi. Ann Surgery 105:1009

[107] Baggio B, G Gambaro, E Ossi, S Favaro, A Borsatti (1983) Increased urinary excretion of renal enzymes in idiopathic calcium oxalate nephrolithiasis. J Urol 129:1161

[108] Hackett RL, PN Shevock, SR Kahn (1990) Cell injury associated calcium oxalate crystalluria. *J.Urol.* 144:1535

[109] Khan SR, PN Shevock, RL Hackett (1989) Urinary enzymes and calcium oxalate urolithiasis. J Urol 142:846

[110] Doyle IR, RL Ryall, VR Marshall (1991) Inclusion of proteins into calcium oxalate crystals precipitated from human urine: a highly selective phenomenon. Clin Chem 37:1589

[111] Leiser J, Molitoris BA (1993) Disease processes in epithelia: The role of the actin cytoskeleton and altered surface membrane polarity. Biochim Biophys Acta 1225:1

[112] Edelstein CL, Ling H, Schrier RW (1997) The nature of renal cell injury. Kidney Int 51:1341

[113] Hackett RL, Shevock PN, Kahn SR (1990) Cell injury associated calcium oxalate crystalluria. J Urol 144:1535

[114] Hackett RL, Shevock PN, Khan SR (1994) Madin-Darby canine kidney cells are injured by exposure to oxalate and to calcium oxalate crystals. Urol Res 22:197

[115] Scheid C, Koul H, Hill WA, Luber-Narod J, Kennington L, Honeyman T, Jonassen J, Menon M (1996) Oxalate toxicity in LLC-PK_1 cells: Role of free radicals. Kidney Int 49:413

[116] Koul H, Kennington L, Honeyman T, Jonassen J, Menon M, Scheid C (1996) Activation of *c-myc* gene mediates the mitogenic effects of oxalate in LLC-PK_1 cells, a line of renal epithelial cells. Kidney Int 50:1525

[117] Koul H, Kennington L, Nair G, Honeyman T, Menon M, Scheid C (1994) Oxalate-induced initiation of DNA synthesis in LLC-PK_1 cells, a line of renal epithelial cells. Biochem Biophys Res Comm 205:1632

[118] Scheid C, Koul H, Hill WA, Luber-Narod J, Jonassen J, Honeyman T, Kennington L, Kohli R, Hodapp J, Ayvazian P, Menon M (1996) Oxalate toxicity in LLC-PK_1 cells, a line of renal epithelial cells. J Urol 155:1112

[119] Scheid C, Koul H, Kennington L, Hill WA, Luber-Narod J, Jonassen J, Honeyman T, Menon M (1995) Oxalate-induced damage to renal tubular cells. Scanning Microsc 9:1097-1107

[120] Schwartz GJ, Barasch J, Q Al-Awqati (1985) Plasticity of functional epithelial polarity. Nature 318:368

[121] Tsuruoka S, Schwartz GJ (1996) Adaptation of rabbit cortical collecting duct HCO3- transport to metabolic acidosis in vitro. J Clin Invest 97:1076

[122] Kajander EO, Çiftçioglu N (1998) Nanobacteria: An alternative mechanism for pathogenic intra-and extracellular calcification and stone formation. Proc Natl Acad Sci USA 95:8274

[123] Fleiszig SMJ, Vallas V, Jun CH< MOK 1, Balkovetz DF, Roth MG, Mostov KE (1998) Susceptibility of epithelial cells to pseudomonas aeruginosa invasion and cytotoxicity is upregulated by hepatocyte growth factor. Infect Immun 66:3443

Summary

Nephrolithiasis (renal stone disease) is a common disorder in industrialized countries. About 10 % of the population will develop kidney stones during lifetime. Stones smaller than 5 mm usually are spontaneously passed with the urine. Surgical intervention or stone destruction techniques are often required to remove larger stones. Approximately 50 % of the patients that formed a renal stone for the first time will do that again within a period of 10 years. Although renal stone disease generally is not life threatening, stones can be very painful and invasive clinical interventions are required for their removal. Furthermore, these clinical procedures and the allied absence from work has a substantial economic impact. Therefore, it is important to disclose the abnormalities underlying renal stone disease. With this knowledge we might be able to develop strategies to prevent stone recurrence.

One of the most important functions of the kidney is the production of a concentrated urine. This is accomplished by the reabsorption of almost all essential nutrients and water filtered at the glomerulus. During this process there is an increase in the concentration of components that are not or less extensively reabsorbed. After the solubility product of certain salts is surpassed (supersaturation) this may lead to the spontaneous formation of crystals (nucleation). Urine normally contains compounds that prevent salt crystals from increasing in size (growth), from clotting (agglomeration) or from interacting with the renal tissue (attachment). Renal stones are the ultimate result of crystals that are not eliminated with the urine (retention). Hence, the events leading to stone formation are, in sequence, saturation, super saturation, crystal nucleation, growth, agglomeration and retention. Calcium oxalate (CaOx) is the most common component of approximately 75% of all stones. In normal urine, the soluble amount of CaOx can be 4 times higher than in pure water. Oxalate plays a more important role in the solubility of CaOx than calcium. Urinary oxalate is increased in many idiopathic calcium stone formers. Hyperoxaluria could in theory be caused by enhanced intestinal absorption or by increased renal secretion of oxalate. It was found that distinct idiopathic calcium stone patients could be identified by an increased transport of oxalate across the membranes of their red blood cells. From this observation it was speculated that oxalate could also be transported faster across the membranes of renal and/or intestinal cells. Therefore, it seemed essential to obtain more knowledge about the cellular handling of oxalate. We studied oxalate transport in various renal

epithelial cell lines. Although oxalate transport was studied extensively, we were unable to detect active oxalate transport in these cells (Chapter 2 and 3). This observation, however, does not necessarily implicate that there is no active transport of oxalate in the kidney. It is conceivable that cells in culture loose their ability for organic anion transport, or that the cell lines used originated from sites in the nephron not involved in oxalate transport. In the mean time, a different view point was reached on the induction of hyperoxaluria. Recent clearance studies demonstrated that in healthy individuals there is no net renal oxalate transport. In many stone formers hyperoxaluria most likely is not caused by an enhanced renal secretion, but by an increased intestinal absorption or an enhanced endogeneous production of oxalate. On the other hand, there are also indications that after an oxalate load, oxalic acid is excreted faster and with higher peaks in the urine of distinct stone formers. These transiently high concentrations of oxalate in the primary urine, for example after meals, could be high enough to trigger the litogenic process. In the latter case a role for oxalate secretion in the kidney cannot be excluded. Although speculative, it is also possible that transient peaks of oxalate in the tubular fluid are induced by an abnormal fast reabsorption of water in early segments of the nephron (Chapter 3).
The next question that we tried to answer was: Why are crystals, that are occasionally formed in the kidneys of all individuals, selectively retained in the kidneys of stone formers? It is conceivable that the epithelium in the kidneys of these patients is more suceptible for crystal adherence. We subsequently used our cell culture models to study crystal-cell interaction. These studies showed that the cell surface of certain cell types indeed can have affinity for crystals. CaOx crystals were generated by mixing calcium with oxalate in water. The addition of a fraction radioactive oxalate during this process results in the formation of radiolabeled crystals that are conveniently to monitor. X-ray diffraction showed that these crystals exclusively consisted of calcium oxalate monohydrate (COM). Coulter Multisizer measurements demonstrated that under the conditions used, crystals were formed with an average size of 2 μm. We also examined the effect of various factors on crystal-cell interaction such as the influence of temperature, pH, crystal concentration and crystal binding kinetics (Chapter 4). The confrontation with crystals at other sites in the body (blood, joints) often leads to a violent inflammatory response accompanied by tissue destruction. We presented evidence that the interaction of renal cells with COM crystals is not necessarily damaging. This was established by measuring the release of cellular (LDH) and membrane associated enzymes

(γ-GT), epithelial barrier integrity (P^{mann}), and cell viability (MTT-test, trypan blue exclusion test). Crystals not only appeared to adhere to the cells, but were also taken up by them (endocytosis). Transmission electron microscopy showed that after a certain period of time endocytosed crystals had disappeared from the cell interior, suggesting that these cells are capable to process a certain amount of crystals. This may reflect a protective physiological mechanism to prevent stone formation.

Next, we investigated the inhibitory effect of polysaccharides, which are well known inhibitors of crystallization, on crystal binding (Chapter 5). These studies showed that polysaccharides occuring naturally in the urine such as glycosaminoglycans, only moderately inhibited crystal binding (IC-50: >100 μg/ml). Synthetic polysaccharides, on the other hand, appeared to be very potent inhibitors (IC-50: ~ 1 μg/ml). Evidence was provided that polysaccharides exert their inhibitory effect by interacting with the crystal surface rather than the cell surface. Provided that there are no unwanted side-effects and that the achievable concentrations in the primary urine are sufficiently high, synthetic polysaccharides perhaps can be applied as drugs in the prevention of stone recurrence.

Crystal binding was further studied during the growth of the cells to confluent and functional monolayers. Monolayers were considered functional after they formed polarized cells with functional tight junctions. The assembly of tight junctions is monitored by measuring the transepithelial electrical resistance (TER). Epithelial polarity is indicated by the predominant presence of Na^+,K^+-ATPase in the basolateral membrane of MDCK and LLC-PK_1 cells (Chapter 7), selectively uptake of the glucose analog α-methyl glucoside at the apical membrane and the vectorial transport of solutes and water by intact monolayers formed by LLC-PK_1 cells (Chapters 2 and 3). Binding studies demonstrated that crystals avidly associated with the surface of subconfluent MDCK cultures but not or only hardly with the surface of functional monolayers. The epithelial cells reobtained affinity for crystals during the repair from mechanically inflicted wounds. Confocal microscopy showed that during the process of wound healing crystals selectively adhered to the surface of migrating cells at the border of the wound and to cells that temporary formed a scar at sites where wounds were closed. The tissue is protected again after the tissue is regenerated and the barrier integrity is restored (Chapter 6). To investigate whether the ability to repulse crystals is specific for MDCK cells, we also studied crystal binding to LLC-PK_1 cells (Chapter 7). These studies showed that the level of crystal binding to these cells, in contrast to MDCK cells,

did not decrease upon the formation of confluent and polarized monolayers. Perhaps this is not coincidental since MDCK cells in culture retained many characteristics of late segments of the nephron (distal tubule/collecting ducts), an area where the level of stone salt supersaturation frequently is high enough for crystal formation. LLC-PK_1 cells, on the other hand, express morphological and functional characteristics of early segments of the nephron (proximal tubule). In this part of the kidney crystals are only to be expected during extreme hyperoxaluria such as that observed in distinct hereditary disorders. These results suggest that, in contrast to the proximal tubule, the tissue in the collecting duct normally is protected from crystal binding. Alterations in the composition of the epithelial surface in late segments of the nephron, for example during wound healing, may induce conditions that lead to a transiently enhanced cell surface affinity for crystals, which ultimately results in the formation of a renal stone.

Samenvatting

Nefrolithiasis (niersteenvorming) is een algemeen voorkomende ziekte in geïndustrialiseerde landen. Ongeveer één op de tien mensen krijgt in zijn/haar leven een niersteen. Stenen die minder dan 5 mm groot zijn worden meestal spontaan uitgeplast. Stenen die groter zijn moeten echter vaak chirurgisch of door schokgolven verwijderd worden. Ongeveer de helft van de mensen die voor het eerst een steen maken zal dat binnen een periode van 10 jaar opnieuw doen. Hoewel nierstenen over het algemeen niet levensbedreigend zijn, veroorzaken ze enorm veel pijn en zijn de klinische procedures om ze te verwijderen erg ingrijpend. Bovendien hebben deze behandelingen en het daarmee samenhangende werkverzuim een behoorlijke economische impact. Het is dan ook van belang om te weten te komen wat de onderliggende afwijkingen zijn bij het ontstaan van nierstenen. Met deze kennis kunnen wellicht maatregelen genomen worden die de terugkeer van een steen voorkomen.

Een van de belangrijkste funkties van de nier is het produceren van een geconcentreerde urine. Dit wordt bereikt door de terugresorptie in de tubuli van vrijwel alle essentiële voedingsstoffen en water uit het glomerulair filtraat. Tijdens dit proces neemt de concentratie in de tubulaire vloeistof van componenten die niet of minder teruggeresorbeerd worden toe. Wanneer het oplosbaarheidsproduct van bepaalde zouten overschreden wordt (supersaturatie) kan dit leiden tot spontane kristalvorming (nucleatie). Normale urine bevat stoffen die voorkomen dat deze zout-kristallen toenemen in grootte (groei), samenklonteren (agglomeratie) of een interaktie aangaan met het nierweefsel (binding). Nierstenen zijn het uiteindelijke gevolg van kristallen die achterblijven in de nier (retentie). De volgorde van de processen die uiteindelijk tot nierstenen leiden is dus: saturatie, supersaturatie, kristal nucleatie, -groei, -agglomeratie en -retentie. Calcium oxalaat (CaOx) vormt het hoofdbestanddeel van ongeveer drie kwart van alle stenen. In normale urine kan de concentratie van CaOx vier keer hoger zijn dan z'n oplosbaarheid in zuiver water. Oxalaat speelt een belangrijkere rol in de oplosbaarheid van CaOx dan calcium. De concentratie van oxaalzuur is verhoogd in de urine van veel idiopatische calcium steenvormers. In theorie zou deze hyperoxalurie veroorzaakt kunnen worden door een verhoogde opname van oxaalzuur in de darm of een verhoogde sekretie in de nier. Vooral na het vinden van een verhoogde flux van oxaalzuur over de celmembraan van erythrocyten bij bepaalde steenpatienten werd er gespeculeerd over de mogelijkheid dat een structureel veranderd

transporteiwit in de membraan niet alleen zou kunnen leiden tot een verhoogd flux in rode bloedcellen maar wellicht ook in nier- en/of darmcellen van deze patienten. Meer kennis over cellulair transport van oxaalzuur leek daarom van essentieel belang. Het transport van oxaalzuur werd door ons bestudeerd in verschillende niercellijnen. Hoewel het transport van oxaalzuur uitgebreid onderzocht werd waren wij niet in staat om aktief oxaalzuur transport in deze cellen aan te tonen (Hoofdstuk 2 en 3). Dit betekent echter niet dat er geen aktief transport van oxaalzuur in de nier zou kunnen plaatsvinden. Het zou kunnen zijn dat cellijnen in kweek de mogelijkheid tot organisch anion transport verliezen, of dat de door ons gebruikte cellen afkomstig zijn van segmenten van de nier die niet betrokken zijn bij het transport van oxaalzuur. Inmiddels is er in de literatuur ook een wat ander inzicht bereikt over de manier waarop hyperoxalurie verklaard zou kunnen worden. Recente klaringsstudies hebben aangetoond dat er bij gezonde mensen geen netto oxaalzuur sekretie plaatsvindt in de nier. Bij veel niersteenpatienten lijkt hyperoxalurie niet veroorzaakt door een verhoogde oxaalzuur sekretie in de nier maar door verhoogde opname in de darm of verhoogde endogene produktie van oxaalzuur in de lever. Aan de andere kant zijn er ook aanwijzingen dat oxaalzuur na een oxalaat belasting sneller en met hogere pieken wordt uitgescheiden in de urine van bepaalde steenpatienten. Deze kortstondig hoge concentraties van oxaalzuur in de tubulaire vloeistof, zoals bijvoorbeeld na maaltijden, zouden wellicht hoog genoeg zijn om het lithogene proces te initiëren. In dit laatste geval zou oxaalzuur sekretie door de nier wel een rol kunnen spelen. In theorie kan een abnormaal snelle water terugresorptie in vroege segmenten van het nefron ook leiden tot zulke kortstondig hoge oxaalzuur concentraties (Hoofdstuk 3).

De volgende vraag die we geprobeerd hebben te beantwoorden is: Hoe komt het dat kristallen, die door ieder individu gemaakt worden, alleen achterblijven in de nieren van steen patienten? Een van de mechanismen waarmee kristal retentie in de nier verklaard zou kunnen worden is wanneer het celoppervlak affiniteit zou hebben of krijgen voor de in de tubulaire vloeistof circulerende zoutkristallen. Gebruikmakend van onze celkweek modellen hebben we daarop de interaktie van CaOx kristallen met niercellen bestudeerd. Deze studies lieten zien dat het celoppervlak van bepaalde cellen inderdaad affiniteit kan hebben voor kristallen. CaOx kristallen werden verkregen door calcium en oxaalzuur met elkaar te mengen. Door toevoeging van een zekere hoeveelheid radioaktief gemerkt oxaalzuur worden er radioaktieve kristallen gevormd die goed te monitoren zijn. In

eerste instantie hebben we met röntgen diffraktie vastgesteld dat deze methode uitsluitend calcium oxalaat monohydraat (COM) kristallen oplevert. Coulter Multisizer metingen hebben aangetoond dat de kristallen onder de door ons gekozen condities een gemiddelde grootte van 2 μm hebben. Verder hebben we het effekt van diverse faktoren, zoals de invloed van temperatuur, pH, en kristal concentraties op de binding in detail onderzocht, alsook de bindings kinetiek (Hoofdstuk 4). Hoewel de confrontatie met kristallen op andere plaatsen in het lichaam (bloed, gewrichten) vaak tot heftige onstekingsreakties en celdood leidt, hebben wij laten zien dat de interaktie tussen niercellen en kristallen niet noodzakelijkerwijs schadelijk is voor het weefsel. Kristallen bleken niet alleen te binden aan het celoppervlak maar werden na verloop van tijd ook door de cellen opgenomen (endocytose). Deze aktieve interaktie tussen cellen en kristallen gaf geen meetbare celschade, zoals het vrijkomen van intracellulaire (LDH) en membraangebonden enzymen (γ-GT), het aantasten van de permeabiliteit van het epitheel (P^{mann}) of het aantasten van de levensvatbaarheid van de cellen (MTT-test, trypanblauw exclusie-test). Bovendien werd met transmissie electronen microscopie duidelijk dat geendocyteerde kristallen na enige tijd niet meer in de cellen aanwezig waren, hetgeen suggereert dat deze niercellen in staat waren een zekere hoeveelheid geassocieerde kristallen te verwerken. Dit zou een natuurlijke protektie kunnen zijn tegen steenvorming.

Vervolgens hebben we onderzocht of het bedekken van de kristallen bijvoorbeeld met polysacchariden een methode zou kunnen zijn om kristalbinding tegen te gaan (Hoofdstuk 5). Hieruit bleek dat in de urine voorkomende polysacchariden zoals glycosaminoglycanen, die uit de literatuur bekend zijn als remmers van kristallisatie, vrij matige remmers van kristalbinding zijn (IC-50: $>$ 100 μg/ml). Synthetische polysacchariden daarentegen bleken veel meer remmende aktiviteit te hebben (IC-50: $\sim$ 1 μg/ml). Tevens werd bewezen dat deze stoffen hun effekt uitoefenen op het kristaloppervlak en niet op het celoppervlak. Synthetische polysacchariden zouden dus mogelijk gebruikt kunnen worden om steenvorming te voorkomen, op voorwaarde dat de concentraties in de tubulaire vloeistof voldoende hoog kunnen worden en er geen ongewenste bijwerkingen zijn.

Daarna hebben we de binding van kristallen aan het oppervlak van deze cellen tijdens hun ontwikkeling in funktionele monolagen onderzocht. Monolagen werden funktioneel beschouwd wanneer membraan bestanddelen gepolarizeerd verdeeld werden en er tussen de cellen funktionele stevige verbindingen (tight junctions) gevormd werden. De montage van deze

stevige verbindingen tussen cellen kan worden gevolgd door het meten van de transepitheliale electrische weerstand (TER). Epitheliale polariteit werd aangetoond door de aanwezigheid van Na^+,K^+-ATPase voornamelijk in de basolaterale membraan van MDCK en LLC-PK_1 cellen (Hoofdstuk 7), de selektief apicale opname van de glucose analoog α-methyl glucoside en het vectoriale transport van opgeloste stoffen en water door LLC-PK_1 cellen (Hoofdstukken 2 en 3). Crystal bindingsstudies toonden aan dat kristallen zich gretig verbonden met het celoppervlak van subconfluente cultures van MDCK cellen, maar niet of nauwelijks met het oppervlak van funktionele monolagen. Het epitheel kreeg opnieuw affiniteit voor kristallen tijdens de reparatie van mechanisch toegebrachte weefselschade. Confocale microskopie liet zien dat de kristallen zich tijdens dit proces selektief hechtten aan het oppervlak van migrerende cellen aan de rand van de wond en aan cellen die tijdelijk een litteken vormden op plaatsen waar de wond werd gesloten. Het weefsel was weer beschermd tegen kristaladhesie nadat de wond was geheeld en de integriteit van de epitheliale barière volledig was hersteld (Hoofdstuk 6).

Om te onderzoeken of de eigenschap om kristallen af te stoten specifiek is voor MDCK cellen werden deze studies herhaald met LLC-PK_1 cellen. Hieruit bleek dat in tegenstelling tot MDCK cellen, de hoeveelheid kristaladhesie aan LLC-PK_1 cellen niet omlaag ging tijdens de vorming van confluente en gepolariseerde monolagen. Misschien is dit niet toevallig aangezien MDCK cellen vooral overeenkomen met cellen in late segmenten van het nefron (distale tubulus en/of de verzamelbuizen), een gebied waar de oververzadiging van de primaire urine regelmatig hoog genoeg is voor kristal vorming. LLC-PK_1 cellen daarentegen hebben morfologische en funktionele eigenschappen van cellen uit vroege segmenten van het nefron (proximale tubulus). In dit deel van de nier zijn kristallen alleen te verwachten bij zeer hoge oxaalzuurwaarden in het plasma zoals dat voorkomt bij sommige erfelijke vormen van hyperoxaluria (Hoofdstuk 7). Deze resultaten suggereren dat, in tegenstelling tot het weefsel in de proximale tubulus, de cellen in de verzamelbuizen normaal beschermd zijn tegen de adhesie van kristallen. Een verandering in de samenstelling van het celoppervlak in late segmenten van het nefron, zoals bijvoorbeeld tijdens het herstel van schade, zou kunnen leiden tot een kortstondig verhoogde affiniteit van het weefsel voor kristallen dat uiteindelijk resulteert in het ontstaan van een niersteen.

List of publications

Verkoelen CF, Boom van der BG, Kok DJ, Houtsmuller AB, Visser P, Schröder FH, Romijn JC (1998) Cell type-specific acquired protection from crystal adherence by renal tubule cells in culture, submitted

Verkoelen CF, Boom van der BG, Houtsmuller AB, Schröder FH, Romijn JC (1998) Increased calcium oxalate monohydrate crystal binding to injured renal tubular epithelial cells in culture. Am J Physiol 274:F958

Verkoelen CF, Kok DJ, Boom van der BG, Jonge de HR, Schröder FH, Romijn JC (1998) LLC-PK_1 cells as model system to study proximal tubule transport of water and other compounds relevant for renal stone disease. Accepted for publication in Urol Res

Verkoelen CF, Boom van der BG, Schröder FH, Romijn JC (1997) Cell cultures and nephrolithiasis. World J Urol 15:229

Verkoelen CF, Romijn JC, Boevé ER, Schröder FH (1997) Cell cultures as a model in the study of nephrolithiasis. It J Mineral Electrol Metab 10:57

Verkoelen CF, Boom van der BG, Romijn JC (1996) Cell density dependent calcium oxalate crystal binding to sulphated proteins at the surface of MDCK cells. in: Urolithiasis. CYC Pak, MI Resnick, GM Preminger (eds), Millet The Printer, Inc, Dallas, pg 20

Verkoelen CF, van der Boom BG, Romijn JC (1996) Transport of glucose, chloride, bicarbonate, phosphate, fluid, *p*-aminohippurate and oxalate by LLC-PK_1 cells. in: Urolithiasis, CYC Pak, MI Resnick, GM Preminger (eds), Millet The Printer, Inc, Dallas, pg 347

Verkoelen CF, Romijn JC, Bruijn de WC, Boevé ER, Cao LC, Schröder FH (1995) Association of calcium oxalate monohydrate (COM) crystals with MDCK cells. in: Renal stones, aspects on their formation, removal and prevention, H-G Tiselius (ed), Akademitryck AB, Edsbruk, pg 34

Verkoelen CF, Romijn JC, Cao LC, Boevé ER, Bruijn de WC, Schröder FH (1995) Crystal-cell interaction inhibition by polysaccharides. J Urol 155:749

Verkoelen CF, Romijn JC (1995) Oxalate transport and calcium oxalate renal stone disease. Urol Res 24:183

Verkoelen CF, Romijn JC, Bruijn de WC, Boevé ER, Cao LC, Schröder FH (1995) Association of calcium oxalate monohydrate crystals with MDCK cells. Kidney Int 48:129

Verkoelen CF, Romijn JC, Bruijn de WC, Boevé ER, Cao LC, Schröder FH (1993) Absence of a transcellular oxalate transport mechanism in LLC-PK$_1$ and MDCK cells cultured on porous supports. Scann Microsc 3:1031

Verkoelen CF, Romijn JC, Schröder FH, Schalkwijk WP and Splinter TAW (1988) Quantitation of polyamines in cultured cells and tissue homogenates by reversed-phase liquid chromatography of their benzoyl derivates. J Chrom 426:41

Cao LC, Deng G, Boevé ER, Bruijn de WC, Water de R, Verkoelen CF, Romijn JC, Schröder FH (1996) Zeta potential measurements and particle size analysis for a better understanding of urinary inhibitors of calcium oxalate crystallization. Scanning Microsc 10:110

Bruijn de WC, Water de R, Boevé ER, Run van PR, Vermaire PJ, Miert van PP, Romijn JC, Verkoelen CF, Cao LC, Schröder FH (1996) Lectin-cytochemistry of experimental rat nephrolithiasis. Scanning Microsc 9:89

Bruijn de WC, Water de R, Run van PR, Boevé ER, Kok DJ, Cao LC, Romijn JC, Verkoelen CF, Schröder FH (1997) Ultrastructural osteopontin localization in papillary stones induced in rats. Eur Urol 32:360

Cao LC, Deng G, Boevé ER, Romijn JC, Bruijn de WC, Verkoelen CF, Schröder FH (1997) Does urinary oxalate interfere with the inhibitory role of glycosaminoglycans and semisynthetic sulfated polysaccharides in calcium oxalate crystallization? Eur Urol 31:485

Bruijn de WC, Boevé ER, Run van PR, Miert van PP, Water de R, Romijn JC, Verkoelen CF, Cao LC, Schröder FH (1995) Etiology of calcium oxalate nephrolithiasis in rats. I. Can this be a model for human stone formation. Scanning Microsc 9:103

Bruijn de WC, Boevé ER, Run van PR, Miert van PP, Water de R, Romijn JC, Verkoelen CF, Cao LC, Noordende van 't JM, Schröder FH (1995) Etiology of calcium oxalate nephrolithiasis in rats. II. The role of the papilla in stone formation. Scanning Microsc 9:115

Bruijn de WC, Boevé ER, Run van PR, Miert van PP, Romijn JC, Verkoelen CF, Cao LC, Schröder FH (1994) Etiology of experimental calcium oxalate monohydrate nephrolithiasis in rats. Scanning Microsc 8:541

Boevé ER, Cao LC, Verkoelen CF, Romijn JC, Bruijn de WC, Schröder FH (1994) Glycosaminoglycans and other sulfated polysaccharides in calculogenesis of urinary stones. World J Urol 12:43

Splinter TAW, Verkoelen CF, Vlastuin M, Kok TC, Rijksen G, Haglid KG, Boomsma F, van der Gaast A (1992) Distinction of two different classes of small-cell lung cancer cell lines by enzymatically inactive neuron-specific enolase. Br J Cancer 66:1065

Romijn JC, Verkoelen CF, Splinter TAW (1988) Application of the MTT-assay to human prostatecancer cell lines in vitro, establishment of testconditions and assessment of hormone-stimulated growth and drug induced cytostatic and cytotoxic effects. The Prostate 12:99

Romijn JC, Verkoelen CF, Splinter TAW (1987) Problems of pharmacokinetic studies on alpha-difluoromethylornithine in mice. Cancer Chemother Pharmacol 19:30

Romijn JC, Verkoelen CF, Trapman J, Schröder FH (1986) Determination of the survival of human tumor cells implanted in nude mice. Int J Cancer 38:97

Romijn JC, Verkoelen CF, Splinter TAW (1986) Species-dependent differences of the biochemical properties of diamine oxidase. Int J Biochem 18:835

Romijn JC, Verkoelen CF, Schröder FH (1984) Determination of the growth rate of human prostatic cells in primary culture by a morphometric technique. Cell Biol Int Rep 8:363

Curriculum vitae

Carl Friedrich Verkoelen
- Geboren op 22 december 1953 te Rotterdam
- Getrouwd met Esther de Otter
- Twee kinderen, een dochter Carlie (5) en een zoon Sjors (4)

1970	MULO-A, Herman Heijermansschool, Rotterdam
1971-1972	Ferro Holland BV, Rotterdam
1972-1977	Balansafdeling, Inwendige Geneeskunde III, Academisch Ziekenhuis Dijkzigt, Rotterdam
1974	MBO analytisch-chemisch, van 't Hoff Instituut, Rotterdam
1975	HBO-A klinisch-chemisch, van 't Hoff Instituut, Rotterdam
1977-1979	Pfizer BV, Rotterdam
1979-1980	Radio Biologisch Instituut TNO, Rijwijk
1980-1988	Experimentele Urologie, Erasmus Universiteit Rotterdam
1988-1991	Medische Oncologie, Academisch Ziekenhuis Dijkzigt, Rotterdam
1991-1998	Experimentele Urologie, Erasmus Universiteit Rotterdam
1996	Klinisch-chemisch ingenieur, HLO Polytechnische Faculteit Hogeschool Rotterdam en Omstreken, Delft
vanaf 1999	Vaste wetenschappelijke aanstelling binnen de steengroep van de afdeling Experimentele Urologie, Erasmus Universiteit Rotterdam

Dankwoord

Hierbij wil ik graag iedereen danken die een bijdrage heeft geleverd aan de totstandkoming van dit proefschrift. Zonder iemand te kort te willen doen, wil ik enkele mensen in het bijzonder willen bedanken. In de eerste plaats mijn co-promotor en leermeester Hans Romijn. Beste Hans, we werken nu al zo'n 18 jaar samen. Hoewel het oorspronkelijk niet de bedoeling was, is er nu dus een proefschrift. Bedankt voor je wijze lessen, je niet aflatende steun en vriendschap. Zonder jou was dit boekje er zeker niet gekomen. Professor Schröder ben ik dankbaar voor het in mij gestelde vertrouwen. Zonder uw steun had ik dit onderzoek niet kunnen doen. Burt wil ik bedanken voor al het werk dat hij de afgelopen jaren heeft gedaan. Het was allemaal niet zo eenvoudig als het soms wel eens leek. Uiteindelijk ben je steeds zelfstandiger geworden. Ik hoop dat we nog lang samen zullen werken want we hebben nog een hoop te doen. Mijn kamergenoten, Wytske, Erik Jan, en Nicole zou ik willen bedanken voor de vele stimulerende discussies en de gezelligheid. Corrina, je weet het hé, je wordt bedankt. Burt en Erik Jan wil ik ook bedanken dat ze mijn paranimfen wilden zijn. Johan, Jerome, Hans V, Wilma, Monique, Sigrun, Marja, Maxim en Viola zou ik willen bedanken voor de gezellige sfeer binnen onze groep. Zoals jullie weten: Holle stikstofvaten klinken het leegst. Robert, bedankt voor alle tips. Gert-Jan, met wie ik ook al zo lang prettig samenwerk, zou ik willen bedanken voor het regelen van een nieuwe computer op mijn kamer in het Nefkens gebouw. De leden en ex-leden van de steengroep: de Bruijn, Annelies, Cao, Egbert, Dik, Ruud, Cindy, Niels en Saima zou ik willen bedanken voor hun samenwerking. Verder dank ik Pim van Schalkwijk (klinische chemie), Pim Visser (SEM), Adriaan Houtsmuller (CLSM), Peter van Run (TEM) en Hugo de Jonge (fysiologie) voor de prettige en vruchtbare samenwerking. Ik hoop in de toekomst nog eens een beroep op jullie te kunnen doen. Mijn moeder wil ik bedanken voor haar steun, liefde en vertrouwen en het feit dat ze altijd voor me klaar staat. Esther wil ik vooral bedanken voor haar nuchterheid en de organisatie van alle zaken thuis. Verder hoop ik dat ook jouw opleiding gaat lukken. Mijn schoonmoeder Jo wil ik sterkte wensen en bedanken voor de opvang van de kinderen. Mijn broers, Hennie en Peter omdat ze me vanuit alle uithoeken van de wereld altijd weer weten te vinden. De leden van de kleine commissie wil ik bedanken voor de snelle afhandeling en het kritisch lezen van dit proefschrift. Uiteraard wil ik ook de Nierstichting bedanken voor het financiëren van het onderzoek.